Title
Tyrosinase inhibitors identified from phytochemicals and their mechanism of control

Author
Murray, Anne Frances

Publication Date
2016

Peer reviewed|Thesis/dissertation

Tyrosinase inhibitors identified from phytochemicals and their mechanism of control

By

Anne Frances Murray

A dissertation submitted in partial satisfaction of the

requirements for the degree of

Doctor of Philosophy

In

Environmental Science, Policy and Management

in the

Graduate Division

of the

University of California, Berkeley

Committee in Charge:

Professor Isao Kubo, Chair
Professor David Wood
Professor Leonard Bjeldanes

Fall 2016

Tyrosinase inhibitors identified from phytochemicals and their mechanism of control

by

Anne Frances Murray

Doctor of Philosophy in

Environmental Science, Policy and Management

University of California, Berkeley

Professor Isao Kubo, Chair

The enzyme tyrosinase is responsible for catalyzing the first steps of the melanin formation pathway. Essential oil of the fresh leaves of *Polygonumodoratum* (Polygonaceae), commonly known as Vietnam coriander, was found to inhibit the oxidation catalyzed by tyrosinase (EC 1.14.18.1). Twenty-five scent compounds were characterized in the essential oil by GC-MS analysis. Aldehyde compounds are noted to be the most abundant, followed by alcoholic compounds but to a much lesser extent. Alkanals; dodecanal (55.49%), and decanal (11.57%); were the two most abundant in the essential oil, followed by anisaldehyde (6.35%). Dodecanal and decanal inhibited the oxidation of both L-tyrosine and L-3,4-dihydroxyphenylalanine (L-DOPA) catalyzed by mushroom tyrosinase. The alkanals tyrosinase inhibitory activity was likely caused by nonspecific disruption of the tertiary structure of tyrosinase. This inhibitory activity increased when the enzyme was preincubated with longer chain length alkanals. Yet, this activity did not translate to inhibiting melanin production.

In our search for plant derived tyrosinase inhibitors, benzaldehydes were explored. A series of benzaldehyde structural analogues inhibited the tyrosinase-catalyzed oxidation of L-3,4-dihydroxyphenylalanine (L-DOPA) and a few suppressed melanogenesis activity. The mechanism behind tyrosinase suppression has not been well understood. In cell free experiments, it is likely that the aldehyde group forms a Schiff base with the primary amino acid group on the enzyme. The hydroxyl and methoxy groups then contribute by stabilizing a newly formed complex that suppresses the enzyme. To better understand the mechanisms behind this activity the structurally similar compound isovanillin (3-hydroxy-4-methoxybenzaldehyde) was explored. Possible inhibition mechanisms are discussed.

The final class of phytochemicals explored for their enzyme inhibition mechanisms were tannins. The hydrolysable tannin gallic acid has been reported as a tyrosinase inhibitor but the mechanism has not been clearly understood. Enzymatic assays found that gallic acid inhibited the oxidation of L-3,4-dihydroxyphenylalanine (L-DOPA) catalyzed by mushroom tyrosinase but the tannin was not oxidized when mixed with the enzyme. The available oxygen in the reaction mixture was used for the oxidation of gallic acid and L-DOPA. The enzymatically

generated intermediates produced complex mixtures, and thus gallic acid suppressed the initial rate of pigmented product formation. Gallic acid was oxidized by a redox reaction to the corresponding *o*-quinone. Thus, the enzymatically oxidized tannins and dopaquinone oxidized gallic acid as redox-cyclers. This redox reaction generated *o*-quinones condensing with one another through a Michael type addition, yielding a relatively stable dibenzotropolone intermediate, purpurogallincarboxylic acid. The two major tannins were also found to exhibit cytotoxicity against murine B16-F10 melanoma cells but not significantly suppress melanin production.

Chapter 1

General Introduction

Melanin is a biopolymer which is crucial to the health and longevity of most plant and animal species(Solomon and others 1996). Specifically, melanin is responsible for ultraviolet (UV) protection acting as a free radical scavenger and as a radiation sink preventing damage to DNA, proteins and other critical cellular components(Kollias and others 1991; Riley 1997).

In mammals and insects, melanin is also responsible for pigmentation, which contributes to reproductive ability through mate attraction, functions in camouflage, mimicry and social communication (Sugumaran 2002; Stoehr 2006; Roulin 2014; Drury and others 2015; Galvan and Alonso-Alvarez 2009).In insects, melanin acts as part of the immune system response (Marmaras 1996) by physically encapsulating invasive pathogens. As a result, inhibiting melanin production offers an attractive approach to create effective insecticides. Melanin is also formed as a byproduct of decay in fruits and vegetables, resulting in a characteristic browning (Kim and Uyama 2005); controlling melanin formation presents opportunities in food sciences. The unregulated production of melanin in humans characterizes melanoma skin cancer (Valentini 2007). Consequently, regulating melanin formation is of significant interest for medical application.

Plant natural products have been demonstrated a successful melanin formation inhibitors(Kubo and others 2003; Kubo and Kinst-Hori 1999; Satooka and Kubo 2011)and are particularly attractive because to their short environmental persistence and often weakly (or non) toxic nature compared to synthetic chemicals(Surh 2003; Batish and others 2008; Rajendran and Sriranjini 2008; George and others 2014). Plant natural products structural and chemical diversity are at the core of their activity as melanin formation inhibitors.

Applications of Melanogenesis inhibitors

Melanin plays many important and vital roles in organisms, yet, melanin synthesis can be disrupted leading to diseases such as melanoma skin cancer and melasma (brown spotting)(D'Orazio and others 2013; Lee and others 2015). Melanoma incidence has increased during the past few decades and is a source of growing and sustained health concern in the United States (Lomas and others 2012). The most frequent treatment for melanoma is to physically remove the tumor (resection); melanoma occurs at the melanocytes, located within the epidermis, making direct topical treatments possible also. However, melanoma cells often metastasize, leading to tumors in other tissues (Brozyna and others 2013) and requiring the patient to undergo chemotherapy or radiation treatments. Melanoma has a low response rate to chemotherapy despite intense research(Hamid and others 2013),making the identification of melanoma-specific drugs even more crucial. Discovering new melanin formation inhibitors and understanding their activity mechanisms is instrumental to developing effective treatments related to melanin disorders. Further, chemotherapy patients often experience negative side effects such as hair loss or immune suppression due to the general cytotoxicity of treatments

towards healthy cells/tissue (Conklin 2000), which may be relieved by identifying compounds which specifically target melanin producing cells.

Melanogenesis inhibitors also have applications in food preservation. Fresh fruits and vegetables contain the enzyme polyphenol oxidase - which initiates the melanin formation pathway in plants - in their epidermis. Damaging the epidermis by cutting or friction exposes the enzyme to oxygen, enabling the melanin formation process and generating browning, characteristic of decay. Preventing or delaying the enzymes ability to catalyze this reaction would prolong the shelf life and preserve the visible quality of the product. Another area that melanin inhibitors have potential application is pest insect control. As noted above, melanin play a crucial role in insect immune response, UV protection, and coloration, but also contributes towound healing, and scleratization of the insect cuticle; suppressing melanin production would be detrimental to insect health and thus presents opportunities for insect control agents (Sansinenea and others 2015).For example, topical application of a melanin formation inhibitor may result in the insect cuticle not hardening. Specifically, cuticular proteins would not be oxidized by catechols, (*N*-acylcatecholamines oxidation is prevented by inhibitors)(Suderman and others 2010) preventing cross-linking that forms oligomers and subsequently polymers. This would leave the larva susceptible to UV-damage and/or exposure to fungi, bacteria from the surrounding environment.

Natural Products

Natural products are compounds produced by bacteria, archea, fungi, animals and plants and are classified into primary and secondary metabolites (Rao and Ravishankar 2002). Primary metabolites are essential to the function of the organism and include, for example, amino acids. Secondary metabolites also play a crucial role relating to an organism' fecundity, defense, immune response and communication (pheromones), but are not essential for organism survival. The wide range of applications for secondary metabolites in organism functionality motivates the development of a broad range of structurally and chemically diverse organic compounds. As described by (Harborne 1998), there are three major classes of secondary metabolites, alkaloids, phenols and terpenoids.

In my work, I focus on small (<600 Da) plant derived secondary metabolites, termed phytochemicals, to inhibit melanin formation. Plant derived secondary metabolites have a long (prehistoric) history of use by humans for medical treatments. Examples of successful medicinal treatments using phytochemicals include salicylates from the willow tree (*Salix alba* L) which are used to treat pain and inflammation, alkaloids from the seeds of the poppy *Papaversomniferum* which is the precursor to morphine, and quinine, derived from (*Cinchona succirubra* Pav. ex Klotsch) and is an FDA approved treatment for malaria(Dias and others 2012). Plants, which have historically been demonstrated as being non-toxic and medicinally beneficial, are often the basis for modern medicine. For example, over the past 70 years about 48% of the small molecules used for cancer drug treatments are either natural products or directly derived from their structures (Newman and Cragg 2012). Based on this past success it is likely that other uninvestigated natural products could have potential as cancer therapies.

In addition to medicinal treatments, phytochemicals contribute to generally improved health. For example, a diet that includes green teas, fruit and chocolate can suppress inflammation, improve cardiac health and immunity (Dixon and Sumner 2003). These health benefits are the result of the anti-oxidant properties that are induced by phytochemicals found in these foods (Pandey and Rizvi 2009).

Although many drug relevant phytochemicals have been discovered and applied within modern medicine, many plants (or their compounds) have not yet been investigated for their medicinal properties. Continued investigations into the activity of phytochemicals present great potential for new compound discovery and can be the basis for novel applications in existing and emerging fields.

Melanin

Chemistry of Melanin Formation

Broadly, melanin is a biopolymer formed from the oxidized quinones generated from oxidized L-DOPA. The melanin formation pathway was established by (Pugh and Raper 1927), and is termed melanogenesis (Figure 1).The enzyme tyrosinase catalyzes two steps during melanogenesis. In the first of these steps, the mono-phenol L-tyrosine is ortho-hydroxylated to form an ortho-diphenol, L-DOPA(L-3,4 dihydroxyphenylalanine)(Equation **a**). In the second step, L-DOPA is oxidized to form the ortho-quinone dopaquinone (Equation **b**). These steps each consume molecular oxygen from the solution. Then through non-enzymatic processes, dopaquinone is quickly cyclized via a 1,4 addition to form leucodopachrome, then through a oxidation-reduction exchange forms dopachrome. Dopachrome is slowly oxidized further to 5,6-dihydroxyindoles and 5,6-dihydroxyindole-2-carboxylic acid (DHIs and DHICA)(Figure 1)(Kitajima and Moro-oka 1993). These compounds then polymerize to form melanin.

(a)

(b)

The first step of the melanin formation pathway is the hydroxylation of L-tyrosine at the ortho-position , catalyzed by tyrosinase, to form L-DOPA. This step occurs slowly since only a small fraction (≈15%) (Chang 2009) of the resting conformation of tyrosinase can catalyze this reaction. As a result, this is the rate-limiting step in the melanin formation pathway (Sarangarajan and Apte 2006), resulting in a delay in activity or a 'lag period'. The self-resultant lag-period is unique to tyrosinase (Ramsden and Riley 2014). The polymerized melanin forms two different types of pigment found in both animals and plants: (1) eumelanins (black/brown) or (2) pheomelanin (yellow/reddish). Eumelanin is the more common of the two

types and is made up of indole monomers (5,6-dihydroxyindoles and 5,6-dihydroxyindole-2-carboxylic acid, abbreviated as DHI and DHICA, respectively)(Meredith and Sarna 2006). Pheomelanin is less common and is composed of benzothiazine (benzene rings with thiolmoites) backbone (Ito and Wakamatsu 2008).

Melanin Formation in Plants and Animals

In mammals, melanogenesis occurs in melanocytes, which are specialized collections of tissues and ligands at the base of the epidermal layer in skin(Lin and Fisher 2007). Within melanocytes there are specialized organelles called melanosomes that produce and store melanin. Melanosomes are derived from the endosomal system, a network of membrane transport shuttles, which is derived from the Golgi complex. The key melanogenic enzymes are tyrosinase and TYRP1 and TRYP2, both transmembrane proteins, and are shuttled to the melanosomes (Wasmeier and others 2008). Once the enzymes arrive at the melanosomes they initiate melanin synthesis. After melanin is synthesized, the melanosomes is transported along microtubules and through motor proteins to the basal epidermal layer. This mechanism of transporting melanosomes helps the melanin polymer – which is insoluble in aqueous solutions – to be transferred to other cells in the organism such as keratinocytes, the dominant skin basal cell type or brain tissue (Cichorek and others 2013).

In lower vertebrates, including insects, melanin formation occurs in hemocytes, for example oenocytoids in lepidoptera (Gonzalez-Santoyo and Cordoba-Aguilar 2012).Oenocytoids contain cytoplasmic phenoloxidase (tyrosinase equivalent in invertebrate systems) precursors that play a role in melanization (Lavine and Strand 2002). In invertebrates, hemocytes are part of the immune response and are located in the circulating hemolymph (Gillespie and others 1997).For example, when foreign pathogens are detected circulating in the insect hemoplymph a complex signaling cascade sends hemocytes to surround the pathogen (Browne and others 2013). The collection of hemocytes secrete melanin and encapsulate the invasive body, preventing its further growth(Solano 2014). By identifying an effective melanogenesis inhibitor, these secretions may be suppressed, and result in the insect immune system being compromised significantly. This illustrates a key difference between melanin formation organelles in insects compared to mammals: pigment granule movement in response to extracellular stimuli in insects occurs on the order of minutes, compared to mammals, which take hours. Spiders (order *Araneae*) are one of the few types of organisms that do not produce melanin (Decker and others 2007).

Tyrosinase

Tyrosinase (EC 1.14.18.1) is a binuclear type III copper containing protein (Hatcher and others 2014). At the active site there are two copper ions, CuA and CuB, both coordinated by three nitrogen atoms from six histidine residues, to which a dioxygen is bound in a μ-η2:η2-

peroxodicopper(II) active coordination (Figure 1.2)(Mirica and others 2006). Tyrosinase has four structural conformations determined by the oxidation state of the two copper ions;Emet, Edeoxy, Eoxy and Edeact (Berreau and others 1999).Each of these states has different catalytic properties and residue coordination. The unique mono-oxygenase and oxidase activity is a result of the oxidation state of the enzyme active site. The purified enzyme is 85% Emet form and 15% Eoxy(Chang 2009). The Emet confirmation has a hydroxyl ion bound between the two copper ions (Cu^{2+}) and can oxidize diphenols. Recalling the melanin formation pathway (Figure 1), the Emet conformation catalyses the oxidation of L-DOPA into dopaquinone. Once the ortho-quinone is formed a water molecule is released and the enzyme confirmation transitions from Emet to Edeoxy. Once in the Edeoxy state, the copper ions are both reduced to Cu(I) and cannot bind with mono or diphenols. In the Edeoxy state, dissolved dioxygen from solution rapidly binds between the Cu ions, converting tyrosinase to the Eoxy state(Sarangarajan and Apte 2006)(Figure 1.3).

Eoxy is the primary active form of tyrosinase, $[Cu(II)_2 \cdot O_2]$, and can hydroxylate monophenols (such as L-tyrosine) into diphenols (such as L-DOPA) and oxidize diphenols into ortho-quinones (such as dopaquinone). The Eoxy confirmation can react with these substrates to follow three different pathways: binding with a catechol (diphenol, for example L-DOPA) Eoxy can be converted to (1) Edeact (Cu(0) and Cu(II)) or (2) Emet; reacting with a diphenol (L-DOPA), (3) Eoxy is converted to Edeoxy (Figure 1.3). The Edeact confirmation is unable to catalyze any further reactions in the melanin formation pathway, and is thus considered inactive. The rate of conversion from Eoxy to Edeact is dependent only on the enzyme concentration (independent of the bound or soluble or product concentration) and does not require oxygen (Ramsden and Riley 2014). The conversion to Emet enables further reaction along the melanin formation pathway. Specifically, the Eoxy conformation converts L-tyrosine to L-DOPA, then the resultant L-DOPA reacts with Emet to form dopaquinone and Edeoxy. In the last case, Eoxy binds with a monophenol releasing a diphenol and converting (oxidizing) to the Edeoxy form. The Edeoxy confirmation cannot bind with either substrate, but unlike Edeact, Edeoxy can absorb dioxygen from solution to be converted back to the active Eoxy confirmation (Figure 1.4).

Other type III copper proteins that also contain this same oxygen binding peroxide bridge(Solomon and others 2001) are catechol oxidase, phenol oxidase (insect derived tyrosinase), polyphenol oxidase (plant derived tyrosinase) all of which share the same EC number as tyrosinase. Mushroom derived tyrosinase is commercially available and is often used as a model system for plant or insect derived tyrosinase. Commercially available tyrosinase is extracted from the *Agaricus bisporus*, the common button mushroom. *Agaricusbisporus* derived tyrosinase is a tetrameter that is composed of two heavy chains that are 43 kDa each and a two lighter 14 kDa for a total of 114 kDa. The structure of *A. bisporus* tyrosinase has been identified by X-ray crystallography for one of the enzymes four conformations (Ismaya and others 2011). This work mapped out the structure of the active site, the driver of enzyme activity, specifically the di-copper ion complex and the placement of amino acid residues surrounding the active site. This active site is located inside a hydrophobic binding pocket (Nithitanakool and others 2009). Mushroom derived tyrosinase is unique among the above listed similar compounds in that the active site is not sterically blocked when it binds dioxygen in a peroxide structure (Rolff and others 2011).

Objectives

In my dissertation, I investigate plant derived natural products and structurally similar compounds, as potential melanin formation inhibitors. My approach focuses on interrupting the melanin formation pathway by inhibiting the enzyme tyrosinase. This enzyme is responsible for catalyzing two reactions within the melanin formation pathway (termed melanogenesis). Inhibiting the enzyme tyrosinase thus presents an attractive approach to disrupt melanin formation.

In chapter 2, I identify two aliphatic aldehydes extracted from Vietnamese coriander as effective inhibitors. In this work, the role of the aliphatic side chain length was of interest. In chapter 3, I identify anisaldehyde, extracted from cashew oil, but also found in the Vietnamese coriander, as a strong inhibitor. This compound has an aldehyde head group, similar to the aliphatic compounds in chapter 2, but also an aromatic tail. I investigate the role of the chemical moieties on the aromatic ring in determining the inhibitory efficacy. In chapter 4, I seek to identify the inhibitory qualities of phenols, which is one of the largest classes of plant derived compounds. This work builds on previous demonstrations and further promotes plant natural products as potential melanin formation inhibitors.

Figures

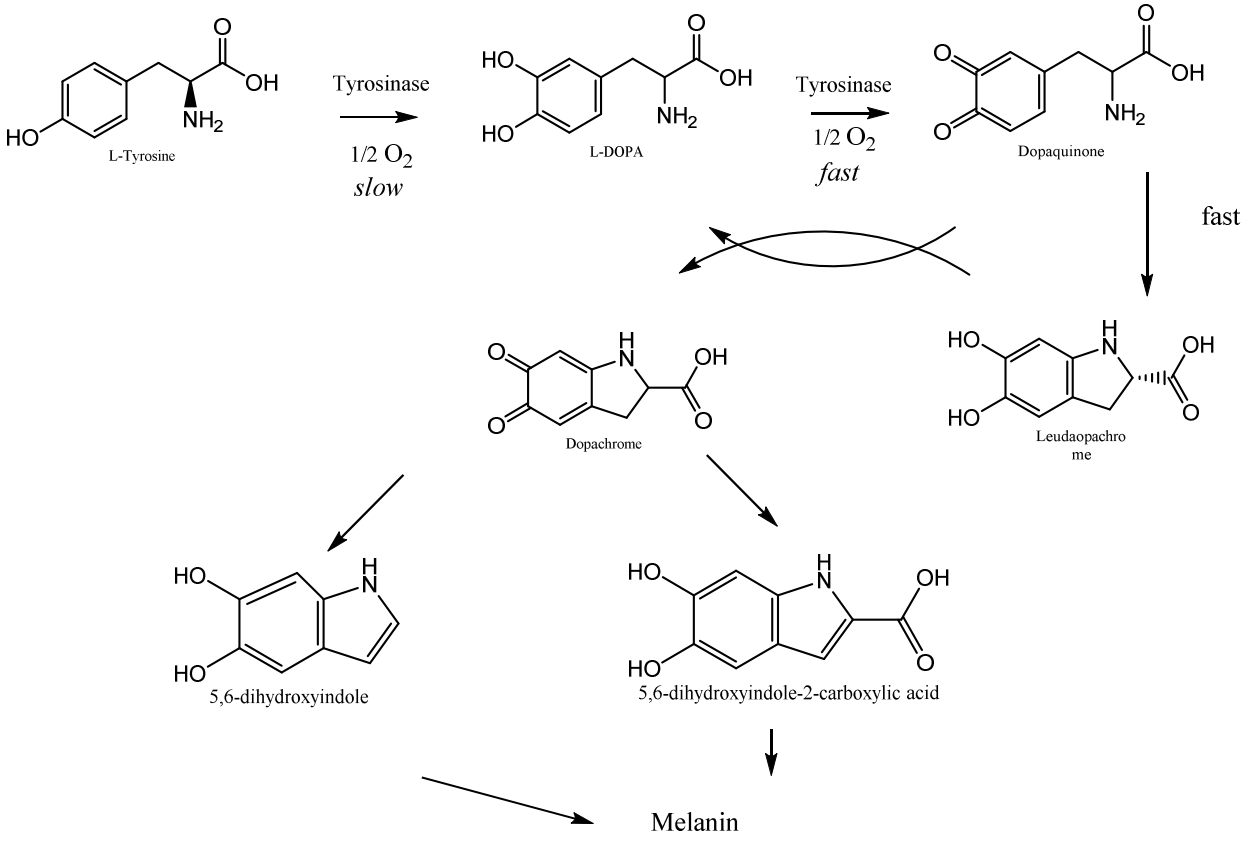

Figure 1.1 Melanin synthetic pathway

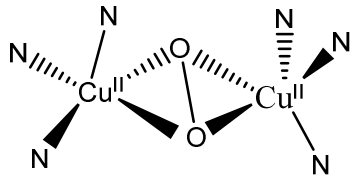

Figure 1.2 Structure of tyrosinase active site in μ-η2:η2-peroxodicopper(II) active coordination

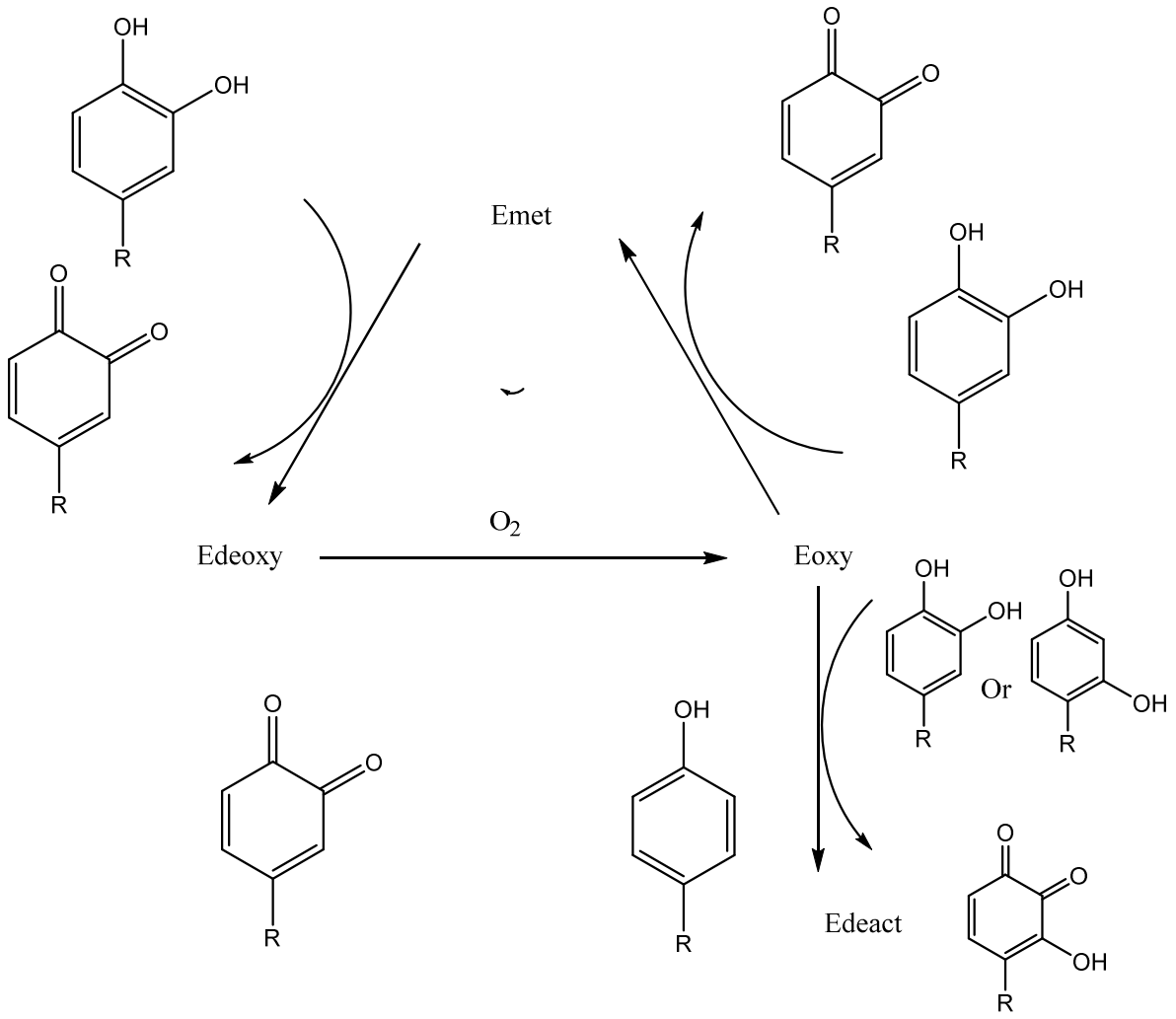

Figure 1.3 Different states of tyrosinase and conformational change of the enzyme

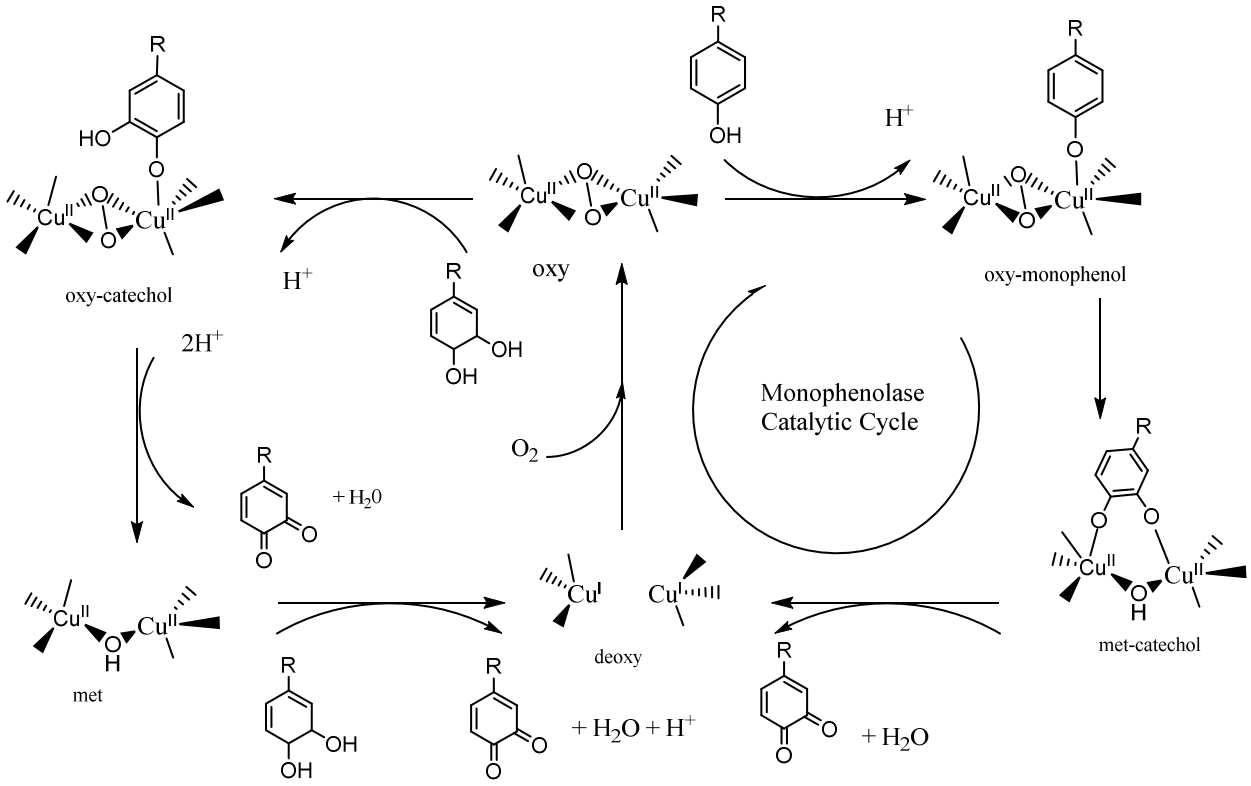

Figure 1.4 Catalytic cycles of tyrosinase. The right panel is the monophenol catalytic cycle

References

1. Batish DR, Singh HP, Kohli SK, Kaur S. 2008. Eucalyptus essential oil as a natural pesticide. For. Ecol. Manage. 256(12):2166-74.

2. Berreau LM, Mahapatra S, Halfen JA, Houser RP, Young VG, Tolman WB. 1999. Reactivity of peroxo- and bis(mu-oxo)dicopper complexes with catechols. Angewandte Chemie-International Edition 38(1-2):207-10.

3. Browne N, Heelan M, Kavanagh K. 2013. An analysis of the structural and functional similarities of insect hemocytes and mammalian phagocytes. Virulence 4(7):597-603.

4. Brozyna AA, Jozwicki W, Janjetovic Z, Slominski AT. 2013. Expression of the vitaimin D-activating enzyme 1 alpha-hydroxylase (CYP27B1) decreases during melanoma progression. Hum. Pathol. 44(3):374-87.

5. Chang T-S. 2009. An Updated Review of Tyrosinase Inhibitors. Int. J. Mol. Sci. 10(6).

6. Cichorek M, Wachulska M, Stasiewicz A, Tyminska A. 2013. Skin melanocytes: biology and development. Postepy Dermatologii I Alergologii 30(1):30-41.

7. Conklin KA. 2000. Dietary antioxidants during cancer chemotherapy: Impact on chemotherapeutic effectiveness and development of side effects. Nutrition and Cancer-an International Journal 37(1):1-18.

8. D'Orazio J, Jarrett S, Amaro-Ortiz A, Scott T. 2013. UV Radiation and the Skin. Int. J. Mol. Sci. 14(6):12222-48.

9. Decker H, Hellmann N, Jaenicke E, Lieb B, Meissner U, Markl J. 2007. Minireview: Recent progress in hemocyanin research. Integr. Comp. Biol. 47(4):631-44.

10. Dias DA, Urban S, Roessner U. 2012. A Historical Overview of Natural Products in Drug Discovery. Metabolites 2(2):303-36.

11. Dixon RA, Sumner LW. 2003. Legume natural products: Understanding and manipulating complex pathways for human and animal health. Plant Physiology 131(3):878-85.

12. Drury JP, Anderson CN, Grether GF. 2015. Seasonal polyphenism in wing coloration affects species recognition in rubyspot damselflies (Hetaerina spp.). J. Evol. Biol. 28(8):1439-52.

13. Galvan I, Alonso-Alvarez C. 2009. The expression of melanin-based plumage is separately modulated by exogenous oxidative stress and a melanocortin. Proc. R. Soc. B-Biol. Sci. 276(1670):3089-97.

14. George DR, Finn RD, Graham KM, Sparagano OAE. 2014. Present and future potential of plant-derived products to control arthropods of veterinary and medical significance. Parasites Vectors 7:12.

15. Gillespie JP, Kanost MR, Trenczek T. 1997. Biological mediators of insect immunity. Annu. Rev. Entomol. 42:611-43.

16. Gonzalez-Santoyo I, Cordoba-Aguilar A. 2012. Phenoloxidase: a key component of the insect immune system. Entomologia Experimentalis Et Applicata 142(1):1-16.

17. Hamid O, Robert C, Daud A, Hodi FS, Hwu WJ, Kefford R, Wolchok JD, Hersey P, Joseph RW, Weber JS, Dronca R, Gangadhar TC, Patnaik A, Zarour H, Joshua AM, Gergich K, Elassaiss-Schaap J, Algazi A, Mateus C, Boasberg P, Tumeh PC, Chmielowski B, Ebbinghaus SW, Li XN, Kang SP, Ribas A. 2013. Safety and Tumor Responses with Lambrolizumab (Anti-PD-1) in Melanoma. N. Engl. J. Med. 369(2):134-44.

18. Harborne AJ. 1998. Phytochemical Methods A Guide to Modern Techniques of Plant Analysis, 3rd ed: Chapman and Hill.

19. Ismaya WT, Rozeboom HJ, Weijn A, Mes JJ, Fusetti F, Wichers HJ, Dijkstra BW. 2011. Crystal Structure of Agaricus bisporus Mushroom Tyrosinase: Identity of the Tetramer Subunits and Interaction with Tropolone. Biochemistry 50(24):5477-86.

20. Ito S, Wakamatsu K. 2008. Chemistry of mixed melanogenesis - Pivotal roles of dopaquinone. Photochem. Photobiol. 84(3):582-92.

21. Kim YJ, Uyama H. 2005. Tyrosinase inhibitors from natural and synthetic sources: structure, inhibition mechanism and perspective for the future. Cell. Mol. Life Sci. 62(15):1707-23.

22. Kitajima N, Moro-oka Y. 1993. Dalton perspectives. [small micro]-[small eta]2:[small eta]2-Peroxide in biological systems. Journal of the Chemical Society, Dalton Transactions (18):2665-71.

23. Kollias N, Sayre RM, Zeise L, Chedekel MR. 1991. Photoprotection by melanin. J. Photochem. Photobiol. B-Biol. 9(2):135-60.

24. Kubo I, Chen QX, Nihei K, Calderon JS, Cespedes CL. 2003. Tyrosinase inhibition kinetics of anisic acid. Zeitschrift Fur Naturforschung Section C-a Journal of Biosciences 58(9-10):713-8.

25. Kubo I, Kinst-Hori I. 1999. 2-hydroxy-4-methoxybenzaldehyde: A potent tyrosinase inhibitor from African medicinal plants. Planta Medica 65(1):19-22.

26. Lavine MD, Strand MR. 2002. Insect hemocytes and their role in immunity. Insect Biochemistry and Molecular Biology 32(10):1295-309.

27. Lee HS, Goh MJ, Kim J, Choi TJ, Lee HK, Na YJ, Cho KH. 2015. A systems-biological study on the identification of safe and effective molecular targets for the reduction of ultraviolet B-induced skin pigmentation. Sci Rep 5:11.

28. Lin JY, Fisher DE. 2007. Melanocyte biology and skin pigmentation. Nature 445(7130):843-50.

29. Lomas A, Leonardi-Bee J, Bath-Hextall F. 2012. A systematic review of worldwide incidence of nonmelanoma skin cancer. British Journal of Dermatology 166(5):1069-80.

30. Meredith P, Sarna T. 2006. The physical and chemical properties of eumelanin. Pigment Cell Research 19(6):572-94.

31. Mirica LM, Rudd DJ, Vance MA, Solomon EI, Hodgson KO, Hedman B, Stack TDP. 2006. mu-eta(2):eta(2)-Peroxodicopper(II) complex with a secondary diamine ligand: A functional model of tyrosinase. Journal of the American Chemical Society 128(8):2654-65.

32. Newman DJ, Cragg GM. 2012. Natural Products As Sources of New Drugs over the 30 Years from 1981 to 2010. Journal of Natural Products 75(3):311-35.

33. Nithitanakool S, Pithayanukul P, Bavovada R, Saparpakorn P. 2009. Molecular Docking Studies and Anti-Tyrosinase Activity of Thai Mango Seed Kernel Extract. Molecules 14(1):257-65.

34. Pandey KB, Rizvi SI. 2009. Plant polyphenols as dietary antioxidants in human health and disease. Oxidative Medicine and Cellular Longevity 2(5):270-8.

35. Pugh CEM, Raper HS. 1927. The action of tyrosinase on phenols. With some observations on the classification of oxidases. Biochemical Journal 21(6):1370-83.

36. Rajendran S, Sriranjini V. 2008. Plant products as fumigants for stored-product insect control. Journal of Stored Products Research 44(2):126-35.

37. Ramsden CA, Riley PA. 2014. Tyrosinase: The four oxidation states of the active site and their relevance to enzymatic activation, oxidation and inactivation. Bioorganic & Medicinal Chemistry 22(8):2388-95.

38. Rao SR, Ravishankar GA. 2002. Plant cell cultures: Chemical factories of secondary metabolites. Biotechnol. Adv. 20(2):101-53.

39. Riley PA. 1997. Melanin. International Journal of Biochemistry & Cell Biology 29(11):1235-9.

40. Rolff M, Schottenheim J, Decker H, Tuczek F. 2011. Copper-O-2 reactivity of tyrosinase models towards external monophenolic substrates: molecular mechanism and comparison with the enzyme. Chemical Society Reviews 40(7):4077-98.

41. Roulin A. 2014. Melanin-based colour polymorphism responding to climate change. Glob. Change Biol. 20(11):3344-50.

42. Sansinenea E, Salazar F, Ramirez M, Ortiz A. 2015. An Ultra-Violet Tolerant Wild-Type Strain of Melanin-Producing Bacillus thuringiensis. Jundishapur J. Microbiol. 8(7):6.

43. Sarangarajan R, Apte SP. 2006. The polymerization of melanin: a poorly understood phenomenon with egregious biological implications. Melanoma Res. 16(1):3-10.

44. Satooka H, Kubo I. 2011. Effects of Thymol on Mushroom Tyrosinase-Catalyzed Melanin Formation. Journal of Agricultural and Food Chemistry 59(16):8908-14.

45. Solano F. 2014. Melanins: Skin Pigments and Much More—Types, Structural Models, Biological Functions, and Formation Routes. New Journal of Science 2014:28.

46. Solomon EI, Chen P, Metz M, Lee SK, Palmer AE. 2001. Oxygen binding, activation, and reduction to water by copper proteins. Angewandte Chemie-International Edition 40(24):4570-90.

47. Solomon EI, Sundaram UM, Machonkin TE. 1996. Multicopper oxidases and oxygenases. Chemical Reviews 96(7):2563-605.

48. Stoehr AM. 2006. Costly melanin ornaments: the importance of taxon? Funct. Ecol. 20(2):276-81.

49. Suderman RJ, Dittmer NT, Kramer KJ, Kanost MR. 2010. Model reactions for insect cuticle sclerotization: Participation of amino groups in the cross-linking of Manduca sexta cuticle protein MsCP36. Insect Biochemistry and Molecular Biology 40(3):252-8.

50. Sugumaran H. 2002. Comparative biochemistry of eumelanogenesis and the protective roles of phenoloxidase and melanin in insects. Pigment Cell Research 15(1):2-9.

51. Surh YJ. 2003. Cancer chemoprevention with dietary phytochemicals. Nat. Rev. Cancer 3(10):768-80.

52. Wasmeier C, Hume AN, Bolasco G, Seabra MC. 2008. Melanosomes at a glance. Journal of Cell Science 121(24):3995-9.

Chapter 2

Effects of aliphatic aldehydes on tyrosinase and melanoma cells

Introduction

Plant natural products have been the focus of long-term research due to their applications to food and medical technologies, and consumer products, including cosmetics (Rastogi 2001; Cai and others 2004; Soto and others 2015). Essential oil plant extracts have been at the core of this research and have found success as inhibitors of enzyme activity (Sharma and others 2007). For example, extracts from *Mandia whitei* have been demonstrated as melanogenesis inhibitors (Kubo and Kinst-Hori 1999; Kim and Uyama 2005), making them attractive for medicinal therapies to treat diseases such as melanoma skin cancer. A challenge of this research is found in the wide variety and sources of plant natural products. Identification of effective inhibitors – especially those safe for human consumption – often relies on a scientific consideration of homeopathic medications and detailed observation of often overlooked details.

Vietnamese coriander (*Polygonum odoratum*) is a food spice used in south-east Asian countries including Vietnam, Thailand and Malaysia(Sakunpak and others 2015). *P. odoratum* is also used for homeopathic medicinal treatments for upset stomachs and has shown anti-inflammatory activity (Fujita and others 2015). What makes *P. odoratum* of interest as a melanogenisis inhibitor is the observation that its leaves do not brown once they have been exposed to air by e.g. breaking or crushing. Since browning in vegetables is due to melanin formation, this suggests biochemicals in *P. odoratum* are melanogenisis inhibitors, possibly by inhibiting the tyrosinase enzyme.

In this work, a steam distilled extract from *P. odoratum* was tested as a melanogenesis inhibitor. Gas chromatography-mass spectroscopy (GC-MS) of the extract (Table 2.1), termed kesom oil, revealed 73% of the compounds present were aldehydes, with the most prevalent compounds being dodecanal, decanal, and anisaldehyde. Dodecanal is commonly used in flavor and fragrance products due to its pungent soapy, citrus smell (Bayraktar and Onoğur 2011). Decanal has a distinct citrus odor and is used in flavor and cosmetic products (Hunter, 1996).The third most abundant active compound, anisaldehyde, is an aromatic compound that is extensively used as a fragrance enhancer in soaps (Surburg and Panten 2010). It is noted that the third most abundant compound is pentacosane, which has no active group, and was not tested. Since these aldehydes are widely used in consumer products, their toxicity is acceptably low and they are expected to present few human health concerns (Tisserand and Young 2014). While anisaldehyde has been previously reported as a tyrosinase inhibitor (Ha and others 2005; Nitoda and others 2007), the were aliphatic aldehydes, decanal and dodecanal, have never been reported, to our knowledge, as a tyrosinase or melanogenesis inhibitor. Individual testing of these compounds using oxygen consumption assays and photo-spectroscopy identify them as effective inhibitors of the tyrosinase enzyme. Further investigations using fluorometry showed that the major aldehydes did interact at the enzyme active pocket in tyrosinase, confirming their potential as a melanogenesis inhibitor. The efficacy of these inhibitors is suggested to be related to the aldehyde head groups and side chain length. To investigate this, saturated and unsaturated analogues were tested with variable side chain length.

Results

Essential Oil

RT	Compounds	% content
30.16	Dodecanal	55.49
19.39	*n*-Decanal	11.57
65.8	Pentacosane	7.26
18.29	*p*-Anis aldehyde	6.35
33.58	*n*-Dodecanol	3.3
63.23	2*E*-Dodecenal	2.5
31.94	α-Humulene	2.41
39.42	Humulene epoxide II	1.51
24.85	Undecanal	1.31
23.26	*n*-Decanol	1.13
38.17	allo-Aromadendrene epoxide	1.08
65.45	2*E*-Tridecenal	1.07
37.73	Methyl vanillin	0.86
28.53	*n*-Undecanol	0.56
59.53	neoiso-Menthol	0.45
43.1	4-methylhexyl-2-methylbutyrate	0.43
42.53	β-Bisabolol	0.41
46.25	Drimenol	0.39
39.93	Tetradecanal	0.34
64.19	Triacontane	0.33
35.13	β-Panasinsene	0.33
13.66	*n*-Decane	0.26
11.48	3-Methyl-4-heptanone	0.05
52.14	Polygodial	0.01

Table 2.1 GC-MS determined composition of essential oil from *P.odoratum*

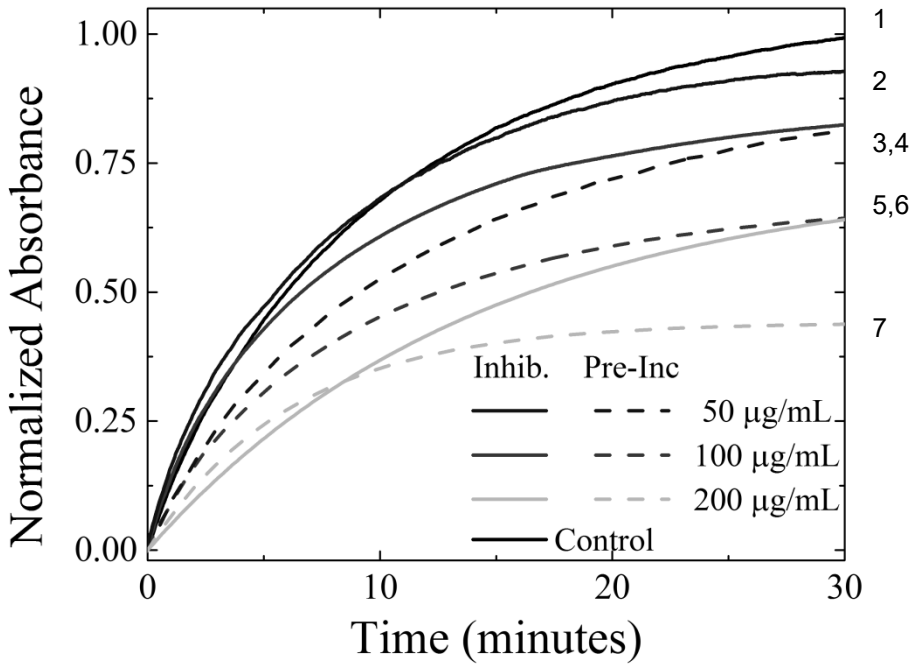

Figure 2.1 Normalized UV-Vis absorption of 250 µM of L-DOPA at 475 nm (1) of essential oil inhibition at 50 µg/mL (2) and 10 minute preincubated 50 µg/mL (3) , inhibition at 100 µg/mL (4) and preincubation for 10 minutes at 100 µg/mL (5), inhibition 200 µg/mL (6) and preincubation 200 µg/mL (7). Essential oil was screened prior to the GC-MS identification of the structural makeup so the concentrations were tested based on a weight per volume basis

Initial screening was performed on the essential oil (EO) using both UV-VIS absorption and dissolved oxygen assays as a preliminary screening to determine if it included inhibitory compounds. While the UV-VIS data monitors dopachrome formation, which at the core of our focus, oxygen consumption assays offer an alternative method to monitor the progression of the reaction, and is sensitive both to DOPA and tyrosine catalysis. Comparisons between the UV-VIS and oxygen consumption assays can also be used to elucidate the inhibitory mechanism. Inhibitory assays performed with the extracted essential oil, monitoring UV-VIS absorption, Fig. 1, and oxygen consumption, Fig. 2. For low concentrations (50 µg/mL), the UV-VIS absorption shows only a slight inhibition of 7%. Increasing the concentration to 100 µg/mL, and subsequently to 200 µg/mL, further suppressed dopachrome formation by 17% and 36%, respectively. Comparing these results to the preincubation assay (shown in dashed lines in Figure 2.1), the 10 minute preincubation period doubled inhibitory activity; for the 50 µg/mL, 100 µg/mL, and 200 µg/mL concentrations, dopachrome production is reduced by 19%, 36% and 56%, respectively.

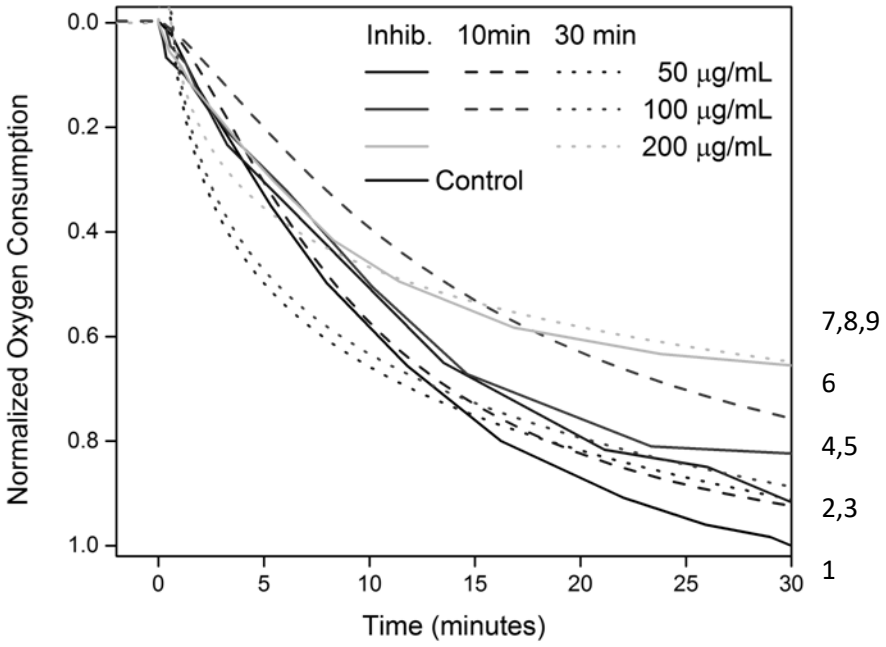

Figure 2.2 Oxygen consumption assay of the oxidation of 250 μM of L-DOPA (1) in the presence of essential oil inhibition at 50 μg/mL (2) 10 minute preincubated 50 μg/mL (3), and 30 minute preincubated 50 μg/mL (4), inhibition at 100 μg/mL (5), preincubation for 10 minutes at 100 μg/mL (6), preincubation for 30 minutes at 100 μg/ inhibition (7), 200 μg/mL (8)and preincubation 200 μg/mL (9)

Oxygen consumption assays were performed on the same solutions of essential oil (Figure 2.2) and show similar inhibitory activity as the UV-VIS data. For concentrations of 50 μg/mL, oxygen monitoring showed only slight inhibition, with a 9% reduction in oxygen consumption, relative to the control. Increasing the concentration to 100 μg/mL and 200 μg/mL,showed suppressed oxygen consumption and dopachrome formation by 18% and 36%, respectively.

A key difference between the UV-VIS and oxygen consumption data is observed when comparing the preincubation assays. While the UV-VIS data showed a doubling of the inhibitory efficacy with a 10-minute preincubation, the oxygen consumption showed only an incremental increase in the inhibitory activity. For concentrations of 50 μg/mL, 100 μg/mL, and 200 μg/mL, oxygen consumption was only further reduced by 2%, 3% and 1%, respectively.

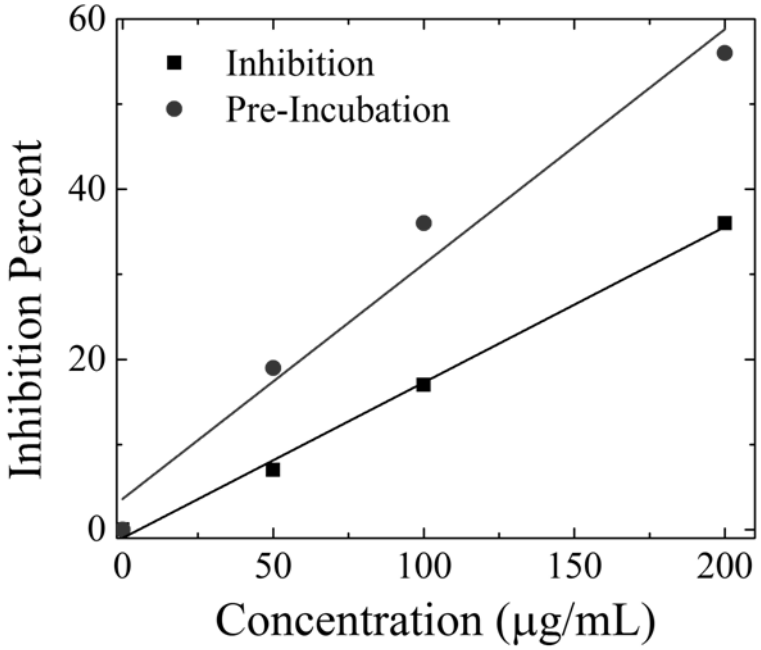

Figure 2.3 Inhibitory efficacy of essential oil as a function of concentration based on dopachrome formation, inhibition (closed square) and preincubation (closed circle)

The essential oil inhibition based on the UV-VIS datais plotted against concentration for both the inhibition and preincubation assays (Figure 2.3). The results show a clear linear relationship, suggesting a strong dose dependent inhibition for concentrations below 200 μg/mL.At this concentration the essential oil is below the saturation limit of inhibitory activity since we did not observe a leveling off of inhibition activity.

For comparison, we examined the natural substrate, L-tyrosine, which is a precursor to L-DOPA in the melanin formation pathway and also relies on tyrosinase to catalyze its hydroxylation. The essential oil showed weak inhibitory activity at a concentration of 50 μg/mL of 9%, in agreement with the L-DOPA values (data not shown). At 100 μg/mL the essential oil showed a 30% reduction of dopachrome formation compared to the control (Figure 2.4). This level of inhibition is much higher than the L-DOPA results, which showed approximately 17% inhibition. Following oxygen consumption at the identical concentration we observed only 1% increase in the consumption of oxygen. Preincubation experiments performed on100μg/mL L-tyrosine substrate for 10 minutes showed a 4% decrease compared to the control (data not shown).This suggests that on this substrate the inactivation of the enzyme occurs without consuming oxygen. This disqualifies K-cat type inhibition as a mechanism in this extract.

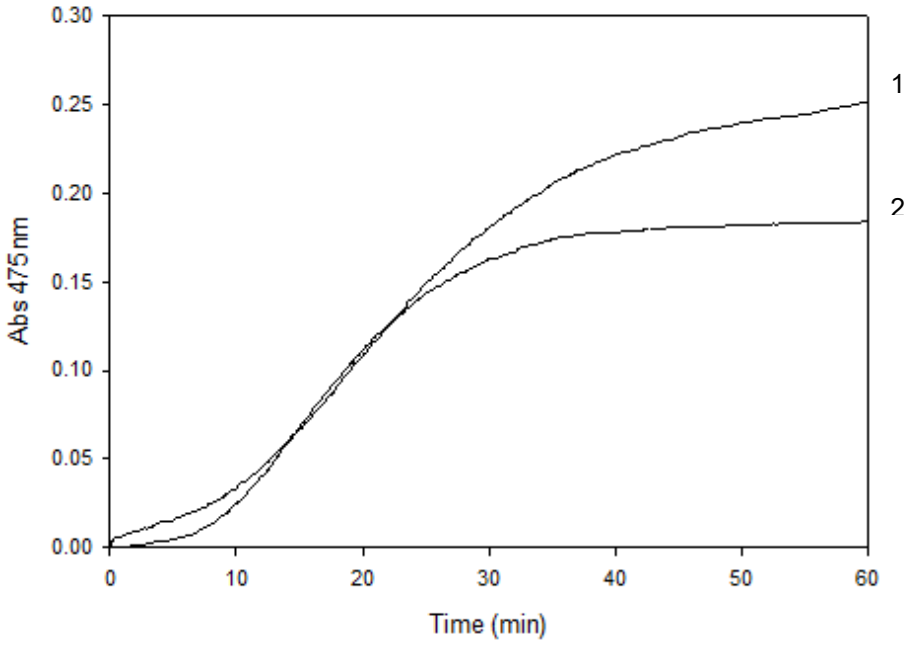

Figure 2.4 UV-Vis absorption of the oxidation of 500 μM of L-tyrosine (1) and 100 μg/mL (2) essential oil.

The activity of the essential oil at the enzyme active site was examined using fluorescence. Control measurements measured on tyrosinase and L-DOPA show that during the first 10 minutes the intensity is approximately constant. Then, after ≈10 minutes, the fluorescence signal increases. We attribute this lag in intensity to competition at the enzyme active pocket between the L-DOPA and the fluorescence probe (N-Phenyl-1-naphthylamine, abbreviated 1-NPN).

Introducing the essential oil, at the low concentration of 50 μg/mL fluorescence remained constant until 10 minutes then increased significantly, similar to the control. This is consistent with the EO interacting only with a small fraction of the enzymes in solution. For a higher concentration of 100 μg/mL there was a notable decrease in overall fluorescence after 30 minutes, suggesting that there was very strong EO binding at the active pocket (Table 2.2). This is consistent with the dose dependent model discussed earlier. Additionally the notable delay in fluorescence decrease was unique to the essential oil, likely a result of the various compounds interacting.

The inhibitory and preincubation assays suggest that within the essential oil there are compounds that bind, possibly in a time dependent manner, to the enzyme and inhibit its activity, thus motivating further investigations of the major compounds.

Time (min)	50 μg/mL	100 μg/mL	L-DOPA
0	100	100	100
3	105	132	95
10	300	105	80
30	200	50	125

Table 2.2 Percentage fluorescence of the essential oil of the oxidation of 500 μM of L-DOPA

Dodecanal

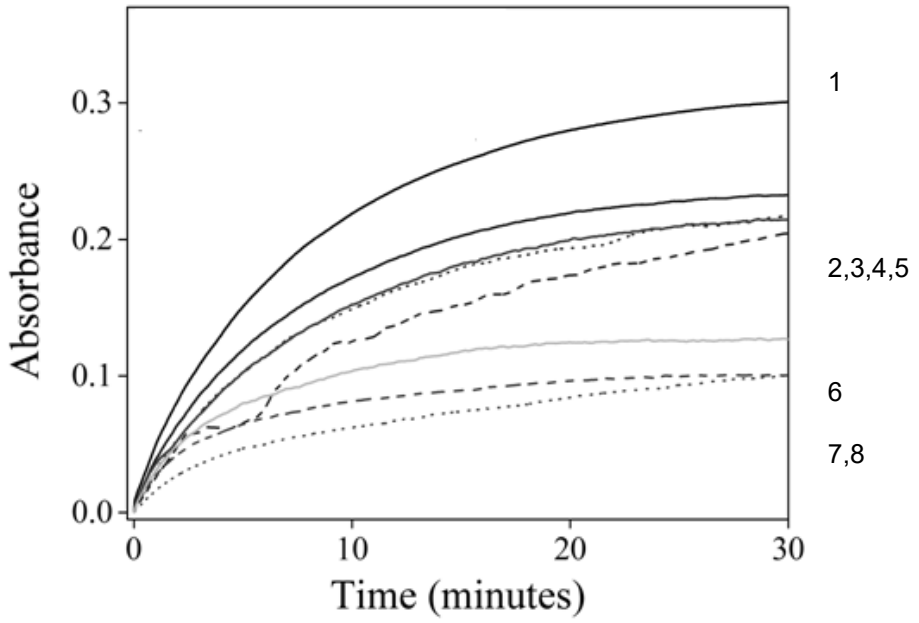

Figure 2.5.UV-Vis absorption of the oxidation of 250 μM of L-DOPA (1) at 475 nm in the presence of dodecanal at 250 μM (2), 500 μM (3), 250μM preincubated for 10 minutes (4) and 250 μM 20 minutes (5) and 1000 μM(6), 500 μM preincubated for 10 minutes (7) and 500μM 20 minutes (8)

Dodecanal is identified as the most abundant (55%, 304.9μM) compound in the essential oil (Table 2.1). Inhibition assays performed using dodecanal as an inhibitor on an L-DOPA substrate showed strong inhibitory properties based on the UV-VIS plots (Figure 2.5). At the lowest tested concentration of 250 μM dodecanal reduced enzyme activity by 23% after 30 minutes. When the concentration was increased to 500 μM a 30% reduction in dopachrome

formation occurred then subsequently a 57% reduction at 1 mM. Preincubaiton for 10 minutes showed increased inhibition activity at the higher concentrations; at 250μM the activity only slightly increased, to 30%, while at 500 μM a 67% reduction in dopachrome formation occurred. There does appear to be some recovery of enzyme activity with the longer preincubation assays suggesting some reversibility in the inhibitory mechanism.

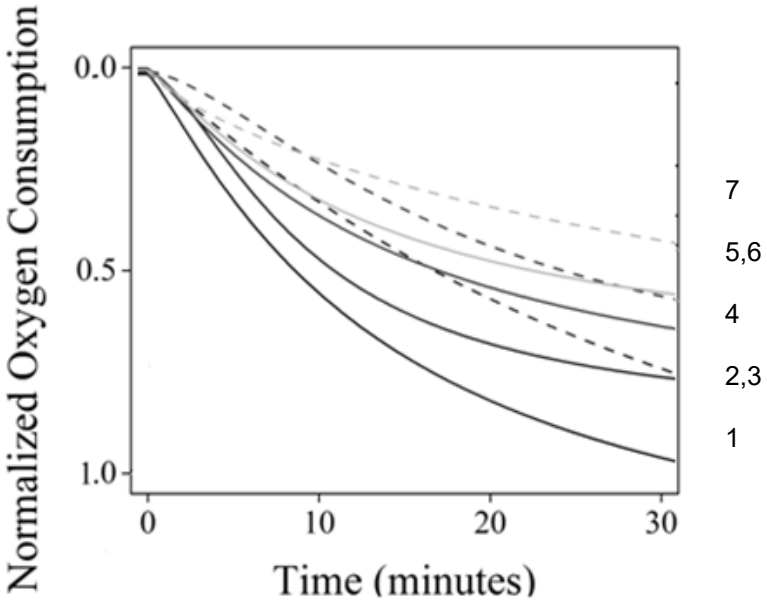

Figure 6. Oxygen consumption assay of the oxidation of 250 μM of L-DOPA (1) in the presence of dodecanal at 250 μM (2), 250 μM preincubated for 10 minutes (3), 500 μM(4), 500 μM preincubated (5) and 1000 μM (6), 1000 μM (6) preincubated for 10 minutes (7)

Oxygen consumption assays were also performed testing dodecanal and confirmed the inhibitory activity. Measurements performed on a L-DOPA substrate at 250 μM showed a 25% reduction in activity, at 500 μM a 36% reduction and at 1 mM a 43% reduction. A preincubation period of 10 minutes reduced oxygen consumption at higher concentrations (at 250 μM the inhibition was unchanged, remaining at 25%) at 500 μM there was an additional reduction of activity of 7% and at 1 mM an additional13% reduction (Figure 2.6). The preincubation curves show some recovery in enzyme activity (Fig. 6 dashed lines). This suggests that the inhibition mechanism may have a reversible component.

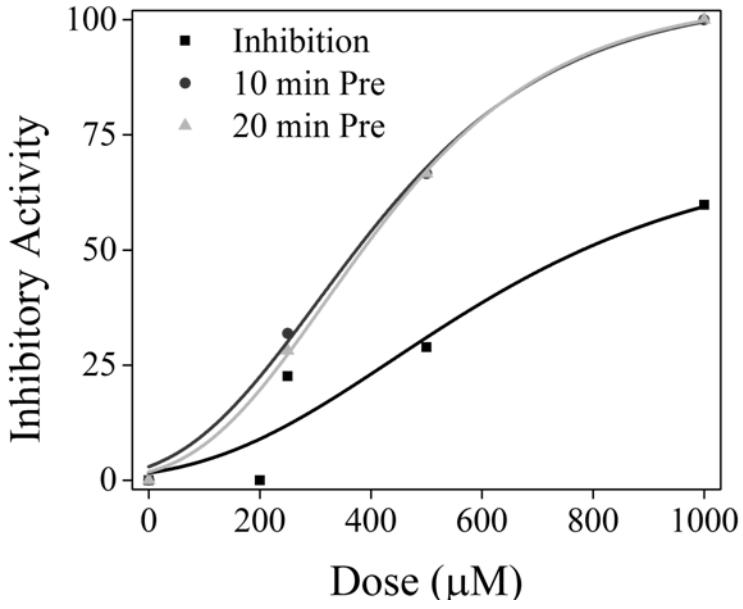

Figure 2.7. Inhibitory efficacy of dodecanal as a function of concentration based on dopachrome formation

The inhibitory activity of dodecanal on dopachrome formation is extracted from the UV-VIS data and plotted (Figure 2.7). These results show a sigmodial dose response, suggesting a critical concentration for inhibition. A preincubation period of 10 minutes increased the activity of dodecanal notably. However, the 10 minute and 20 minute preincubations show little difference, indicating that the inhibitory mechanism occurs on a time scale of 10 minutes.

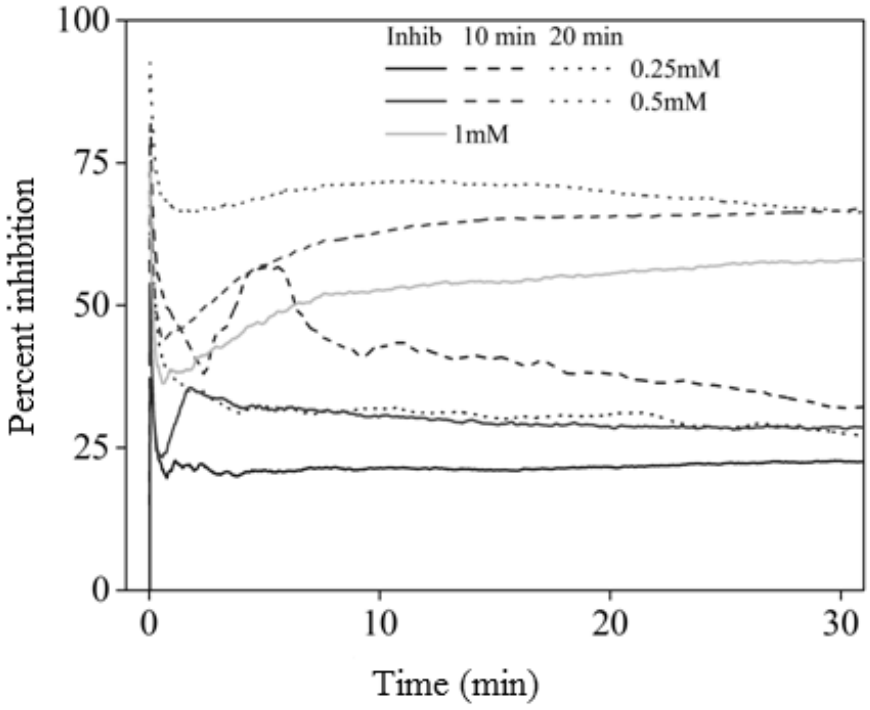

Figure 2.8. Percent inhibition oftyrosinase by dodecanal as a function of time, colors included for ease of distinction; 250 μM , 500 μM (and 1000 μM)

This time dependent inhibitory activity was investigated further by dividing the dopachrome formation curves by the control (Figure 2.8). These curves provide insight into the inhibitory mechanism. The inhibition and preincubation curves generated from the 250 μM solutions show little dependence, remaining constant at approximately 20% and 30%, respectively. This indicates that, at these concentrations, dodecanal interacts with tyrosinase mostly within the first minutes of the assay (quickly). In-contrast, the 500 μM solution has a strong time dependent inhibition, showing increasing inhibition for 3-4 minutes, and decreased time dependence, with increased preincubation time. Further, the 10 minutes and 20 minutes preincubation plots converge to the same inhibition efficacy after the 30 minute measurement. This suggests that at the higher concentrations we see slightly different mechanism of activity, the initial inhibitory interaction occurs on a time-scale of approximately 5-8 minutes but the inhibitory activity continues beyond 12 minutes.

The effect of dodecanal on the enzyme was further explored by HPLC (250 μM dodecanal, 100 μM L-DOPA substrate). For these measurements, the inhibitor, enzyme and substrate were combined, then every 10 minutes the solution was sampled and measured by HPLC. In the presence of the inhibitor, the L-DOPA peak area continue to decrease quickly throughout the assay compared to the control, corresponding to inhibitory activity (Figure 2.9).

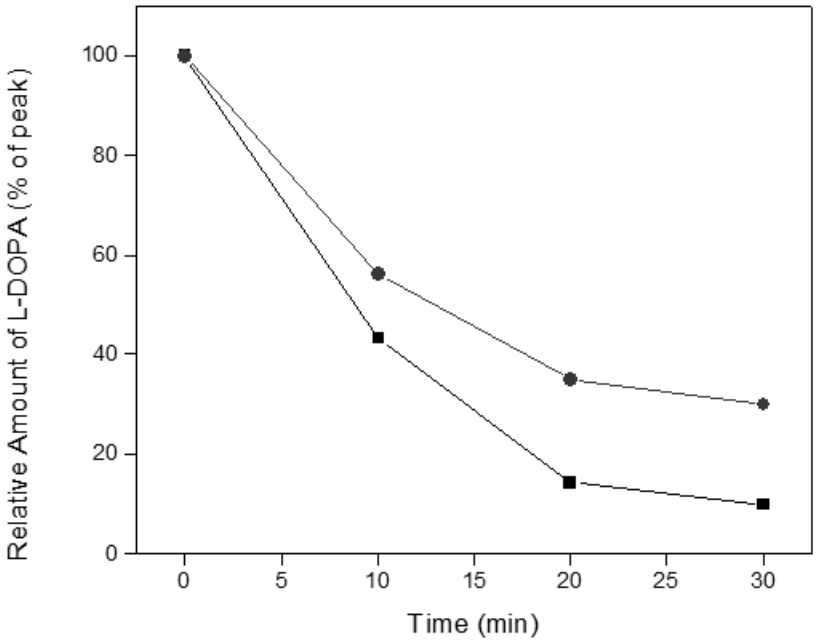

Figure 2.9 . HPLC analysis of L-DOPA (100 μM) oxidation by tyrosinase in absence (closed square) or presence (closed circle) of mixture of dodecanal (250 μM)

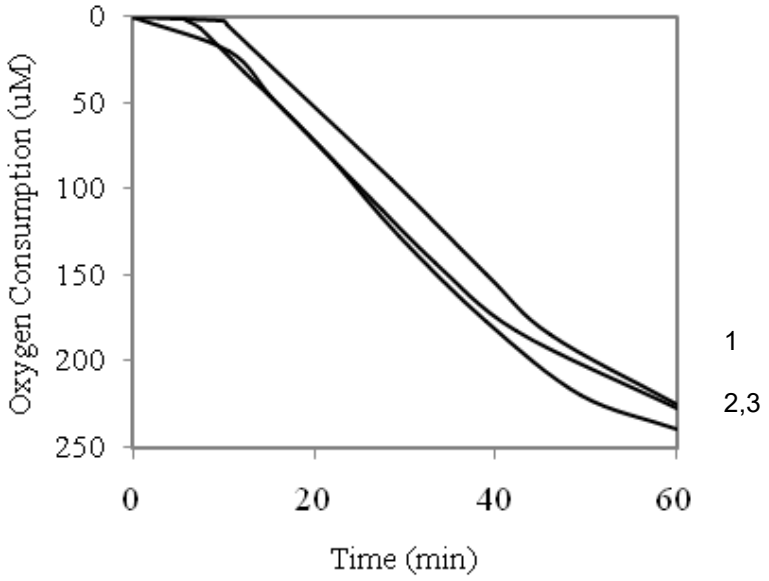

Figure 2.10. Oxygen consumption of dodecanal at 250 μM (2) and 500 μM (3)in the presence of 500 μM L-tyrosine (1)

We followed the inhibition reaction measuring dopachrome formation with L-tyrosine as the substrate and we observed activity at 2% inhibition at 200 μM dodecanal and suppressing activity 11% at 1mM after 60minutes.

Inhibition assays measured by oxygen consumption show a 2% *increase* in amount of oxygen being consumed (Figure 2.10) at 250 μM and 7% at 500 μM. Compared to the control, the lag phase was shortened in the presence of dodecanal. The decrease in the lag phase suggests that the dodecanal promotes the formation of L-DOPA, which then is rapidly catalyzed to dopaquinone, resulting in the apparent increase in oxygen consumption. One possible mechanism for this effect is that dodecanal promotes a change in the tyrosinase confirmation from Emet to Edeoxy. When dodecanal was preincubated with L-tyrosine there is a 17% decreased in oxygen consumption and an extended lag phase compared to the control after the 60 minute period (data not shown). This would suggest that dodecanal was interacting with Eoxy.

To specifically isolate the tyrosinase catalyzed steps, we use the substrate *N*-acetyl-L-tyrosine. In the melanin formation pathway, tyrosinasecatalyzes L-tyrosine to form L-DOPA, and subsequently dopaquinone, which then cyclizes to form leukodopachrome. Replacing the amine group in L-tyrosine with an acetyl group, forming *N*-acetyl-L-tyrosine, presents a new substrate which can still be hydroxylated and oxidized by tyrosinase to form *N*-acetyl-L-dopaquinone, but cannot cyclize further to *N*-acetyl-Leukodopachrome (Figure 2.11). This isolates the effect of the inhibitor on the tyrosinase-catalyzed reaction to dopaquinone. Inhibitory assays were performed using the HPLC peak area to monitor the concentration of *N*-acetyl-L-tyrosine (Figure 2.12). For a 250 μM dodecanal concentration, consumption of *N*-acetyl-L-tyrosine was reduced by 24% relative to the control after 60 minutes. This suggests the inhibitor acts slowly after 30 minutes and appears to be a monophenolase, inhibitor but cannot inhibit completely.

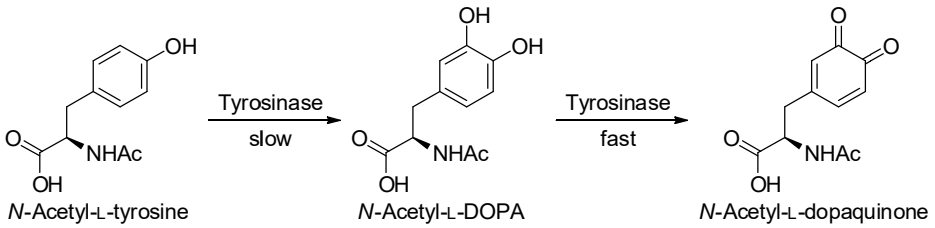

Figure 2.11 N-acetyl-l-tyrosine pathway

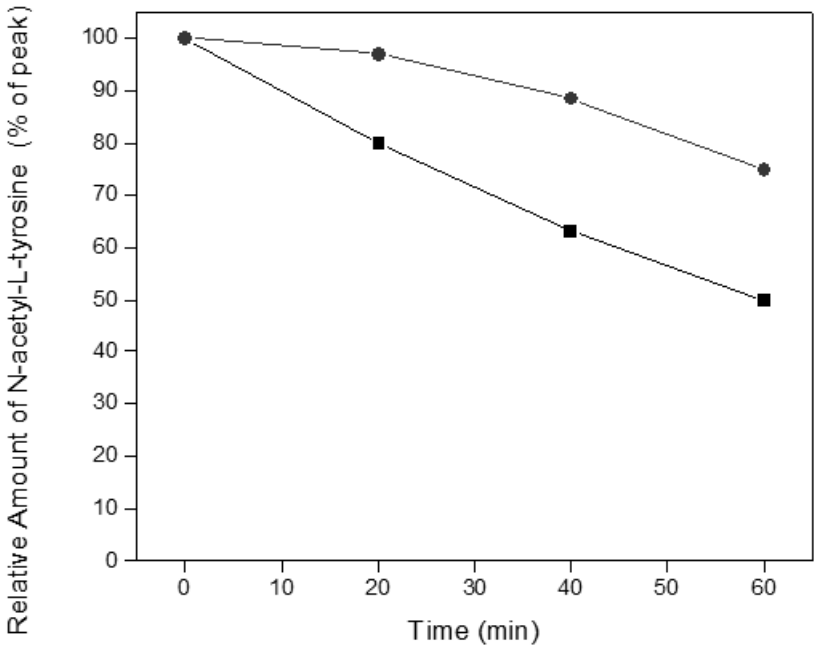

Figure 2.12. Relative HPLC peak area for 100 µM *N*-acetyl-L-tyrosine in the absence (open sqaure) or presence (closed circle) of 250 µM dodecanal and tyrosinase

The binding activity of dodecanal was investigated using fluorescence spectroscopy with an L-DOPA substrate. The fluorescence at low concentrations (50µM) was similar to the control, suggesting weak binding of dodecanal at the enzyme active site (Table 2.3). For higher concentration of 300 µM there is a significant (80%) decrease in fluorescence, suggesting that 1-NPN cannot access the active pocket likely due to dodecanal occupation.

Time (min)	50μM	300 μM	L-DOPA
0	100	100	100
10	140	60	95
20	80	50	80
35	100	20	125

Table 2.3 Percentage fluorescence of dodecanal of the oxidation of 500 μM of L-DOPA

Decanal

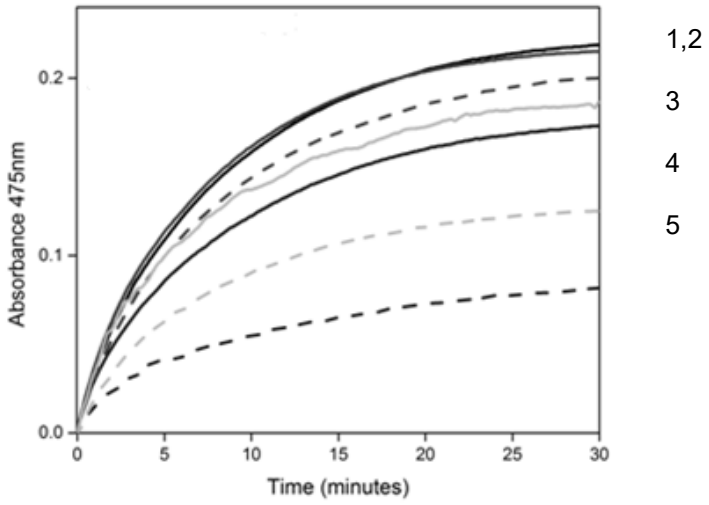

Figure 2.13 UV-Vis absorption of the oxidation of 250 μM of L-DOPA (1) at 475 nm in the presence of decanal at 125 μM (2), 125 μM preincubated for 10 minutes (3), 250 μM (4), 250 μM preincubated for 10 minutes (5), 500 μM (6) and500 μM preincubated for 10 minutes (7)

Decanal was the second most abundant compound (12%) at 74.17 μM in the essential oil. UV-VIS spectroscopy measured for test solutions with 125 μM of L-DOPA, in the presence of decanal and did not appreciably suppress dopachrome formation (Figure 2.13). Increasing the concentration of decanal to250 μM, 500 μM showed a 16% and 23% suppression in activity, respectively. Preincubation improved inhibition efficacy 10%, 44% and 64% for 125 μM, 250 μM and 500 μM. This suggests a time dependent inhibition mechanism.

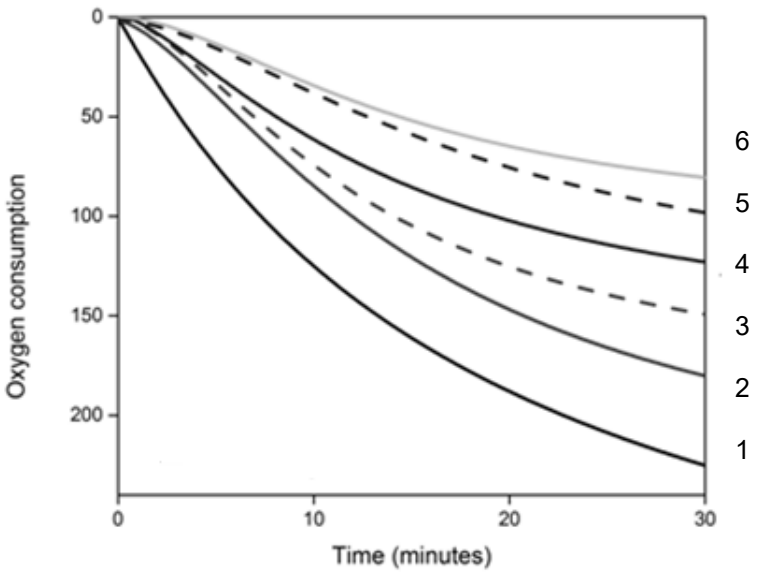

Figure 2.14. Oxygen consumption assays performed with the inhibitor decanal at 250 μM of decanal (2), 250 μM preincubated for 10 minutes (3), 500 μM (4), 500 μM preincubated for 10 minuttes (5)and suppression at 1 mM (6) on250 μM L-DOPA (1)

Oxygen consumption assays performed on a similar test solution show a 23% suppression of activity in inhibition measurements performed at 250 μM of decanal, 46% suppression at 500 μM, and 62% suppression at 1 mM. A 10 minute preincubation period increased the inhibitor activity of to 33% for 250 μM and 56% for 500 μM (Figure 2.14).

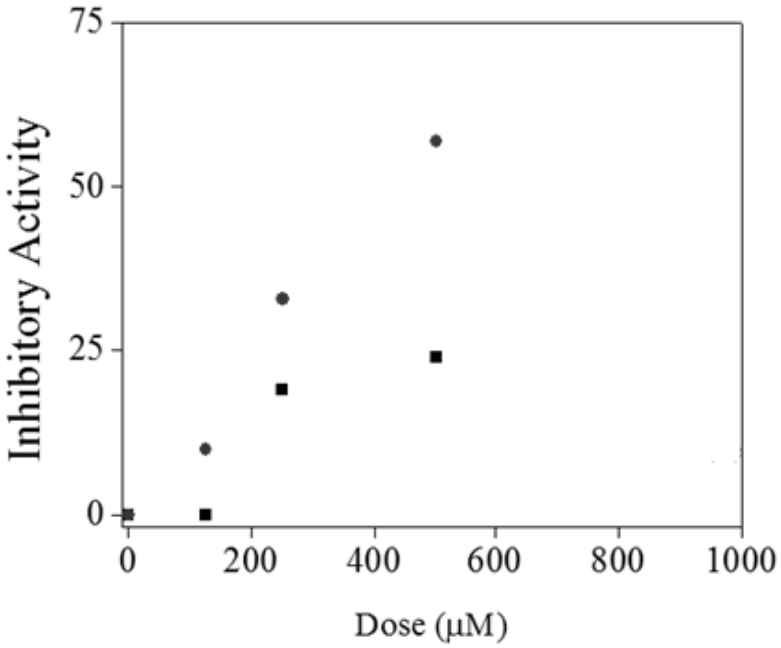

Figure 2.15 Dopachrome inhibition activity from L-DOPA, as a function of decanal concentration, incubation (closed square) and preincubation (closed circle)

The inhibitory activity of decanal was collated from the UV-VIS data (Figure 2.15) and shows a sigmodial dose response. A preincaubtion period of 10 minutes increased the inhibitory activity of decanal greatly, an additional 10 minutes of incubation did not improve activity. Comparing these results with dodecanal (Figure 2.7) shows that decanal is a less-effective inhibitor for inhibition assays and in the preincubation assays. These compounds are chemically similar with the side chain length being the only significant difference, suggesting their inhibitory efficacy is related to their chain length.

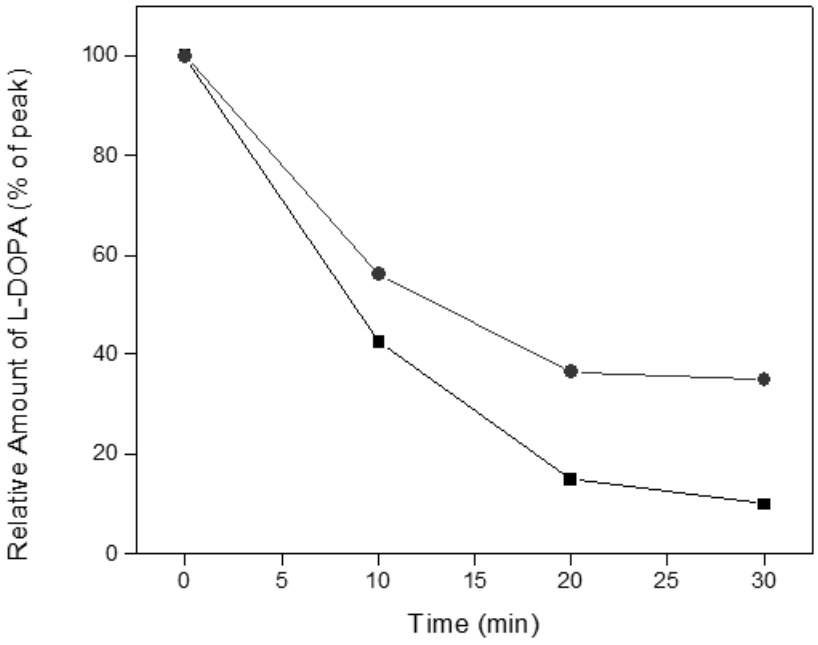

Figure 2.16. Peak area from HPLC of L-DOPA (100 μM) in the absence (closed square) or presence (closed square) of decanal (250μM) and tyrosinase

The inhibition activity of decanal on tyrosinase was explored by HPLC analysis based on the same test mixture. Similar to the dodecanal solution (Figure 2.9), the L-DOPA peak quickly decreased within the first 10 minutes of the reaction, and continued to decrease though out the 30 minutes.

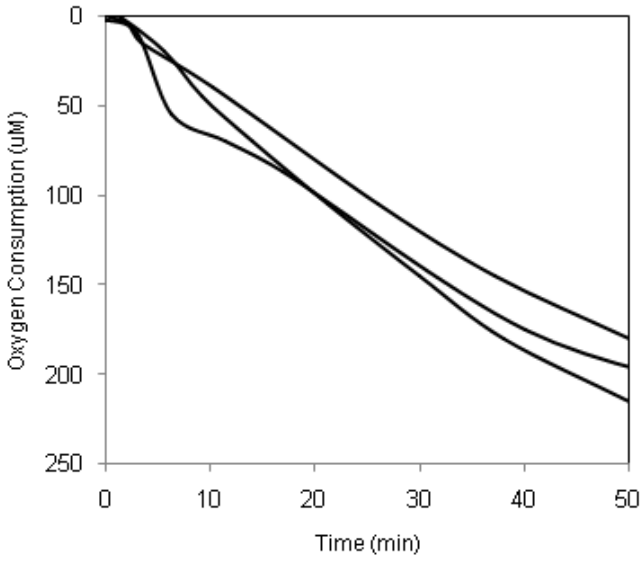

Figure 2.17 Oxygen consumption of decanal (2) 700 μM and (3) 1000 μM on L-tyrosine (1) 500

The inhibitory activity of decanal was investigated using L-tyrosine as an alternative substrate. In both oxygen consumption (Figure 2.17) and UV-VIS inhibitory assays, decanal showed no inhibitor activity at concentrations below 100 μM. At 250μM decanal shows a 7% decrease of oxygen consumption, and at 700 μM a 15% inhibition. The lag phase observed in L-tyrosine assays was not extended or curtailed. Preincubation of 700 μM decanal with L-tyrosine further reduced oxygen consumption by 4%. These results show decanal is a weaker inhibitor on L-tyrosine than L-DOPA, similar to dodecanal (Figure 2.10).

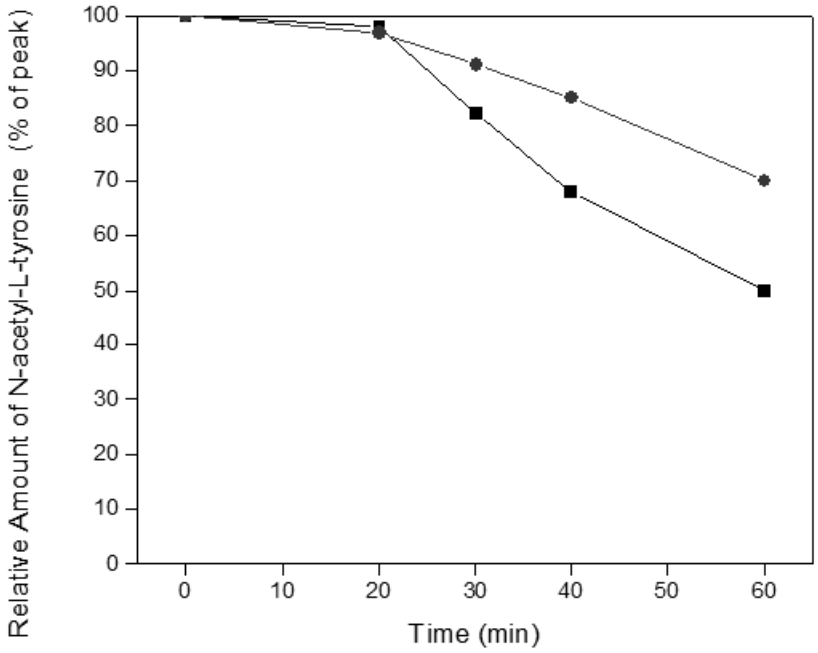

Figure 2.18 HPLC peak area of *N*-acetyl-L-tyrosine at 100 μM in the absence (closed square) or presence (closed circle) of decanal at 250 μM and tyrosinase

We then tested the inhibitory activity of decanal on the substrate *N*-acetyl-L-tyrosine. Once again, this substrate isolates enzymatic processes by halting the formation pathway before *N*-acetyl-leukodopachrome (Figure 2.11). The inhibitory assay (Figure 2.18) shows decanal inhibited the reaction with *N*-acetyl-L-tyrosine by 28% after 60 minutes. This supports that decanal is a comparable monophenol inhibitor to dodecanal.

The binding activity of decanal was investigated using fluorescence spectroscopy. Fluorescence measured at low concentrations (50μM of decanal, Table 4) increased by 100% over 30 minutes. This suggests the decanal enables more 1-NPN to enter the active site, or it makes the active site more hydrophobic. At higher concentrations (300 μM) there was a 50% decrease in fluorescence signal suggesting that decanal binds at the active pocket. The decanal and dodecanal fluorescence (Table 2.4) show similar trends and quantitatively similar suppression of the fluorescence signal. This suggests that, despite their difference in inhibitory efficacy, they share a common presence at the hydrophobic active pocket.

Time (min)	50μM	300 μM	L-DOPA
0	100	100	100
5	150	55	95
10	200	25	80
30	-	56	125

Table 2.4 Percentage fluorescence of decanal of the oxidation of 500 μM of L-DOPA

Anisaldehyde

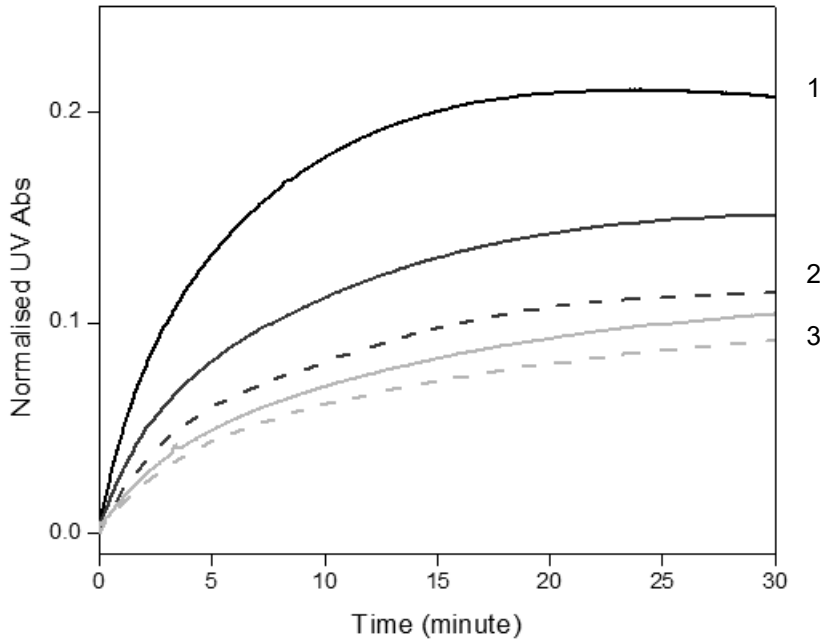

Figure 2.19 UV-Vis absorption of the oxidation of 250 μM of L-DOPA at 475nm of dopachrome formation of anisaldehyde at 125 μM (2), preincubated 10 mins (3) and 300 μM (4), preincubated 10 minutes (5) on L-DOPA (500 μM)(1)

The last major compound investigated was anisaldehyde, present at 46.69 μM (6.35%) in the essential oil. Anisaldehyde was previously reported to inhibit the tyrosinase-catalyzed oxidation of L-DOPA (Kubo and others 2003). The UV-VIS data (Figure 2.19) identifies anisaldehyde as a significantly stronger inhibitor than the other aliphatic aldehydes. At

concentrations of only 125 μM there was 27% inhibition and 50% inhibition at 300 μM. Preincubation assays performed for 10 minutes further improvement anisaldehyde inhibitory efficacy, reducing enzyme activity to 45% at 125 μM and 56% for 300 μM.

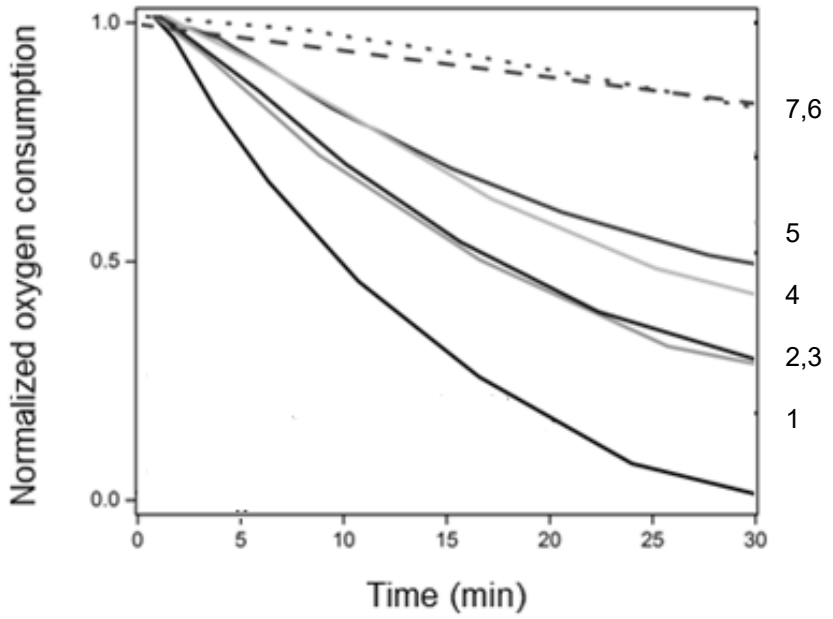

Figure 2.20 Oxygen consumption of Anisaldehyde at 125μM (2), 250μM (3), 500 μM (4) and 1000 μM (5), preincubation of 500 μM for 2 and 10 minutes (6,7) on L-DOPA at 500 μM(1)

Oxygen consumption inhibition assays performed on L-DOPA with anisaldehyde (Figure 2.20) confirm a decrease in enzymatic activity by 28% for 125 μM and 250μM, 48% for 500 μM and 42% for 1 mM. Preincubation at 500 μM for only two minutes reduced enzyme activity by 79%. However, longer preincubation showed no further improvement in inhibition, suggesting a very fast and irreversible reaction between tyrosinase and anisaldehyde. Comparing the side chain groups for the decanal and dodecanal suggested a role of the tail group. Similarly, identifying the common aldehyde head group shared by the aliphatic aldehydes and anisaldehyde suggest a role of the head group – namely the aldehyde group.

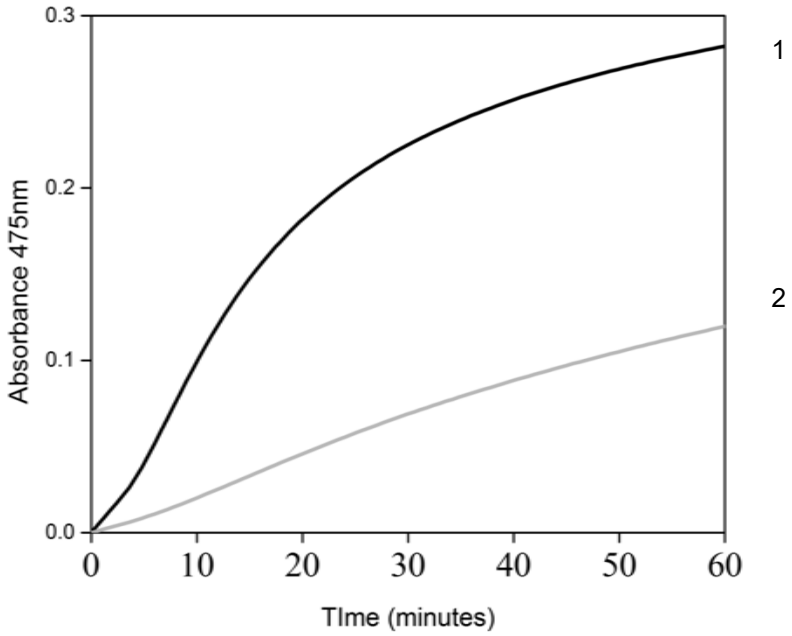

Figure 2.21 Anisaldehyde at 1000 μM (2) following dopachrome formation on L-tyrosine at 500 μM (1)

Inhibitory assays measured using an L-tyrosine substrate and anisaldehyde showed an enhanced lag phase and suppression of dopachrome formation to 69% after 60 minutes. This extended lag phase was not observed in either of the aliphatic aldehydes, and suggests that anisaldehyde directly effects the L-tyrosine to L-DOPA hydroxylation. Preincubation assays (10 minutes preincubation) performed using anisaldehyde on an L-tyrosine substrate, increased inhibition to 78% (Figure 2.21).

Fluorescence measurements were performed on anisaldehyde at 25 μM and 100 μM, with both concentrations showing decreased fluorescence in the first 10 minutes suggesting rapid occupation of the active site (Table 2.5). After 30 minutes, the signal from the100 μM solution dropped 11% then recovered back to its starting value. This suggests that most of the inhibition occurred during the first 10 minutes of the reaction. Anisaldehyde is shown to quickly bind at the active site, but at these concentrations does not entirely suppress enzymatic activity.

Time	25 uM	100 uM	L-DOPA
0	100	100	100
5	83	78	95
15	82	82	86
20	107	84	80
30	89	101	86

Table 2.5 Percentage fluorescence of anisaldehyde of the oxidation of 500 µM of L-DOPA

Imitation essential oil

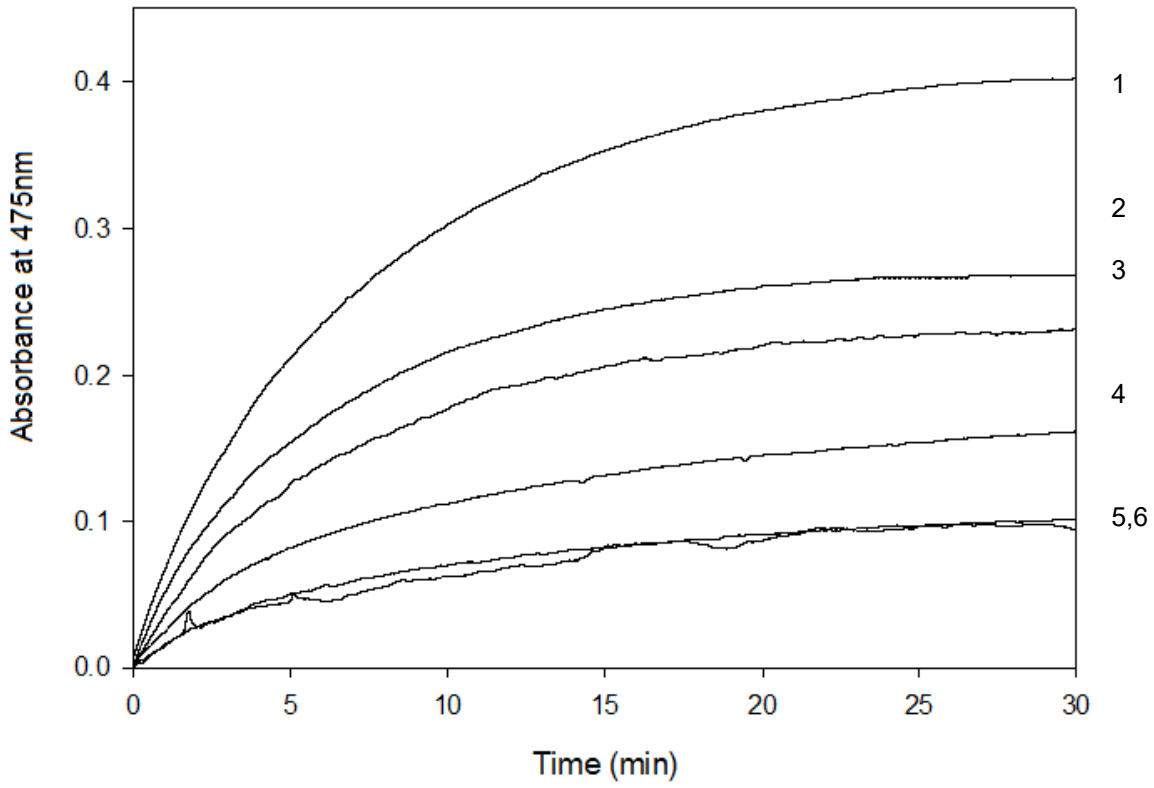

Figure 2.22 UV-VIS absorption at 475 nm of a test solution of 250 µM L-DOPA(1)and 100µg/ml EO (2),Dodecanal (55.49% w/w) with Decanal (12% w/w) (3), Anisaldehyde (6% w/w) Decanal (12% w/w) (4), Anisaldehyde (6% w/w) Dodecanal (55.49% w/w) (5), Dodecanal (55.49% w/w) with Decanal (12% w/w) and Anisaldehyde (6% w/w)(6)

Imitation essential oil using dodecanal, decanal and anisaldehyde was prepared using the ratios determined by the GC-MS analysis. This imitation EO was compared against the extracted EO to determine if the activity observed was a result of all 25 aroma compounds or just these three most abundant (active) compounds. Dopachrome formation showed that the dodecanal and decanal combination was the weakest combination, reducing activity by 42% using a L-DOPA substrate (Figure 2.22). Once anisaldehyde was introduced the solution with decanal suppressed activity by 57% while the dodecanal solution suppressed activity by 73%. The addition of decanal to the dodecanal and anisaldehyde did not further increase its efficacy as an inhibitor.

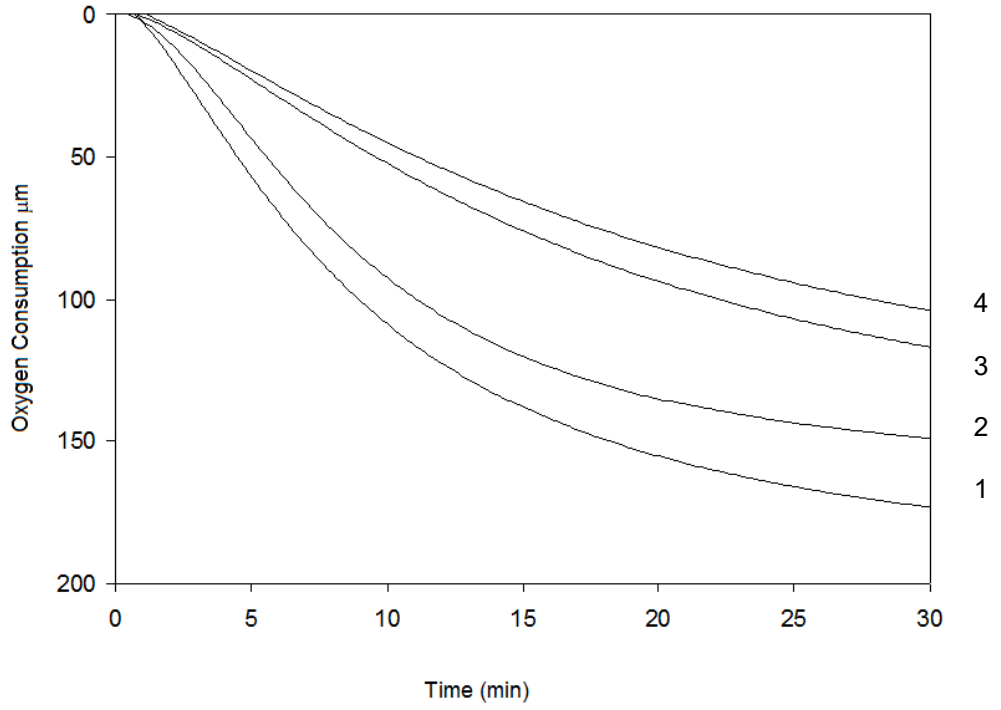

Figure 2.23 Oxygen consumption of Dodecanal (55.49% w/w) with Decanal (12% w/w) (2), Decanal (55.49% w/w) with Anisaldehyde (6% w/w), (3) Dodecanal (12% w/w) with Anisaldehyde (6% w/w (4) in the presence of DOPA (0.5mM)(1)

Similarly, oxygen consumption assays (Figure 2.23) measured on the aliphatic aldehyde imitation EO was the weakest inhibitor, suppressing enzyme activity by 14%. When anisaldehyde was introduced with either decanal or dodecanal, oxygen consumption curves were suppressed by 36% and 43% respectively. This supports our earlier suggestion that chain length plays an important role in enzyme inhibition with aliphatic aldehydes.

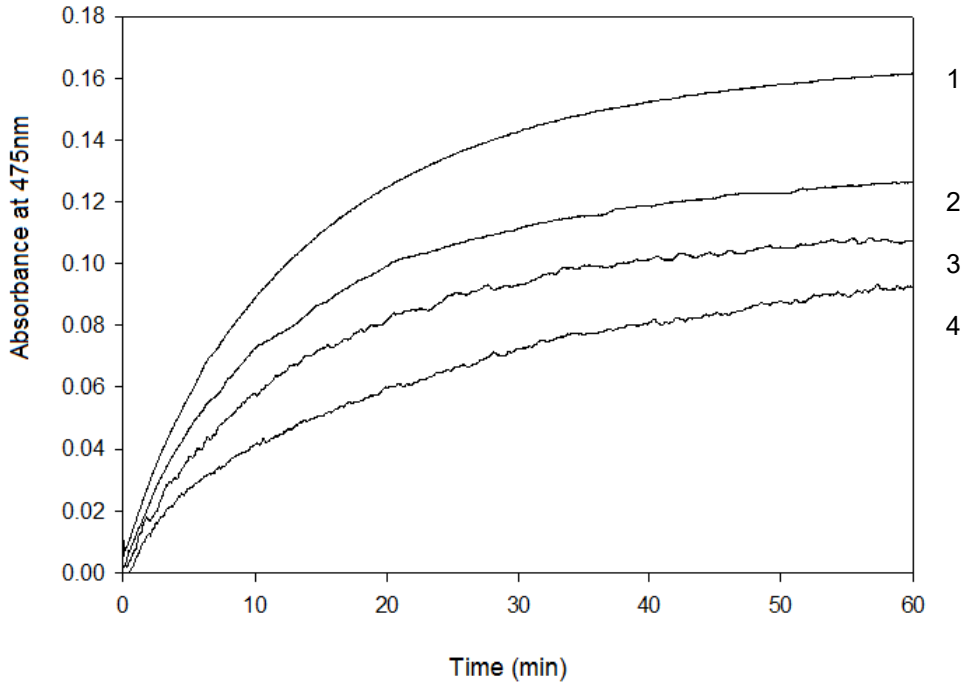

Figure 2.24 UV-VIS absorption of the L-tyrosine (0.25mM) (1) at 475 nm of dopachrome formation of) Dodecanal (55.49% w/w) with Decanal (12% w/w) (2), Decanal (12% w/w) with Anisaldehyde (6% w/w) (3), Dodecanal (55.49% w/w) with Anisaldehyde (6% w/w) (4)

UV-VIS inhibition assays performed on an L-tyrosine substrate (Figure 2.24) had the same inhibitory pattern as the assays performed on L-DOPA, with the dodecanal-decanal combination being the weakest inhibitor, suppressing enzymatic activity by 25%. The combination of anisaldehyde and decanal suppressed enzyme activity by 37%. Once more, the anisaldehyde and dodecanal combination was the strongest enzyme inhibitor, suppressing dopachrome formation by 50%. These results further suggest a relationship between inhibitory activity and chain length in the aliphatic aldehydes.

Structural analogues

To further investigate the role of the tail group, the inhibitory efficacy of shorter chain aliphatic aldehydes, down to hexanal (C6), were investigated; longer chain aliphatic aldehydes are uncommon as a natural product, so we examined only a couple representative compounds. To determined the role of the head group, α,β-unsaturated alkenals and alkanols were tested for inhibition activity. These compounds replace the aldehyde head group with a hydroxy group (alkanols), and a more-reactive unsaturated aldehyde group, which possesses an additional double bond at the 2-site (α,β-unsaturated alkenals).

The alkanals (C6-C12, with an aldehyde head group) were all tyrosinase inhibitors with a trend of increasing inhibitory activity peaking atthe medium length C9 (Table 2.6). In general, preincubation increased alkanal activity on L-DOPA, except the shortest tested compound hexanal (C6). After 10 minutes of preincubation, compounds shorter than C10 had a lower magnitude of suppressed tyrosinase activity, suggesting that the chain length may play a role in the effect of the preincubation. Consistent with the earlier dodecanal and decanal treatments, assays performed using an L-tyrosine substrate showed weaker inhibition activity compared to assays performed on L-DOPA. Additionally preincubation with L-tyrosine did not significantly increase inhibitory activity. The lack of additional efficacy on L-tyrosine suggests that the alkanals poorly affect the Eoxy confirmation, and likely effect the Emet confirmation. Fluorescence measurements (Table 6) show that these compound interact at the hydrophobic pocket throughout the 30 minutes assay, independent of their chain length. This suggests that tyrosinase was still active, and that the alkanals share a similar attraction to the enzyme active site.

Compound	% Enzyme Inhibition on L-DOPA	% Enzyme Inhibition PreInc on L-DOPA	% Enzyme Inhibition on L-tyrosine	Fluorescence %
C6	15	17	11	89
C7	22	25	7	80
C8	40	45	16	75
C9	42	50	10	25
C10	24	62	11	56[a]
C12	30	67	8	20[b]

Table 2.6 for enzyme activity measured by UV-Vis in the presence of alkanals at 500 μM, unless otherwise noted; a) tested at 300 μM and b) tested at 200 μM

Unsaturated Alkenals and Alkanols

To further understand the activity of the aldehyde head group we examined the more-reactive unsaturated 2E-alkenals. These compounds were active inhibitors of dopachrome formation when applied to an L-DOPA substrate, and were slightly weaker at suppressing enzyme activity than the alkanals (Table 2.7). Fluorescence supported that these compounds were present at the active pocket (data not shown). In contrast with the saturated alkenals, preincubation did not significantly improve the inhibitory efficacy of the 2E-alkenalson either substrate. Assays performed on an L-tyrosine substrate, with 2E-alkenals, suppressed enzyme activity less than assays performed on L-DOPA, and did not extend the lag phase. This further supports our earlier suggestion that the inhibitor only weakly inhibits the Eoxy confirmation. Alkanols were also investigated and were the least active (11% at 500 μM for decanol, for example) compounds on the L-DOPA substrate. Preincubation did not significantly improve inhibition activity. Alkanols were no more active on L-tyrosine and fluorescence supported they weakly interacted at the binding site compared to the other compounds investigated (data not showed).

Compound	% Enzyme Inhibition on L-DOPA	% Enzyme Inhibition PreInc on L-DOPA	%Enzyme Inhibition on L-tyrosine
C6	10	-	10
C7	38.5	39	20
C8	42	51	14
C9	34	34	10
C10	33	36	5
C12	11.4	-	32

Table 2.7 Enzyme activity in the presence of 2E-alkenals at 500 μM, measured using UV-VIS

Shaking effects

All of the examined aliphatic compounds (alkanals, and α,β-unsaturated alkenals) lack an ionic charge on the head group, which suggests hydrophobic interactions are a possible source of activity. If hydrophobic interactions are present in the system, then it is expected that agitation (shaking) of the solution will reversibly re-disperse the compounds into solution, and increase activity. To do this test we conducted a shaking experiment in which the alkanals at were preincubated for 10 minutes while being shaken at 125rpm with the enzyme. The L-DOPA substrate was then added, and dopachrome formation monitored. The resultant inhibition did not show a distinct trend with chain length or dependence on shaking (data not shown). This may be due to the changing contribution of the head group and non-polar tail group, and their ability to stabilize micelle-like structures. Shaking did not change the inhibitory efficacy of the 2E-alkenals when measuring oxygen consumption, further suggesting their mechanism may be similar than the saturated alkenals.

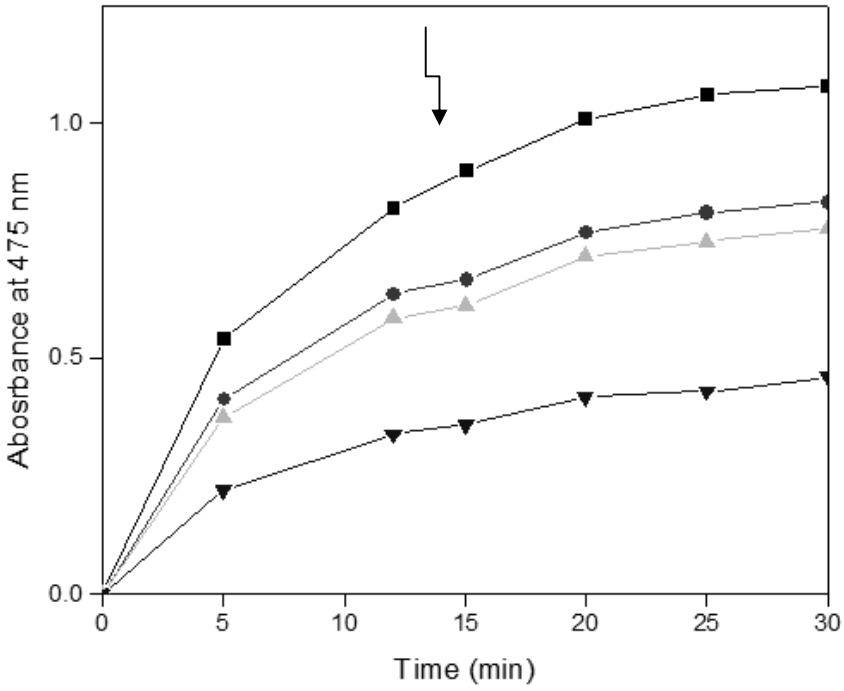

Figure 2.25. UV-VIS absorption of the oxidation of 900μM of L-DOPA (square) at 475 nm of dopachrome formation of essential oil at 100 μg/ml (circle), hexanal at 1000 μM (triangle) dodecanal at 1000 μM (upside down triangle)

In similar assays, a standard assay was performed but with L-DOPA in excess to ensure enough substrate is available to catalyze the reaction after agitation. After 12 minutes the reaction solution was removed, quickly agitated with a vortex mixer for 15 seconds, and then returned to the spectrometer. This procedure can disrupt any hydrophobic bonds, and introduces oxygen to the solution. The resultant dopachrome formation measurements (Figure 2.25) show a distinct jump in absorbance after shaking. It should be noted the amount of available oxygen in the cuvette was approximately 250 μM, thus additional L-DOPA was made available if the enzyme was still active. After 3 minutes the L-DOPA control increased by 0.08 absorbance units, giving a baseline resulting from the oxygen contribution. In comparison, the assays performed with essential oil increased by 0.04 absorbance units, and dodecanal and hexanal increased by 0.02 and 0.03 absorbance units, respectively. These results suggest that indeed there are hydrophobic forces present which contribute to the inhibition and they depend on chain length. The similar slope of the absorption plots on either side of the shaking event suggests that the agitation breaks the hydrophobic construction, dopachrome continues to form, confirming the reversibility.

To determine if there was a hydrophobic aspect to the inhibitory mechanism we investigated two plant derived alkyl resorcinols; cardol, an aromatic ring with a 15 carbon long chain and hydroxyls in the 1 and 3 position and olivetol, identical to cardol but with a shorter 5

carbon tail- to determine if the side chain length was a key to inhibition. Preincubation measuring oxygen consumption on L-DOPA showed cardol reduced dopachrome formation by 30% at 20 µM while olivetol reduced formation by 18% at 500 µM. Additionally, cardol and olivetol were poor inhibitors in the regular L-DOPA inhibition assays, nor did they consume large amounts of oxygen (less than 11%) suggesting that oxygen is not necessary for the inhibition mechanism (data not shown).Thus there appears to be a relationship between side chain length and hydrophobic properties that play a role in enzyme inhibition.

Activity of essential oil components and related aldehydes on B16-F10 melanoma cells

While the testing discussed previously was performed in a 'cell-free' environment, eventual application to medical treatments necessitates testing on living cells. In this section the essential oil extract from *P. ordoratum* and its constituent compounds were tested on cultured murine melanoma cells B16-F10 for cell viability and melanin formation inhibition.

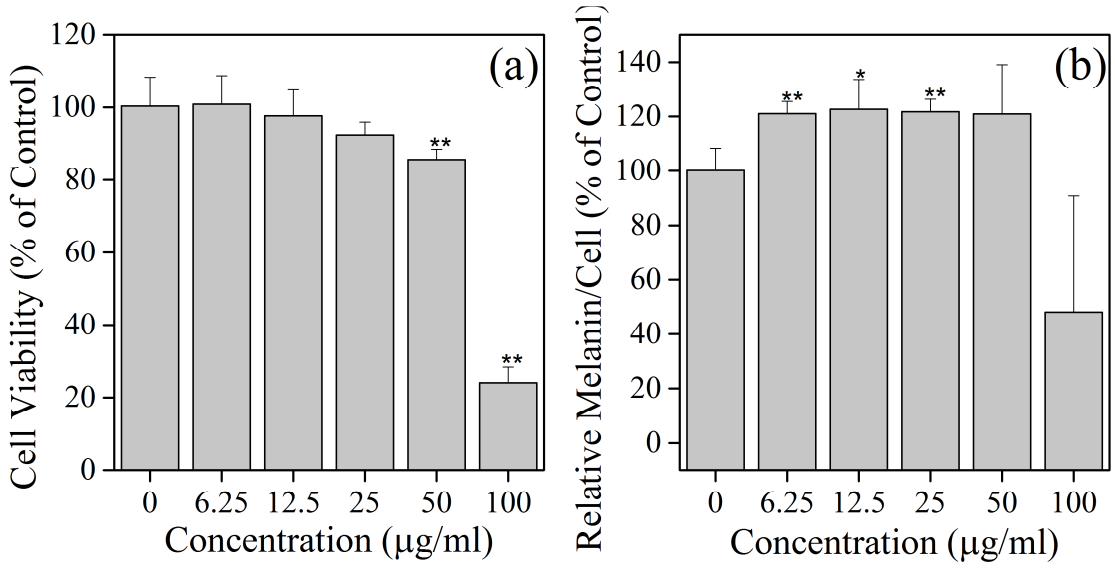

Figure 2.26 (a) Viabilities of B16-F10 melanoma cells after treatment with *P. Ordoratum*; (b) Relative melanin content in B16 melanoma cells after treatment with *P. Ordoratum*. The statistical significance is denoted as follows: *p<0.05, **p<0.01

Similar to the cell-free testing, the essential oil extract was tested first. The above testing showed the EO as an effective tyrosinase inhibitor, showing activity at 100 µg/ml in cell-free testing. This IC_{50} does not always directly correlate to the cellular level testing, as the compound will likely be distributed differently due to the cell's ability to regulate compound distributions. Initial testing of cellular viability showed the essential oil has a weak cytotoxicity up to 100 µg/ml (Figure 2.26a, Table 8), with a calculated IC_{50} of 83 µg/mL. The cell's melanin production was measured and the EO treatment did not reduce melanin formation relative to the control for treatments less-than 100µg/mL, at which toxicity sets in. The cellular melanin content (Figure

2.26b), defined as the melanin production divided by the number of living cells, was lowest in the 100µg/mL treatment. Thus, the onset of inhibition using the EO occurs at similar concentration to the IC_{50} . However, it is possible that the inhibition and toxicity are due to two different compounds. This motivates the testing of the individual major compounds - which were identified above as potential inhibitors - for their efficacy in cellular testing.

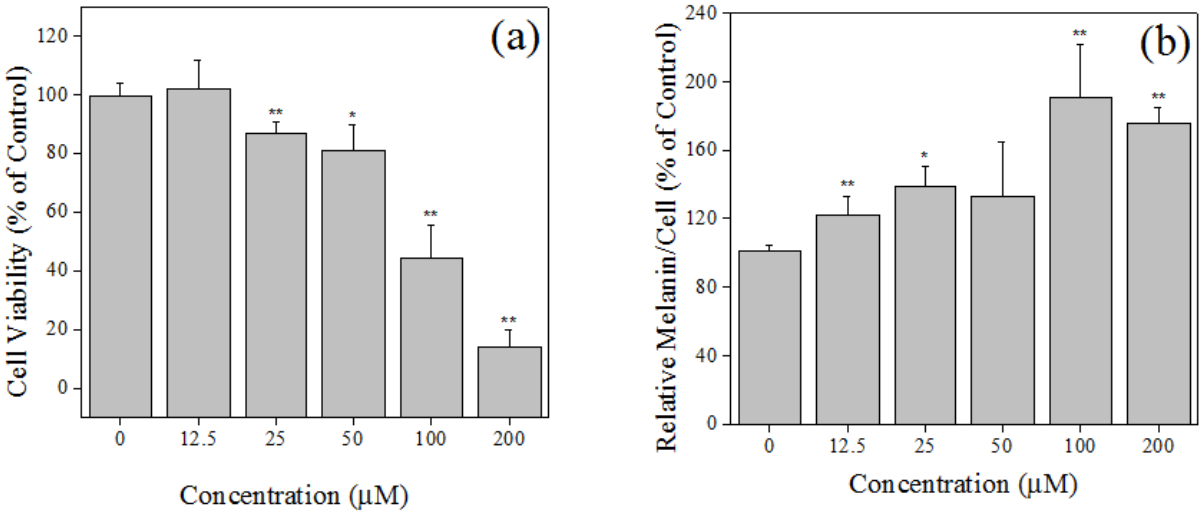

Figure 2.27 (a) Viabilities of B16-F10 melanoma cells after treatment with dodecanal (b) Relative melanin content in B16 melanoma cells after treatment with dodecanal. The statistical significance is denoted as follows: *p<0.05, **p<0.01

Dodecanal was identified as the most abundant compound in EO (55%, Table 2.1)and was shown to be a tyrosinase inhibitor showing activity at 250 µM.In cellular testing, this compound showed a continuously statistically significant decrease in cell viability (Figure 2.27a) with increased concentrations up to 200 µM, with the IC_{50} calculated to be 96 µM. Further, the melanin formation and cellular melanin concentration (Figure 2.27b) was significantly enhanced in most treatments, suggesting that dodecanal potentiated melanin production in the complex cellular system. These results suggest that dodecanal is not a good candidate for melanogenesis inhibition applications.

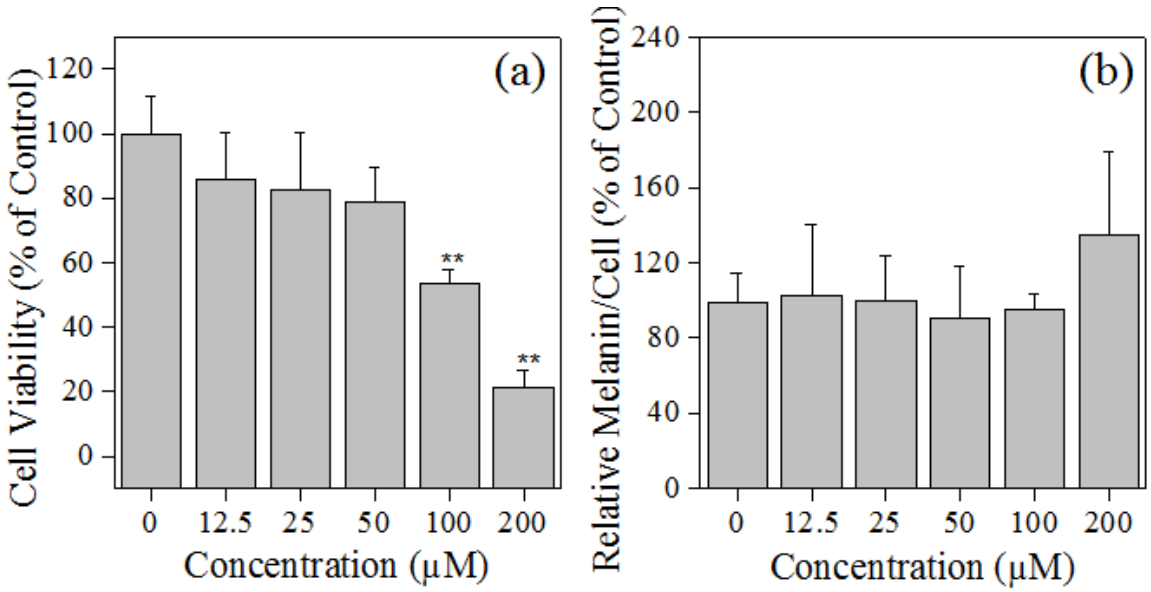

Figure 2.28 (a) Viabilities of B16-F10 melanoma cells after treatment with decanal (b) Relative melanin content in B16 melanoma cells after treatment with decanal. The statistical significance is denoted as follows: *p<0.05, **p<0.01

Decanal was the second most abundant compound identified in the EO (12%, Table 2.1), and was also shown to be a tyrosinase inhibitor (Figure 2.15), showing activity at 250 μM. In cellular experiments, this compound also caused statistically significant continuous decrease in cell viability (Figure 2.28a), similar to dodecanal, with strong cytotoxic activity at concentration exceeding 100 μM. The IC_{50} for cell viability was calculated to be 115 μM, much lower than the concentration necessary to suppress tyrosinase activity in the cell-free experiments, but higher than the dodecanalIC_{50}. Also decanal did not suppress melanin production (Figure 2.28b) and there was no statistical significance in the cellular melanin concentration (Figure 2.28b). These results also suggest decanal is not a good candidate for melanogenesis inhibition applications.

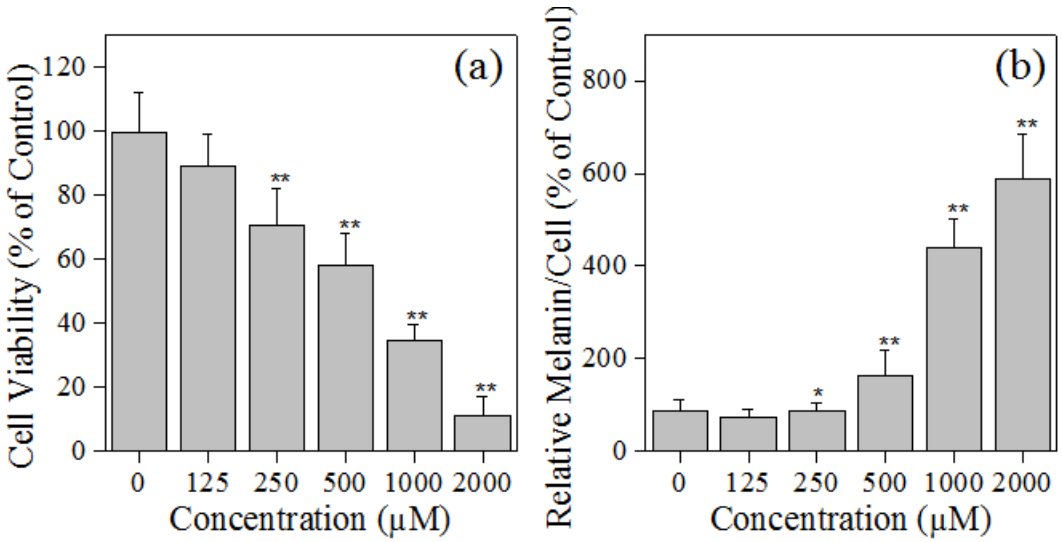

Figure 2.29 (a) Viabilities of B16-F10 melanoma cells after treatment with anisaldehyde (b) Relative melanin content in B16 melanoma cells after treatment with anisaldehyde. The statistical significance is denoted as follows: *p<0.05, **p<0.01

The third most abundant active compound (6%, Table 2.1), and the strongest tested enzyme inhibitor, anisaldehyde, was tested. This compound has previously been reported as a melanogenesis inhibitor (Kubo, 1999) and the IC_{50} was determined to be 790µM (Figure 2.29a). Due to the statistically significant cytotoxicity the amount of melanin produced per cell greatly increased (Figure 2.29b).

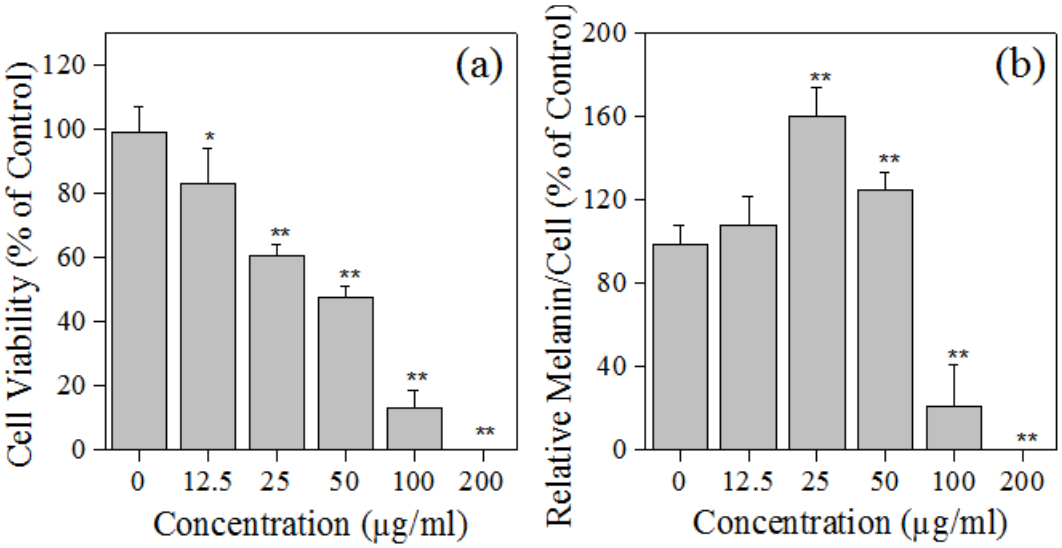

Figure 2.30 (a) Viabilities of B16-F10 melanoma cells after treatment with 2E-dodecanal (b) Relative melanin content in B16 melanoma cells after treatment with 2E-dodecanal. The statistical significance is denoted as follows: *p<0.05, **p<0.01

Recalling that 2E-dodecanal and 2E-decanal - which are structurally similar to dodecanal and decanal - were also effective inhibitors, with ≈30% inhibition at 500 µM concentrations, cellular level testing was also performed. Consistent with these compounds being generally more reactive, 2E-dodecanal was cytotoxic at a much lower concentration (compared to dodecanal) of 12.5 µM (Figure 2.30a),resulting in an IC_{50} of cell viability of only 52 µM. In comparison, 2E-decanal had a lower IC_{50} of 34 µM (Table 8). The 2E-alkenals statistically significantly reduced melanin formation overall (Figure 2.30b), but on a per cell level (Figure 2.30b) actually increased melanin production at the higher concentrations, similar to their saturated analogues. These results suggest that the unsaturated aldehydes are better candidates than their saturated analogues.

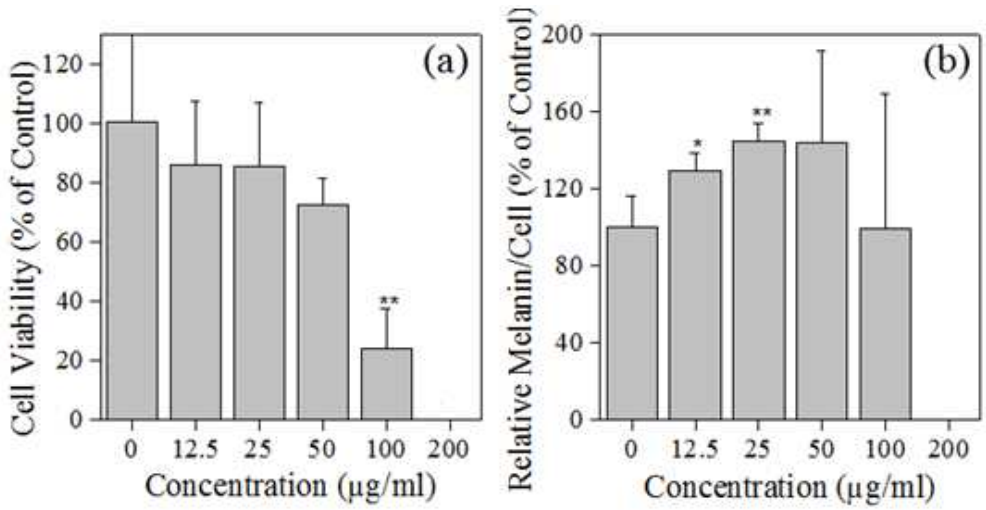

Figure 2.31 (a) Viabilities of B16-F10 melanoma cells after treatment with dodecanol (b) Relative melanin content in B16 melanoma cells after treatment with dodecanol; The statistical significance is denoted as follows: *p<0.05, **p<0.01

Lastly, the alkanols were investigated. These compounds showed reduced tyrosinase inhibition in cell-free experiments, at only 11% inhibition at 500 µM, but were expected to be less-reactive, and thus may show less cytotoxicity. Indeed, cellular viability (Figure 2.31a) remained high until concentrations of 100 µM, comparable to the saturated aldehydes. The IC_{50} was determined to be 63 µM. Also similar to the saturated aliphatic aldehydes, increased concentration of the alkanols slightly increased the overall melanin formation (Figure 2.31b), and the per-cell concentration (Figure 2.31b).

The cellular-level testing results are summarized in Table 2.8, show that the order of cytotoxic activity in decreasing order: unsaturated aldehydes>saturated aldehyde >alkanols. The amount of melanin that was suppressed in increasing order: unsaturated aldehydes >saturated aldehydes = alkanols. Overall the 2E-alkenals (unsaturated) showed the most promise as melanogenesis inhibitors.

Compounds tested	IC_{50} (μM)	Melanin
Anisaldehyde	790	Increase
Hexanal	900	Increase
Decanal	115	Neutral
Dodecanal	96	Increase
2E-Hexanal	16	Increase
2E-Decenal	34	Decrease
2E-Dodecenal	52	Decrease
Hexanol	850	Neutral
Decanol	210	Neutral
Dodecanol	63	Increase

Table 2.8 Cytotoxicity against B16-F10 melanoma cells

Discussion

Vietnamese coriander essential oil and its major components dodecanal, decanal, and anisaldehyde were demonstrated as tyrosinase inhibitors in cell-free assays. The tested compounds share a common aldehyde head group, but have different aliphatic or aromatic tail groups. All of these compounds, as well as the other structurally similar aliphatic aldehydes, and many of the aromatic aldehydes to be discussed in Chapter 3, were effective inhibitors, this suggests that the reactive aldehyde head group may be responsible for the observed inhibitory properties. On the other hand, the fact that the compounds share a common head group but show different inhibitory activity suggests that the side chain group plays an important role in determining their efficacy. In cellular level testing both the essential oil and the refined compounds were shown to be poor melanogenesis inhibitors, often causing cytotoxicity before inhibition of melanin production. In the following we will discuss some possible mechanisms to explain the observed inhibitory activity.

Role of the aliphatic tail length

Testing of the inhibitory activity of the aliphatic aldehydes (Table 6) shows that they are all suppressors on L-DOPA. For inhibition assays, the C8 and C9aliphatic showed the strongest inhibitory activity, while for the preincubation assays, the maximal activity is observed for C10 and C12. Following the suggestion that the aldehyde head group plays a key role in determining the inhibitory activity, a possible explanation for this behavior is that the head group binds at or near the tyrosinase active site, while the aliphatic tail group disrupts enzyme activity.

However, we also observed that none of the saturated aldehydes were strong inhibitors when measured on an L-tyrosine substrate (Table 6). This suggests that the inhibitors preferentially act on the Emet confirmation of tyrosinase. Further, supporting this claim, inhibition of the Eoxy confirmation would result in an extended lag phase, which was not observed in any of the aliphatic aldehyde assays (Figures 2.10 and 2.17). Indeed, if a binding mechanism is responsible for the inhibition, the conformational dependence (activity against Emet and not Eoxy) suggests that the binding occurs near the active site, which is consistent with the provided fluorescence data (Tables 3, 4, and 9).Inhibitor binding at or near the tyrosinase active site has been previously suggested to occur by a Schiff base mechanism, a non-competitive mechanism (Kubo, 1998). Specifically, the double-bound oxygen located on the aldehyde head undergoes a single-replacement with a nitrogen in the active pocket and forms a Schiff base with a primary amino group (Yokoi and others 1990).

Additionally, it has been previously shown (Decker and others 2007) that when aldehydes form Schiff bases with a primary amino group in the tyrosinase active site, in can disrupt their tertiary structure. This work also suggested that hydrophobic interactions which result from the bound compound can then further disrupt enzyme functionality, and may contribute to our observed inhibition. In another work, it has been suggested specifically for

tyrosinase that effectors can bind to the enzyme and can induce conformational transitions (Rolff and others 2011). In this case, conformational changes from Emet to Edeoxy or Eoxy would manifest as inhibition. Since both hydrophobic interactions and Schiff base formation, with aliphatic aldehydes, are known to be reversible, the disruption of the tertiary structure of the enzyme is expected to be reversible. Indeed, this reversibility is observed in the activity assays (Figure 2.25).

The tail length data – which shows increased inhibition only up to C9 (Table 6) – casts doubt on this mechanism. However this can be reconciled by considering the preincubation data. Specifically, preincubation assays showed increased activity compared to the inhibition assays for all chain lengths but to a lesser degree for hexanal (C6) and increased inhibition up to the longest aliphatic chain (C12). These observations both suggest that the binding interaction occurs slowly. In effect, the preincubation assays give the long-side chain time to bind with and disrupt the enzyme tertiary structure. The UV-Vis and oxygen data (Figure 2.8) supports this conclusion. It appeared there was time dependent inhibition since the preincubation assays increased inhibition (Figure 2.5 and Figure 2.8)yet there was not a significant amount of oxygen consumed (Figure 2.2 and Figure 2.6) and the dopachrome formation assays showed increased inhibition the first 10 minutes but not beyond.

To further consider the plausibility of Schiff base formation, we investigated the inhibitory activity of 2E-alkenals (Table 7). These compounds are similar to the simple alkanals but with an additional double bond between the number two and three carbons. Since the double-bonded oxygen is still present on the aldehyde head, we expect these compounds to also form a Schiff base since it has been reported that 2E alkenals form them (Kubo, 1999). Indeed, both inhibition assays and preincubation performed using 2E alkenals on DOPA and L-tyrosine substrates show inhibition, with no notable improvement compared to the simple alkanals. This supports our suggestion that a Schiff base may be forming. Also, the similar inhibitory activity of the alkanals and 2E alkenals suggests that the structure of the side chain near the aldehyde head does not play as prominent a role in the inhibition. This supports our suggestion that the inhibitor may be inducing hydrophobic forces. Additionally, native proteins have poor conformational stability so they are sensitive to hydrophobic disruptions (Decker and others 2007, Gelman, 2013).

In summary, our combined data suggests that the aliphatic aldehydes reversibly bind to the enzyme, likely by a Schiff base mechanism interacting with a primary amino group in the active site. Then the aldehydes either disrupt the tertiary structure reducing functionality by hydrophobic interactions (such as hydrogen bonding), generally relating to side chain length, or induce conformational changes, predominantly effecting the Emet conformation.

Alternative Inhibitory Mechanisms

Two other potential inhibitory mechanisms are also considered. The first of these mechanisms considers the specific structural features of the aliphatic aldehydes. Particularly, the aldehyde head is hydrophilic, while the aliphatic tail is hydrophobic, with longer chains being

more hydrophobic (Otzen and others 2009). When in solution the polar head helps keep the surfactant dissolved as a monomer. As the concentration of the surfactant increases the monomers start to associate via their hydrophobic tails to form micelles, particularly for nonanal (C9) and longer chains (Otzen 2011). The formation of micelles in solution will decrease the number of free molecules able to interact with the enzyme or bind to the active site, leading to the apparent decrease in activity in the inhibitory assays with C10 and C12. However, while this mechanism agrees with the observed chain-length dependence, it does not have a dependence on the enzyme confirmation, which was also observed. This mechanism also relies on the above arguments that the monomers induce inhibition, and the micelle formation decreases activity in longer chain aliphatic, at higher concentrations (Figure 2.32). For these reasons, we suspect this mechanism plays a lesser role in determining the activity.

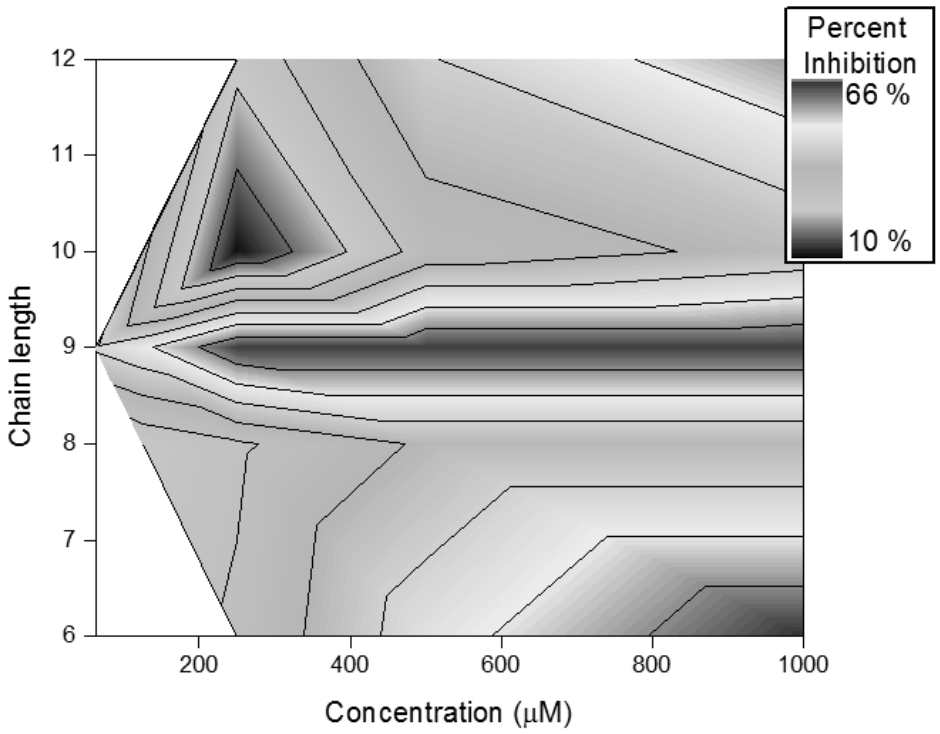

Figure 2.32 Intensity of binding of tyrosinase based on oxygen consumption and inhibition; red indicates stronger inhibitor activity and blue weaker activity

In the second alternative mechanism, we specifically consider an inhibitory mechanism which acts on the Emet confirmation, leaving tyrosinase in the effectively inactive Edeoxy state. In the first step, the aldehyde group is drawn into the tyrosinase Emet active site by electrostatic attraction between the Cu^{2+} ion, and the double bonded oxygen (Figure 2.33a). After entering the active site, the electro-negative oxygen bound between the Cu ions attracts the electropositive C-H group on the aldehyde (Figure 2.33b). Then, the C-H group is oxidized, forming undecylic acid (Figure 2.33c), and changing the confirmation of the tyrosinase from Emet to Edeoxy.

Finally, the aliphatic group rejoins the solution, leaving tyrosinase in the Edeoxy state (Figure 2.33d), which is unable to oxidize DOPA or hydroxylate L-tyrosine.

This mechanism is discounted for two reasons. First, there is no dependence on the chain length of the inhibitor, which is at odds with our observations. Secondly, this mechanism results in a buildup of Edeoxy. On an L-tyrosine substrate, the Edeoxy consumes oxygen from solution to form Eoxy. As a result, there will be increased oxygen consumption, and more rapid conversion of L-tyrosine to L-DOPA, resulting in a reduced lag phase. This was observed only in the dodecanal (C12) inhibition assay. We therefore suggest that this mechanism also only plays a minor role in the inhibitory process.

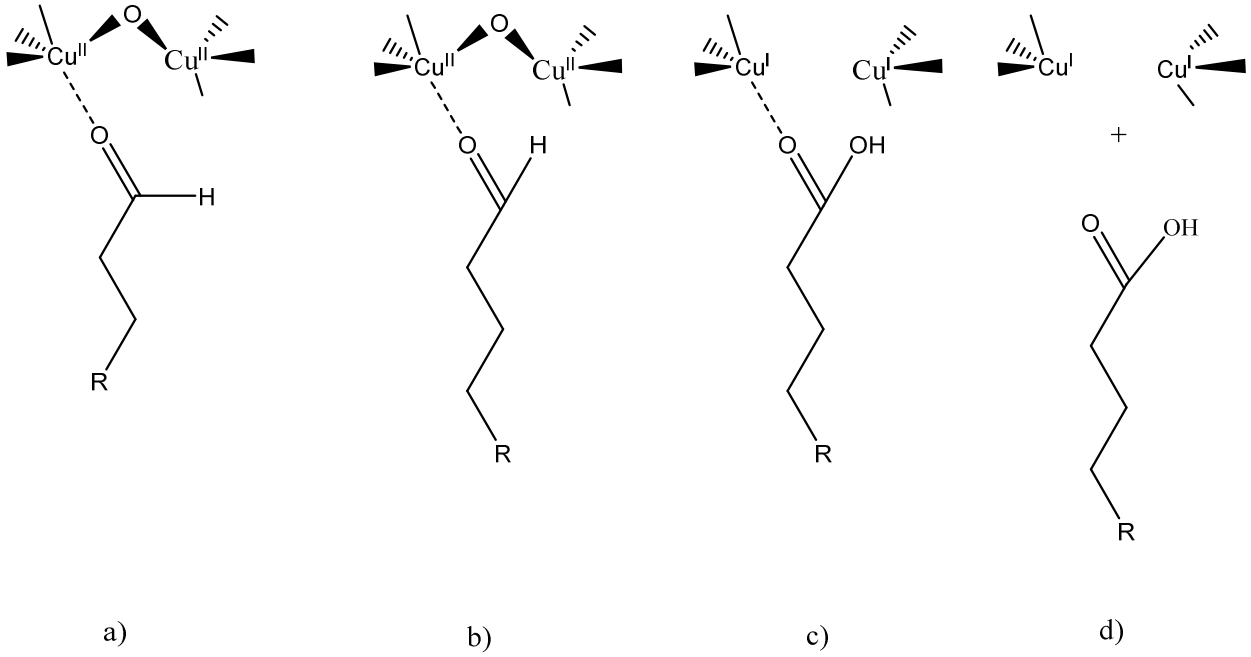

Figure 2.33 Aldehyde reduction of tyrosinase active site

Cells Discussion

Consistent with the enzyme activity, the essential oil did not show cytotoxicity until 100 μg/ml. The amount of alkanals entering into the cytosol or lipid bilayer depends on the length of the alkyl chain (Kubo and Cespedes 2013).The murine cell surface is a phospholipid

bilipid membrane which is made up of a polar head group and a non-polar hydrophobic tail. The hydrophilic head group consists of a choline group with a positively charged nitrogen which presents a possible binging site for the aldehyde group (How 2014). Aldehydes have been experimentally found to form Schiff bases with this phospholipid layer (Solis-Calero and others 2010). It was reported that tetradecanal (C14) was inactive because it could not accumulate in high enough concentrations in the phospholipid lipid bilayer, demonstrating the importance of side chain length (Céspedes and others 2013).Thus, it is possible that the aldehydes are binding with the phospholipid layer on the enzyme membrane, interfering with membrane dynamics leading to cell cytotoxicity. For example, the longer chain alkanals C10,C12 dissolved in the testing medium and were possibly incorporated into the lipid bilayers of the plasma membrane (Franks and Lieb 1986).The short chain alkanals entered the cells by passive diffusion across the plasma membrane and/or through prion channels (Schulz 1992). Once inside the lipid bilayer or cytosol, the aldehyde may react with biologically important materials(Eisenbrand and others 1995) leading to cell death. Previous investigations into aldehyde chain length have shown patterns of toxicity based on chain length. For example, activity against *S. choleraesuis* was distinctly increased with each additional CH_2 group, up to dodecanal (Kubo and others 2004). While here toxicity in human melanoma cells decreased as chain length increased. This difference in activity is not unexpected due to the different nature of these cell walls. The most cytotoxic compound was 2E-dodecenal, and other 2E-alkenals have been reported to have similar activity on V79 cells due to their induced DNA breakage (Janzowski and others 2003). 2E-alkenals ability to form Michael adducts is the source of their activity and makes them particularity potent in cellular systems (Spickett 2013).The general lack of melanogenesis suppression in the cellular assays reflects the complexity of cellular events. While the tested compounds are strong enzyme inhibitors, melanin production may not be inhibited within mammalian pigment cells.

Conclusion

Overall, the major components of *P. ordoratum* essential oil were moderate tyrosinase inhibitors in cell-free assays, yet this activity did not translate to strong melanogenesis inhibition. We suggest an inhibitory mechanism in which the aldehyde moiety binds at the active pocket of tyrosinase (possibly in the Emet confirmation),as a noncompetitive inhibitor by a Schiff base mechanism. Then, over time the hydrophobic alkyl chain interacts with the hydrophobic domains of the enzyme disrupting the enzyme's tertiary structure, reducing activity. All of our tested compounds were demonstrated as tyrosine inhibitors, suggesting the aldehyde head group plays a crucial role in the inhibition mechanism. This presents new opportunities to discover effective tyrosinase inhibitors. Since the principle compounds investigated in this work are used commercially, and are demonstrated tyrosinase suppressors, they could have new useful applications in unexplored areas.

Structures

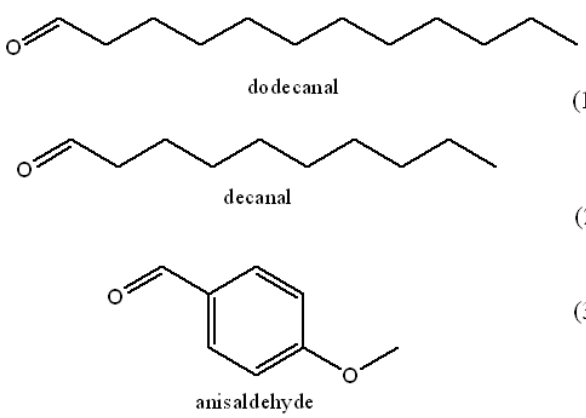

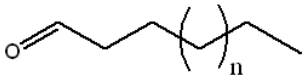

(4): n=0
(5): n=1
(6): n=2
(7): n=3
(8): n=4
(9): n=5
(10): n=6

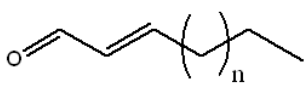

(11): n=0
(12): n=1
(13): n=2
(14): n=3
(15): n=4
(16): n=5
(17): n=6

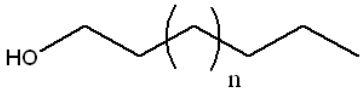

(18): n=0
(19): n=4
(20): n=5

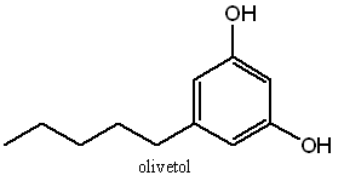

(21)

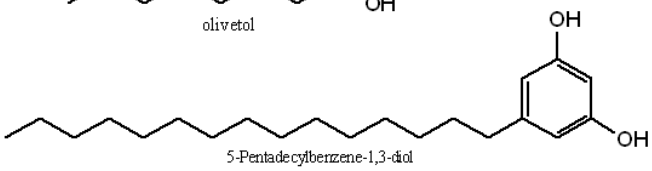

(22)

Figure 2.24 Structure of dodecanal (1), decanal (2), anisaldehyde (3) and related compounds

Materials and Methods

General methods

Methods

General procedures were as previously reported (Nitoda and others 2007, Satooka and Kubo, 2011) with slight modifications. Assays were performed in triplicate.

Materials

Key testing materials such as L-DOPA, L-tyrosine and tyrosinase were purchased from Sigma-Aldrich (Milwaukee, MN, USA). Purified aliphatic aldehydes (saturated and unsaturated), aromatic aldehyde compounds were purchased from the same supplier. N-acetyl-L-tyrosine was purchased from Tokyo Kasei Kogyo Co. Ltd. (Tokyo, Japan).

GC-MS analysis

The composition of essential oil of *P. odoratum* was analyzed by a GC-MS system(GC-17A/QP5050; Shimadzu Co., Ltd., Kyoto, Japan) equipped with a DB-5 column (30 m × 0.25 mm i.d., 0.25 μm film thickness; J & W Scientific Inc.). The temperature program was as follows: 45℃ for 8 min, followed by increases of 2.5 ℃ min^{-1} to 180℃, and 10℃ min^{-1} to 250℃, and holding for 3 min. The other parameters were as follows: injection temperature, 250℃; ion source temperature, 250℃; ionization energy, 70 eV; carrier gas, He at 1.7 mL min^{-1}; injection volume, 1 μL (90 μg/mL Et_2O); split ratio, 1:20; mass range, m/z 50 to 450.

Essential oil

An essential oil (kesom oil) was steam distilled from fresh leaves taken from *P. odoratum*, collected in north east Thailand. Currently there are no commercial products which utilize kesom oil, and limited investigations of its efficacy as a medical compound have been reported. Gas chromatography-mass spectroscopy (GC-MS) measurements of the distilled essential oil show that the major compounds were aliphatic aldehydes comprising 67% of the solution. Twenty-five aroma compounds were identified in the essential oil extract. The most abundant compounds were aliphatic aldehydes dodecanal at 55% (C12) and decanal at 11.5% (C10) followed by anisaldehyde 9% (Table 2.1).

Enzyme

Assays investigate tyrosinase inhibition as a mechanism to suppress melanogenesis. Tyrosinase – mushroom derived– used in the inhibition assays was purchased from Sigma Aldrich and was purified by anion-exchange chromatography using DEAE-Sepharose Fast Flow (Pharmacia, Uppsala, Sweden) as previously described (Espin and Wichers 1999). Tyrosinase initiates the melanin formation cascade by catalyzing the hydroxylation of L-tyrosine, and thenthe oxidation L-DOPA into dopaquinone, then non-enzymatically into dopachrome, and eventually into melanin, as discussed in the General Introduction.

Spectrometry

Photo-spectroscopy (UV-VIS) measurements were performed on a Shimadzu 1700 (Tokyo, Japan) to identify the formation of dopachrome. Absorbance was measured at 475 nm, which corresponds to a strong absorbance of dopachrome. Samples were dissolved in DMSO and only used for experimentation after their dilution. The final concentration of DMSO was always 3%. For inhibition assays, a test solution of 3 ml was prepared consisting of 1.95 ml distilled and filtered H_20, 0.725 ml of 67mM phosphate buffer (pH=6.8), 0.125 ml L-DOPA (from a 6 mM stock) were mixed and incubated at 30° C for 5 minutes. At this point, the 100 µl of the sample solution and 100 µl of the purified tyrosinase in phosphate buffer was added (1 µg/ml) to the mixture in this order. Once tyrosinase was added to the solution the absorbance was measured for 30-60 minutes. For preincubation assays, the preincubation solution- 1.95 ml distilled and filtered H_20, 0.725 ml of 67mM phosphate buffer (pH=6.8), 100 µl of the sample solution and 100 µl of the purified tyrosinase was added (1 µg/ml) and incubated for 10 minute (or 20 minutes) at 30° C, prior to the addition of L-DOPA. Each assay was repeated three times on separate occasions; data was recorded in Probe 2.1v.

Oxygen consumption

Oxygen consumption inhibitory assays can monitor both the catalyzation of L-tyrosine into L-DOPA and L-DOPA into dopaquinone, since both steps consume a single molecular oxygen from solution. Measurements were taken using an OBH 100 oxygen electrode with a water jacket chamber using an YSI 5300 oxygen monitor (all from Yellow Springs Instruments Co., Yellow Springs, OH). For inhibition assays, a test solution of 3 ml was prepared consisting of 1.95 ml distilled and filtered H_20, 0.725 ml of 67mM phosphate buffer (pH=6.8), 0.125 ml L-DOPA (from a 6 mM stock) and the sample candidate were incubated at 30° C for 5 minutes. At this point, 100 µl of the purified tyrosinase in phosphate buffer was added (1 µg/ml). Oxygen consumption was then monitored at 30° C for up to 60 minutes. Each assay was repeated three times on separate occasions to confirm repeatability. Preincubation assays investigated interactions of the inhibitor with tyrosinase. The preincubation solution was prepared as described above. . The results were expressed as oxygen consumption in the unit µM.

HPLC

The high-performance-liquid-chromotography (HPLC) analysis was performed on EYELA pump (Tokyo Rikakikai Co. Ltd., Tokyo, Japan) with an EYELA UV-7000 detector (Tokyo Rikakikai Co. Ltd., Tokyo, Japan) and Develosil ODS-UG-5 column (4.6 x 150 mm, Nomura Chemical Co., Ltd., Japan). The operating conditions were as follows unless otherwise noted: the solvents were 7% MeCN (Acetonitrile) and H_2O containing 0.2 % Trifluoroacetic (TFA), flow rate of 1 ml/min, detection at 280 nm (UV), injected volume of 25µl from the above described 3 ml assay system. The peak area was used to monitor the consumption of substrates and the results were described as the ratio of the area of sample peaks to the control.

Fluorescence

Fluorescence measurements were performed using *N*-Phenyl-1-naphthylamine (1-NPN) to probe the occupancy of the active site. This compound strongly fluoresces in hydrophobic environments (Yin and others 2015), which includes the tyrosinase active site. Thus, as the substrate and/or inhibitor occupy the active site, the fluorescence intensity is expected to decrease. In this work specifically, control fluorescence assays performed on the native L-tyrosine substrate showed an initial drop in signal intensity during the conversion of L-tyrosine to L-DOPA. This drop can be understood as the substrates occupying the active site, and consequentially displacing 1-NPN. Assays performed on the L-DOPA substrate also showed an initial decrease in fluorescence due to the same displacement mechanisms (Yin and others 2015). After this initial decrease, the fluorescence intensity increased, indicating that the probe can access the active site. Generally, the fluorescence signal in the control experiments increase over the 30 minute assay period due to the shrinking amount of L-DOPA available to bind.

Fluorescence measurements were performed on an EnVision Plate reader 2104i (Perkin-Elmer, Waltham, MA,USA), using a 340 nm excitation light and monitoring emissions at 460 nm. Inhibitory assay solutions (3 ml) were prepared as described in the spectroscopy experiments, with the addition of 100 µL of 1-NPN for (20 µM) was added and the solution incubated at 30° C for 10 minutes.. Of this solution 300 µL were then loaded into wells of a 96 well plate, then the candidate inhibitor was added to this solution, then tyrosinase was added. Emissions were measured every 5 minutes for 30 minutes total. To avoid light interference measurements were taken only after the light path way shut for at least 10 seconds.

Cellular assays

Cell mortality assays were performed on B16-F10 murine melanoma cells purchased from ATCC (Manassas, VA, USA), and cultured in continuous log phase growth in Dulbecco's Modified Eagle medium (DMEM) containing 10% fetal bovine serum (FBS). Cells were seeded in 96-well plates (≈2000 cells/well) and incubated at 37° C for 24 hours at 5% CO_2 prior to chemical treatment. Each chemical was applied in duplicate with a final content of 0.1% DMSO, and treated cells were cultured for 72 hours prior to scoring.

The melanin content was quantified as described (Kageyama and others 2004; Venkatasamy and others 2004) with some adjustment. Cells were washed with phosphate-buffered saline (PBS), harvested by trypsinization, and centrifuged for 10 minutes at 1500×*g*. The cell pellets were then dissolved in 1.0 M NaOH that contained 10% DMSO for a 2 hour incubation period at 80° C. Melanin content was determined at 475 nm using a SpectraMax Plus spectrophotometer and SoftMax Pro software (Molecular Devices, Union City, USA).

Cell viability was evaluated through trypan blue exclusion using a Nikon Diaphoto TMD (Nikon, Tokyo, Japan), and a 50% viable cells lost (IC_{50}) was determined. PBS was used to wash cells, and then they were dispersed by trypsinization. A sample of the cells was then diluted with DMEM containing 10% FBS, and then mixed with the trypan blue solution (for a final concentration of 0.1%) at room temperature. Unstained cells (viable cells) were counted within 10 minutes using a hemocytometer after being mixing with the trypan blue

Statistical analysis

The statistical significance was determined by either Student's or Welch's t-test depending on the data variances and $p<0.05$ and $p<0.01$ was considered statistically significant.

References

1. Bayraktar D, Onoğur TA. 2011. Investigation of the aroma impact volatiles in Turkish pine honey samples produced in Marmaris, Datça and Fethiye regions by SPME/GC/MS technique. International Journal of Food Science & Technology 46(5):1060-5.

2. Cai YZ, Luo Q, Sun M, Corke H. 2004. Antioxidant activity and phenolic compounds of 112 traditional Chinese medicinal plants associated with anticancer. Life Sciences 74(17):2157-84.

3. Decker H, Hellmann N, Jaenicke E, Lieb B, Meissner U, Markl J. 2007. Minireview: Recent progress in hemocyanin research. Integr. Comp. Biol. 47(4):631-44.

4. Eisenbrand G, Schuhmacher J, Golzer P. 1995. The influence of gluthatione and detoxifying enzymes on DNA- damage induced by 2-alkenal in primary rat hepatocytes and human lymphoblastoid- cells. Chemical Research in Toxicology 8(1):40-6.

5. Espin JC, Wichers HJ. 1999. Slow-binding inhibition of mushroom (Agaricus bisporus) tyrosinase isoforms by tropolone. Journal of Agricultural and Food Chemistry 47(7):2638-44.

6. Franks NP, Lieb WR. 1986. Partitioning of long chain alcohols into lipid bilayers-implications for mechanimsm of general anesthesia. Proceedings of the National Academy of Sciences of the United States of America 83(14):5116-20.

7. Fujita K, Chavasiri W, Kubo I. 2015. Anti-Salmonella Activity of Volatile Compounds of Vietnam Coriander. Phytotherapy Research 29(7):1081-7.

8. Gelman H, Perlova T, Gruebele M. 2013. Dodine as a Protein Denaturant: The Best of Two Worlds? Journal of Physical Chemistry B 117(42):13090-7.

9. Ha TJ, Tamura S, Kubo I. 2005. Effects of mushroom tyrosinase on anisaldehyde. Journal of Agricultural and Food Chemistry 53(18):7024-8.

10. How CW, Teruel JA, Ortiz A, Montenegro MF, Rodríguez-López JN, Aranda FJ. 2014. Effects of a synthetic antitumoral catechin and its tyrosinase-processed product on the structural properties of phosphatidylcholine membranes. Biochimica et Biophysica Acta (BBA) - Biomembranes 1838(5):1215-24.

11. Janzowski C, Glaab V, Mueller C, Straesser U, Kamp HG, Eisenbrand G. 2003. alpha,beta-unsaturated carbonyl compounds: induction of oxidative DNA damage in mammalian cells. Mutagenesis 18(5):465-70.
12. Kageyama A, Oka M, Okada T, Nakamura S, Ueyama T, Saito N, Hearing VJ, Ichihashi M, Nishigori C. 2004. Down-regulation of melanogenesis by phospholipase D2 through ubiquitin proteasome-mediated degradation of tyrosinase. Journal of Biological Chemistry 279(26):2777

13. Kim YJ, Uyama H. 2005. Tyrosinase inhibitors from natural and synthetic sources: structure, inhibition mechanism and perspective for the future. Cell. Mol. Life Sci. 62(15):1707-23.

14. Kubo I, Cespedes CL. 2013. Antifungal activity of alkanols: inhibition of growth of spoilage yeasts. Phytochemistry Reviews 12(4):961-77.

15. Kubo I, Chen QX, Nihei K, Calderon JS, Cespedes CL. 2003. Tyrosinase inhibition kinetics of anisic acid. Zeitschrift Fur Naturforschung Section C-a Journal of Biosciences 58(9-10):713-8.

16. Kubo I, Fujita K, Nihei K, Nihei A. 2004. Antibacterial activity of akyl gallates against Bacillus subtilis. Journal of Agricultural and Food Chemistry 52(5):1072-6.

17. Kubo I, Kinst-Hori I. 1998. Tyrosinase inhibitors from cumin. Journal of Agricultural and Food Chemistry 46(12):5338-41.

18. Kubo I, Kinst-Hori I. 1999. 2-hydroxy-4-methoxybenzaldehyde: A potent tyrosinase inhibitor from African medicinal plants. Planta Medica 65(1):19-22.

19. Kubo I, Kinst-Hori I. 1999. Tyrosinase inhibitory activity of the olive oil flavor compounds. Journal of Agricultural and Food Chemistry 47(11):4574-8.

20. Lee HS, Goh MJ, Kim J, Choi TJ, Lee HK, Na YJ, Cho KH. 2015. A systems-biological study on the identification of safe and effective molecular targets for the reduction of ultraviolet B-induced skin pigmentation. Sci Rep 5:11.

21. Nitoda T, Fan MD, Kubo I. 2007. Anisaidehyde, a melanogenesis potentiator. Zeitschrift Fur Naturforschung C-a Journal of Biosciences 62(1-2):143-9.

22. Otzen D. 2011. Protein-surfactant interactions: A tale of many states. Biochimica Et Biophysica Acta-Proteins and Proteomics 1814(5):562-91.

23. Otzen DE, Sehgal P, Westh P. 2009. alpha-Lactalbumin is unfolded by all classes of surfactants but by different mechanisms. Journal of Colloid and Interface Science 329(2):273-83.

24. Rastogi SC. 2001. A method for the analysis of intermediates of oxidative hair dyes in cosmetic products. J. Sep. Sci. 24(3):173-8.

25. Rolff M, Schottenheim J, Decker H, Tuczek F. 2011. Copper-O-2 reactivity of tyrosinase models towards external monophenolic substrates: molecular mechanism and comparison with the enzyme. Chemical Society Reviews 40(7):4077-98.

26. Sakunpak A, Suksaeree J, Pathompak P, Charoonratana T, Chankana N, Sermkaew N. 2015. Thin-Layer Chromatography—Densitometry and Thin-Layer Chromatography—Image Analysis for Screening Bile Acid-Binding Activities of Thai Edible Plants. JPC - Journal of Planar Chromatography - Modern TLC 28(5):380-5.

27. Satooka H, Kubo I. 2011. Effects of Thymol on Mushroom Tyrosinase-Catalyzed Melanin Formation. Journal of Agricultural and Food Chemistry 59(16):8908-14.

28. Schulz GE. 1992. Strucutre function relationships in the membrane channel prion as based on a 1.8 angstrom resolution crystal structure. Membrane Proteins : Structures, Interactions and Models 25:403-12.

29. Sharma RA, Steward WP, Gescher AJ. 2007. Pharmacokinetics and pharmacodynamics of curcumin. Adv.Exp.Med.Biol. 595:453-70.

30. Solis-Calero C, Ortega-Castro J, Munoz F. 2010. Reactivity of a Phospholipid Monolayer Model under Periodic Boundary Conditions A Density Functional Theory Study of the Schiff Base Formation between Phosphatidylethanolamine and Acetaldehyde. Journal of Physical Chemistry B 114(48):15879-85.

31. Soto LM, Falqué E, Domínguez H. 2015. Relevance of Natural Phenolics from Grape and Derivative Products in the Formulation of Cosmetics. Cosmetics 2(3).

32. Spickett CM. 2013. The lipid peroxidation product 4-hydroxy-2-nonenal: Advances in chemistry and analysis. Redox Biology 1(1):145-52.

33. Surburg H, Panten J. 2010. Common Fragrance and Flavor Materials: Preparation, Properties and Uses.6 ed. Germany: Wiley-Vch.

34. Tisserand R, Young R. 2014. Essential Oil Safety: A Guide for Health Care Professionals.2 ed. New York: Elsvier.

35. Yokoi H, Takeuchi A, Yamada S. 1990. Esr studies on salicyladehyde schiff base complexes of copper (III) dimer formation on Bis(N-alkylsalcylidenemination- copper (II) complexes and their derivatives in toluene. Bulletin of the Chemical Society of Japan 63(5):1462-6.

36. Venkatasamy R, Faas L, Young AR, Raman A, Hider RC. 2004. Effects of piperine analogues on stimulation of melanocyte proliferation and melanocyte differentiation. Bioorganic & Medicinal Chemistry 12(8):1905-20.

37. Yin J, Choo YM, Duan HX, Leal WS. 2015. Selectivity of odorant-binding proteins from the southern house mosquito tested against physiologically relevant ligands. Frontiers in Physiology 6.

Chapter 3

Effect of benzaldehydes derivatives on tyrosinase and B16 melanoma cells

Introduction

In our continued search for plant derived tyrosinase inhibitors, aromatic aldehydes were are investigated. Plant sourced aromatic aldehydes have been previously identified as effective tyrosinase and melanogenesis inhibitors (Kubo and Kinst-Hori 1999; Kubo and others 2003a). Specifically, 2-hydroxy-4-methoxybenzaldehyde (HMB)(Kubo and Kinst-Hori 1999) and 4-methoxybenzaldehyde (Anisaldehyde) (Kubo and Kinst-Hori 1998), isolated from African medicinal plants *Mondiawhitei* (Asclepiadaceae), *Rhus vulgaris* (Anacardiaceae), and *Sclerocaryacaffra* (Anacardiaceae), were reported as strongmelanogenesis andtyrosinase inhibitors.Both 2-hydroxy-4-methoxybenzaldehyde and 4-methoxybenzaldehyde have an aromatic ring (C_6H_6), with moieties including an aldehyde head group (-CHO), to which their activity is attributed; these structures are part of a common class of compounds derived from the parent compound benzaldehyde.

As shown in Chapter 2, the aldehyde head group plays a significant role in determining the activity of compounds as tyrosinase inhibitors. However, we also demonstrated the role of side-chain length in aliphatic aldehydes, emphasizing the role of the tail group in determining efficacy. In both HMB and anisaldehyde the aromatic ring has a methoxy group ($-OCH_3$) in the *para*-position (4-posistion), while the HMB has an additional hydroxyl (-OH) group in the *meta*-position (2-posistion) – adjacent to the aldehyde head group. HMB was demonstrated to be a more-effective inhibitor than anisaldehyde highlighting the role of these moieties. This motivates an investigation into the role of the moieties in determining the inhibitory efficacy of benzaldehyde derived compounds, including their composition and arrangement.

In this work, aromatic aldehydes with simple moieties are investigated as tyrosinase inhibitors. Using HMB and anisaldehyde as model systems, the moieties are initially removed and benzaldehyde is tested for efficacy. Then, methoxy and hydroxyl functional groups are arranged on the aromatic ring, and their inhibitory activity determined. These results show a strong dependence on the structural arrangement of the functional groups relative to the aldehyde group. For example, the compound vanillin is inactive as an inhibitor but exchanging the arrangement of itsmethoxy and hydroxyl functional groups forms isovanillin, which is an extremely effective tyrosinase inhibitor. The inhibitory activity is investigated on the different confirmations of the enzyme to determine if tyrosinase can be inhibited before achieving its most active form. Further investigations using fluorometry showed that the aromatic aldehydes interact at the tyrosinase active site, confirming the underlying mechanism for tyrosinase inhibition.

Results

Benzaldehyde

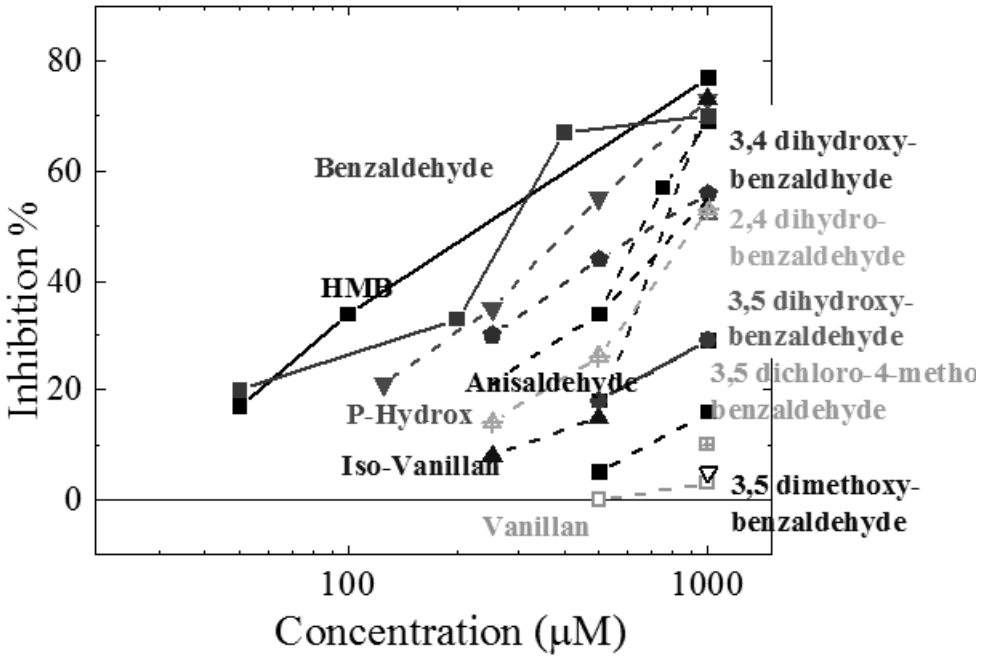

Figure 3.1 Percentage of enzyme inhibition activity of benzaldehydes derivatives on L-tyrosine

We began by investigating the parent compound of our study, benzaldehyde. Benzaldehyde (**1**) showed a dose dependent inhibition response when measuring dopachrome formation on L-tyrosine, suppressing activity by 20%, 35%, 67% and 72% at 50 µM, 200 µM , 400 µM and 1000 µM concentrations (Figure 3.1). These assays showed a slightly extended lag phase compared tothe control (Figure 3.2), suggesting this inhibitor acts on the L-tyrosine to L-DOPA transition. Preincubation assays of benzaldehye did not improve activity further. When measuring oxygen consumption benzaldehyde suppressed enzyme activity by 50% and 55% at 200µM and 400µM respectively (Figure 3.3).

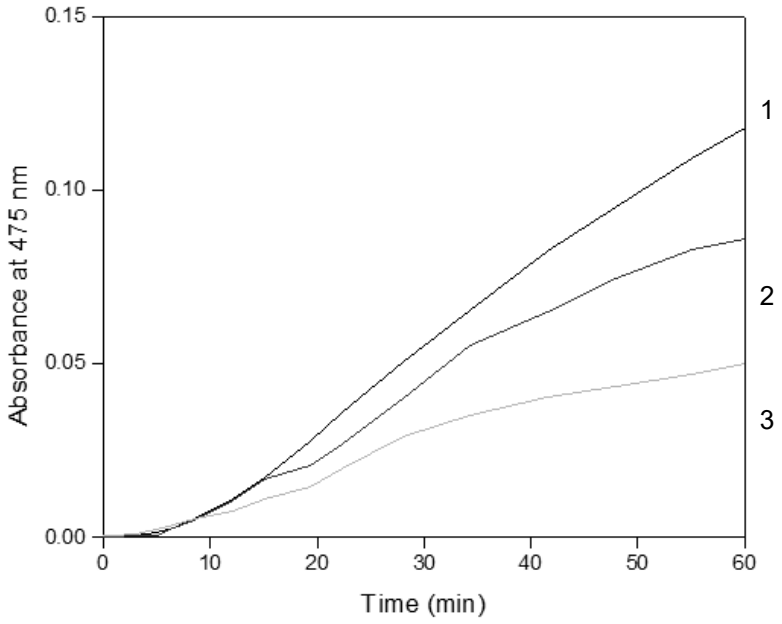

Figure 3.2 UV-VIS spectra at 475 nm obtained in oxidation of 100 μM of L-tyrosine (1) by mushroom tyrosinase in presence of benzaldehyde at 200 μM (2) and 400 μM (3)

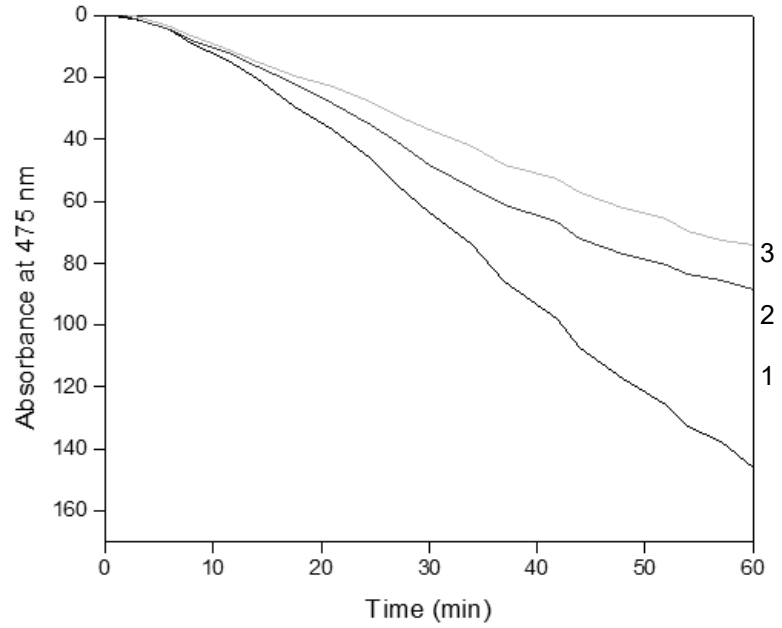

Figure 3.3 Oxygen consumption of oxidation of L-tyrosine (100 μM)(1) by mushroom tyrosinase in presence of benzaldehyde at 200 μM (2) and 400 μM (3)

The effect of benzaldehyde on the tyrosinase-catalyzed oxidation of *N*-acetyl-L-tyrosine was examined. As discussed in Chapter 2, this substrate is catalyzed by tyrosinase to *N*-acetyl-Leukodopachrome, but does not subsequently cyclize, thus isolating the enzymatic steps of the melanin formation pathway. The results (Figure 3.4) showed most of *N*-acetyl-L-tyrosine remained after 30 minutes and was not oxidized. This confirms that benzaldehyde specifically inhibited the tyrosinase catalyzed monophenolase activity and appeared to do so slowly.

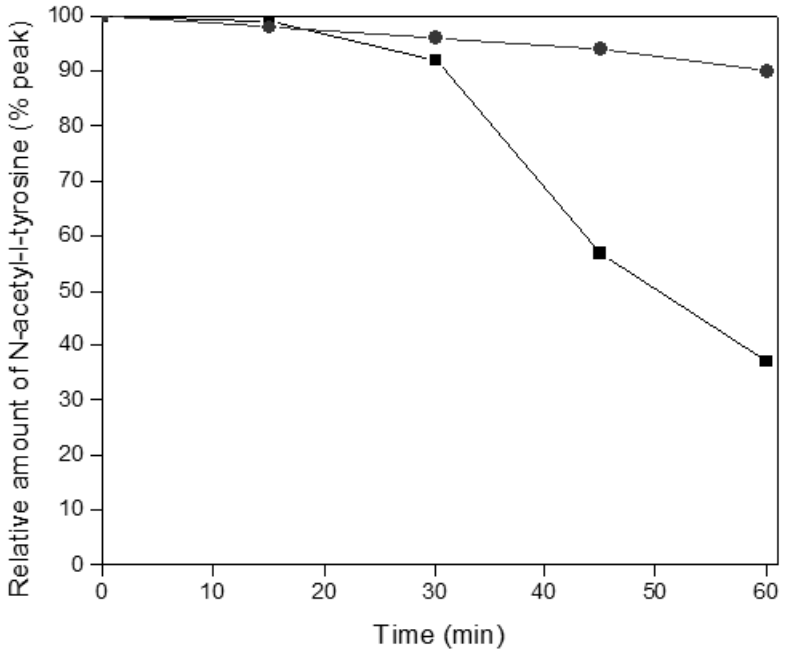

Figure 3.4 HPLC peak area of *N*-acetyl-L-tyrosine (100 µM) oxidation by tyrosinase in absence (closed square) or presence (open circle) of benzaldehyde (400 µM)

Assays performed using an L-DOPA substrate also showed that benzaldehhyde was an active inhibitor (Figure 3.5). Dopachrome formation was suppressed by 15%, 32%, 40 % and 60% at 50µM, 150 µM, 300 µM and 400 µM concentrations, respectively, showing a dose dependent response. Preincubation for 10 minutes of benzaldehyde with tyrosinase prior to the addition of L-DOPA increased activity by 8%, 8%, 8% and 4% for 50 µM, 150 µM, 300 µM and 400 µM, respectively. This minor increase suggests that the compound is an inhibitor rather than an inactivator.

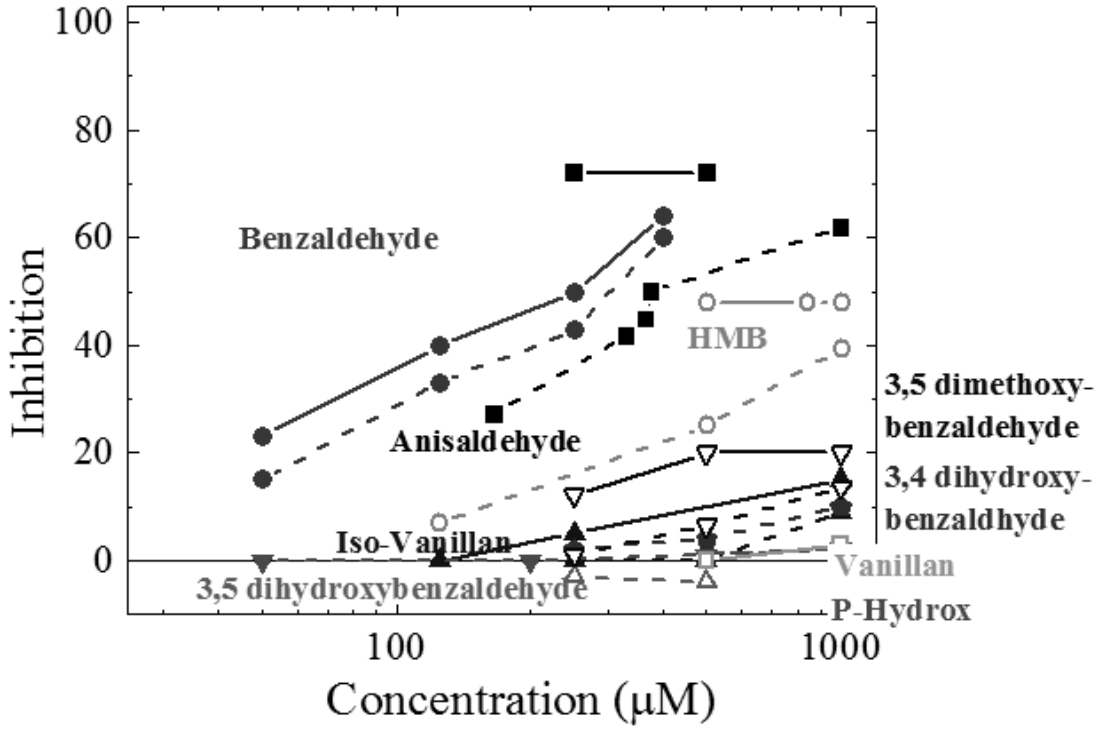

Figure 3.5 Percentage of enzyme inhibition of various benzaldehydes on L-DOPA. Dashed lines are inhibition and solid lines are preincubation assays

Monitoring oxygen consumption in inhibitory assays showed a much weaker inhibition. A weak dose dependent response was observed in the oxygen consumption, with the strongest inhibition at 400 μM suppressing 40% enzyme activity. This is approximately 30% weaker less than the direct UV-VIS spectroscopy assays observed at these concentrations, suggesting the inhibitory mechanism must also consume oxygen (data not shown).

The difference of the inhibition and preincubation assays suggest that benzaldehhyde inactivates the enzyme and inhibition is not the result of products of the reaction. In Chapter 2 we suggested the aldehyde head group plays a crucial role in the inhibition by binding at/near the enzyme active site. To investigate this possibility fluorescence measurements were performed.

As shown in Chapter 2, the control experiments showed an initial decrease in fluorescence signal due to the active site occupation by the substrate. After 10 minutes, sufficient amounts of the substrate was consumed and the signal recovers. In the presence of the inhibitor, the fluorescence signal is not expected to recover due to active site occupation by the test compound. Indeed, the fluorescence data (Table 3.1) shows a 23% overall decrease in signal intensity relative to the control during the first 10 minutes, supporting that benzaldehyde is binding at the active site on tyrosinase. This reduced intensity does not recover throughout the

remainder of the assay, indicating the inhibitor is continuously interacting at the active site. On the L-DOPA substrate there was an immediate decrease in fluorescence during the first 10 minutes of the reaction. After 15 minutes the fluorescence signal was reduced by 25-30% by benzaldehyde at 30 μM, and remained constant until 35 minutes when the fluorescence increased to 93%.

Time	30μM benzaldehyde with L-tyrosine	L-tyrosine control	30μM benzaldehyde with L-DOPA	L-DOPA Control
0	100	100	100	100
5	97	97	70	95
10	93	93	10	80
15	96	87	60	-
20	83	84	70	-
30	81	85	70	125
50	77	-	-	-
60	77	85	-	-

Table 3.1 Percentage of fluorescence of test solutions of L-tyrosine and L-DOPA with tyrosinase, inhibited by benzaldehyde at 30 μM

Single Moiety Benzaldeydes

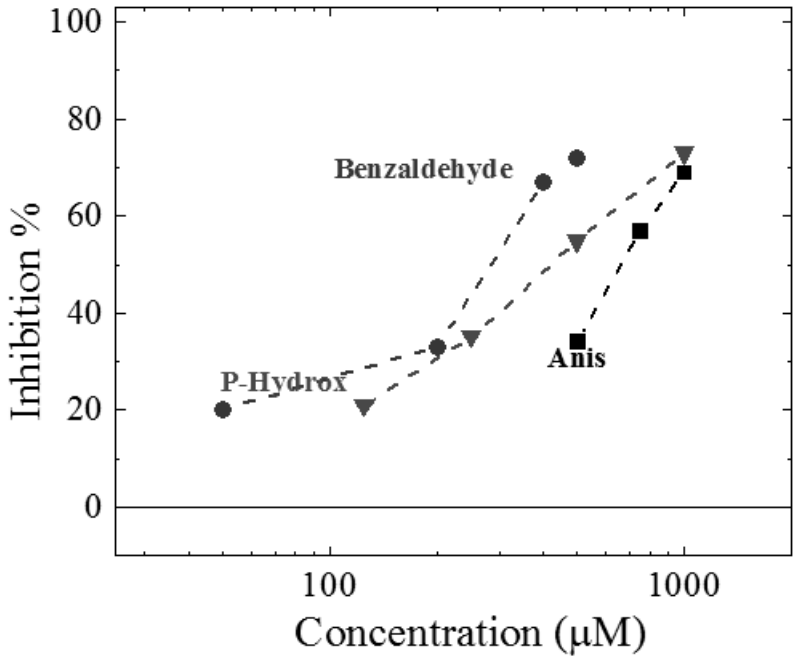

Figure 3.6 Percentage of enzyme inhibition of 4-posistion benzaldehydes on L-tyrosine

Chapter 2 focused on the aliphatic aldehydes, but also showed that anisaldehyde was a strong tyrosinase inhibitor. Compared to its parent compound, benzaldehyde, anisaldehyde has a single methoxy moiety located at the *para*-position. This suggests motivates the possibility of improving enzyme inhibition activity by including moieties to the aromatic ring. In this first section, hydroxyl (-OH) or methoxy (-OCH_3)moieties are introduced at the *para*-position, including 4-methoxybenzaldehyde (anisaldehyde) and 4-hydroxybenzaldehyde (*p*-hydroxy). Supporting this approach, the additions are expected to be strong electron donators, and thus may enhance the activity.

As shown in Chapter 2 anisaldehyde (**2**) was a strong tyrosinase inhibitor. Assays performed with an L-tyrosine substrate showed that anisaldehyde inhibited tyrosinase activity (Figure 3.6), significantly extending the lag phase, and suppressing enzyme activity by 69% at 1 mM; preincubation further improved the activity of anisaldehyde by 3% on L-tyrosine. The UV-VIS data identifies anisaldehydeas a strong inhibitor on L-DOPA (Figure 3.7),suppressing activity by 27% at only 125 μM and 50% at 300 μM. Preincubation at 500 μM for only two minutes reduced enzyme activity by 80% measuring oxygen consumption and 37% measuring dopachrome formation.

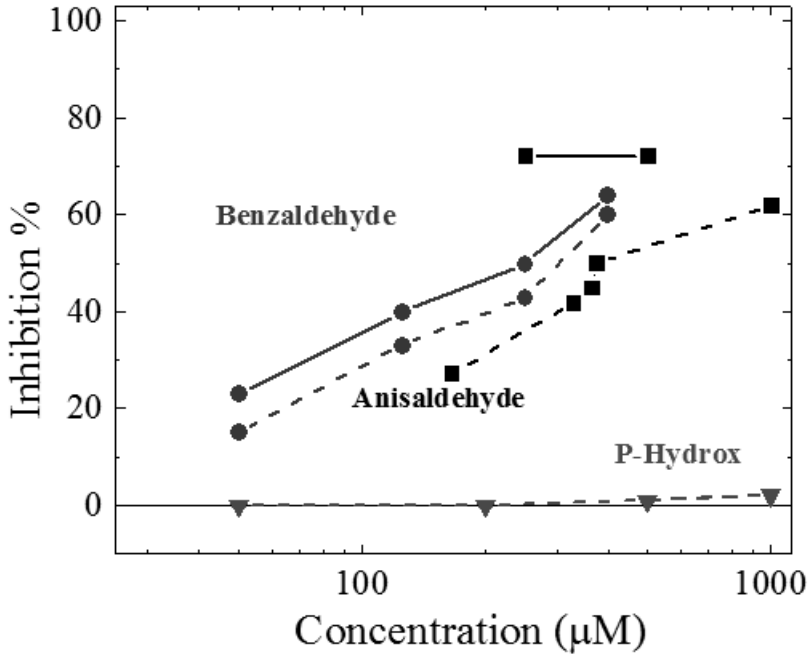

Figure 3.7 Percentage of enzyme inhibition of *para*-benzaldehydes on a L-DOPA substrate

Fluorescence assays probing the tyrosinase active site were performed, measured with test solutions of 25 μM and 100 μM anisaldehyde, tyrosinase, and substrates of L-DOPA and L-tyrosine (Table 3.2). In all of the measurements, the fluorescence signal decreased relative to the control in the first 10 minutes, supporting that most of the inhibitory activity occurred during the first 10-12 minutes of the reaction. This coincides with the conversion of the enzyme to the more active form. In both cases, anisaldehyde decreased the fluorescence signal, but much less than benzaldehyde, despite having three times higher concentration, suggesting less bonding near the active site, consistent with the weaker inhibitory activity.

Time	100μManisaldehyde with L-DOPA	L-DOPA Control	100μManisaldehyde with L-tyrosine	L-tyrosine control
0	100	100	100	100
5	83	95	78	97
15	82	-	82	87
20	107	-	84	84
30	89	125	-	85
50				-
60			83	85

Table 3.2 Percentage of fluorescence of oxidation on L-tyrosine and L-DOPA by tyrosinase on anisaldehyde

These results indicate that the moiety indeed plays a role in determining inhibitory activity. To further investigate the role of the *para*-position moiety, we compared a structural similar compound *para*-hydroxybenzaldehyde(4-hydroxybenzaldehyde).

Inhibitory assays performed with 4-hydroxybenzaldehyde (**3**) caused an extended lag phase up to 5 minutes beyond the control on L-tyrosine, suggesting strong inhibitory activity specifically against the Eoxy or Edeoxy confirmations. In UV-VIS inhibition assays, there was a dose dependent inhibition of monophenolase activity, resulting in dopachrome formation being reduced by 20%,31%,53% and 82% at 125 µM, 250 µM, 500 µM and 1000 µM (Figure 3.8). Following the oxygen consumption in these assays (Figure 9), 4-hydroxybenzaldehyde was a dose dependent inhibitor 17%, 33%, and 66% for 250 µM, 500 µM and 1000 µM.A preincubation increased 4-hydroxybenzaldehyde activity by 17%,

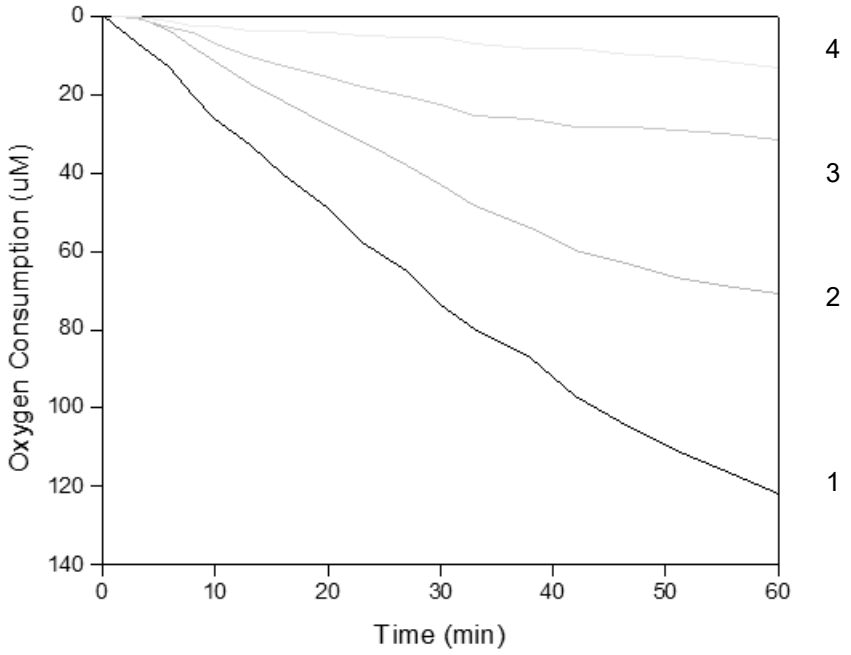

Figure 3.8 Oxygen consumption of oxidation of L-tyrosine (100 µM)(1) by mushroom tyrosinase in presence of *p*-hydroxybenzaldehyde at 100 µM (1) 500 µM (2) and 1000 µM (3)

In addition, the inhibitory activityof 4-hydroxybenzaldehyde on the tyrosinase catalyzed oxidation of *N*-acetyl-L-tyrosine was examined as an alternative substrate. *N*-acetyl-L-tyrosine was poorly oxidized, demonstrating that 4-hydroxybenzaldehyde inhibited the tyrosinase catalyzed monophenolase oxidation of *N*-acetyl-L-tyrosine (data not shown).

Interestingly, 4-Hydroxybenzaldehyde was not an inhibitor on L-DOPA for concentrations up to 1 mM (Figure 3.8). A preincubation period did not potentiate diphenolase

activity. This is strong evidence that 4-hydroxybenzaldehyde is inactive against the Emet confirmation of tyrosinase, but a strong inhibitor of the Eoxy confirmation.The reaction was followed on the HPLC and the4-hydroxybenzaldehydepeak area was not diminished after an hour (data not shown), indicating it is not being consumed during its inhibition activity. 4-hydroxybenzaldehyde is known to be a weak antioxidant (Wang and others 2015). It is unlikely though that the compound was interfering withredox reactions because we did not see a decrease in dopachrome formation on L-DOPA.

The inhibition reaction on L-tyrosinewas followed usingfluorescence.During the first 10 minutes we observed a significant decrease in fluorescence signal during the conversion from Eoxy to Emet/Edeoxy, similar to benzaldehyde (Table 3.1). Over the 30 minute measurement, there was a decrease in fluorescence of 28% supporting that the compound was binding and is dose dependent which is consistent with 4-hydroxybenzaldehyde. It should be noted that the fluorescence did increase back to 100 % suggesting there is some reversibility in the reaction mechanism. In comparison, fluorescence measurements performed on L-DOPA show a smaller decrease initially (21% v. 54%), and after 30 minutes the fluorescence signal is 3% lower than the control, supporting that the inhibitor does initially interact at the active site but does not the entirety of the assay.

Time (min)	**200µM 4-hydroxybenzaldehyde with L-DOPA**	**L-DOPA Control**	**200µM 4-hydroxybenzaldehyde with L-tyrosine**	**L-tyrosine control**
0	100	100	100	100
10	78.7	95	45.5	97
20	-	-	-	87
30	122.7	125	72.7	84
50				-
60			100	85

Table 3.3 Fluorescence of 4-hydroxybenzaldehyde at 200µM on L-DOPA and L-tyrosine

Two other single moiety aromatic aldehydes were also tested: 3-hydroxybenzaldehyde (**4**) and 2-hydroxybenzaldehyde (**5**). These compounds were moderate inhibitors on L-tyrosine, reducing activity to 54% and 52%, respectively, when applied to L-tyrosine at a concentration of 1 mM.Preincubation did not increase these compounds activity on L-tyrosine. On L-DOPA, 3-hydroxybenzaldehyde was not strong inhibitor, reducing activity by 3% at 1 mM.

These results show benzaldeyde, 4-methoxybenzaldehyde (anisaldehyde) and 4-hydroxybenzaldehyde (*p*-hydroxy), 3-hydroxybenzaldehyde, and 2-hydroxybenzaldehyde are all effective inhibitors. Compounds (**1**) and (**2**)were shown to be comparable inhibitors on L-DOPA and L-tyrosine, while (**3-5**) were not an inhibitor of L-DOPA, but was a strong inhibitor of L-tyrosine. This suggests that hydroxyl moiety causes the benzaldehyde to selectively interact with the Eoxy form confirmation of the enzyme conformation.

3,4-benzaldehydes

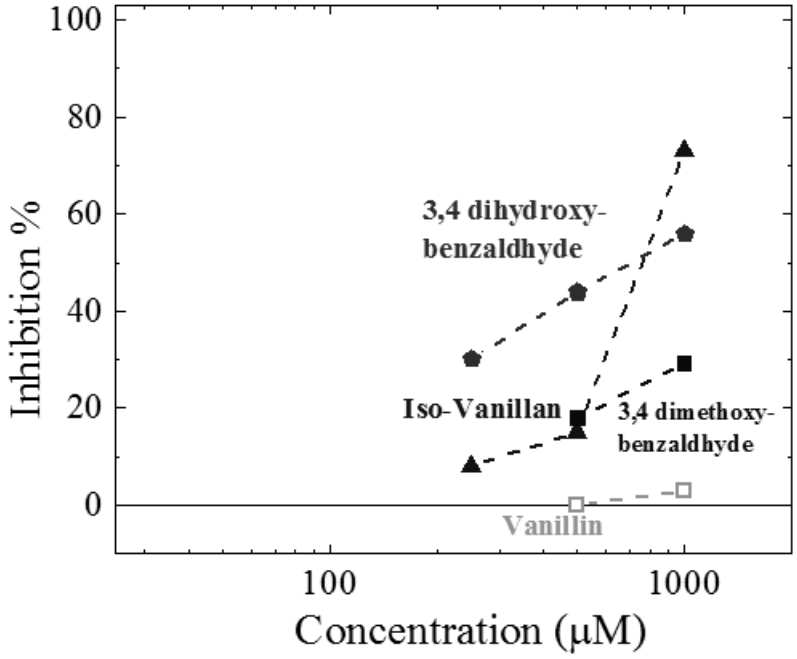

Figure 3.9 Percentage of enzyme inhibition of 3,4 benzaldehydes on L-tyrosine

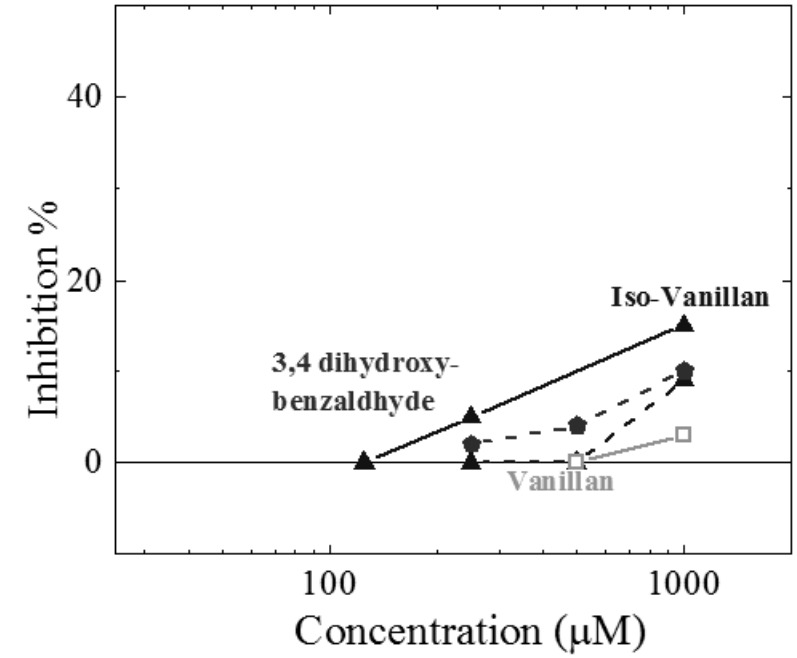

Figure 3.10 Percentage of enzyme inhibition of 3,4 benzaldehydes on L-DOPA

The previous section showed that the addition of a single moiety had a significant effect on the inhibitory activity of our benzaldehyde derived compounds, including making them inhibit only one enzyme confirmation. Based on this observation, it is expected that adding moieties to the aromatic ring may further affect the inhibitory activity. In this section, we build on anisaldehyde (**2**) and p-hydroxybenzaldehyde (**3**) and introduce an additional -OCH_3 and –OH moieties in the *meta*-position. The tested compounds included 4-methoxy-3-hydroxybenzaldehyde (isovanillin) (**6**), 4-hydroxy-3-methoxybenzaldehyde (vanillin) (**7**) 3,4-dihydroxybenzaldehyde (**8**), and 3,4-dimethoxybenzaldehyde (**9**).Inhibitory and preincubation assays performed on L-tyrosine (Figure 3.9) show that some of the examined compounds were effective inhibitors, but assays performed on L-DOPA (Figure 3.10) show an activity of less-than 15% for all the compounds. The specifics for these compounds are discussed below.

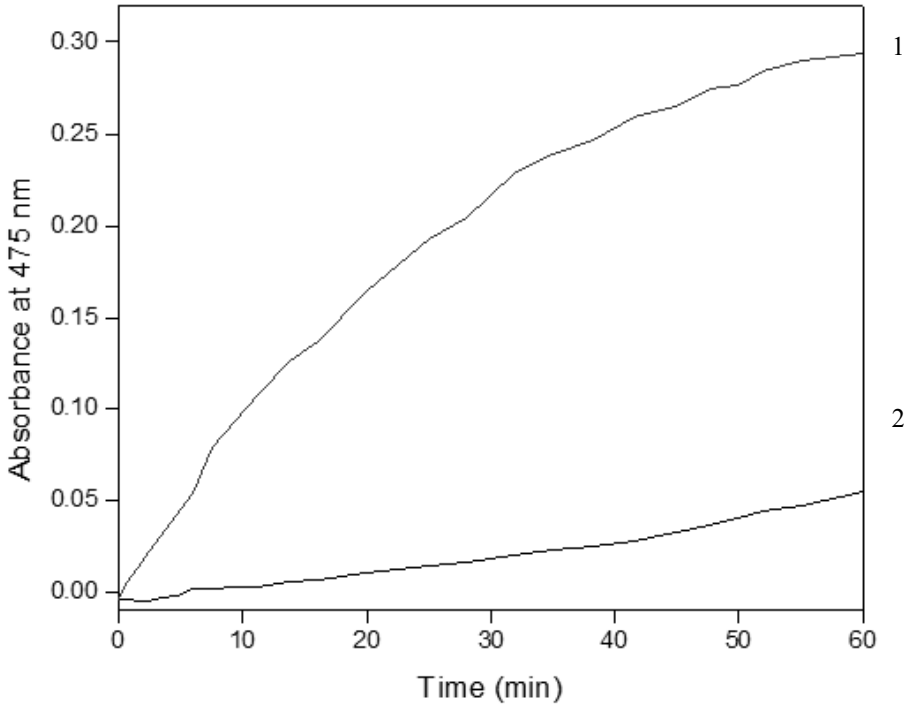

Figure 3.11 UV-Vis absorption isovanillin at 1000 µM (2) in the presence of L-tyrosine (500 µM)(1)

Isovanillin (**6**) was an exceptionally strong monophenolase inhibitor on L-tyrosine (Figure 3.11). When measuring dopachrome formation on L-tyrosine with a 1 mM isovanillin inhibitor, the lag phase persisted for 10minutes (Figure 3.11), much longer than the control. After 60minutes, dopachrome formation was inhibited by 73% compared to the control. Monitoring

oxygen consumption during the same reaction, the test solution inhibited with isovanillin consumed little oxygen during the lag phase (e.g. the first 10 minutes) and at 60 minutes, oxygen consumption was reduced by 15%. Interestingly, the oxygen consumption measured at 500 μM and 1000 μM concentrations consumed identical amounts of oxygen, while concentrations of 250 μM were not reduced at all relative to the control, after 60 minutes. Preincubation of isovanillin with L-tyrosine increased oxygen consumption by 8% and 10% at 250 μM and 500 μM.

Isovanillin reduced tyrosinase activity on L-DOPA by 9% at 1000 μM when measuring oxygen consumption and dopachrome formation (Figure 3.10), and thus was considered a poor inhibitor. Preincubating tyrosinase with isovanillin for 10-minutes increased inhibitory activity on L-DOPA to 16% measuring dopachrome formation but only 6% on the oxygen monitor. The fluorescence assays showed a decrease in fluorescence of 30% over 30 minutes, supporting that isovanillin was binding at the active site.

Time (min)	1000μM Isovanillin with L-tyrosine	1000 μM Vanillin with L-tyrosine	L-tyrosine control
0	100	100	100
10	78.7	100	97
20	-	101	87
30	70	100	84
60	57	102	85

Table 3.4 Percentage of fluorescence of oxidation on L-DOPA and L-tyrosine by tyrosinase on isovanillin and vanillin at 1000μM

The structural analogue of isovanillin is vanillin (**7**), which has the methoxy- and hydroxyl- moieties exchanged. This compound showed weak monophenolase and diphenolase inhibitor activity not exceeding 3% (Figures 3.9 and 3.10). Additionally, preincubation of vanillin did not potentiate additional activity. The HPLC analysis showed L-DOPA was oxidized in the presence of vanillin (data not shown) so it was not interfering with the oxidation process. Fluorescence of vanillin at 150 μM on L-tyrosine (Table 3.4) matches the control throughout the entire 30 minute measurement, confirming that the compound was not strongly interacting at the enzyme active. This example (the activity of isovanillin and vanillin) strongly emphasizes the crucial organization of the moieties in determining inhibitory efficacy. Simply exchanging the location of the moieties is demonstrated to entirely suppress inhibitory activity.

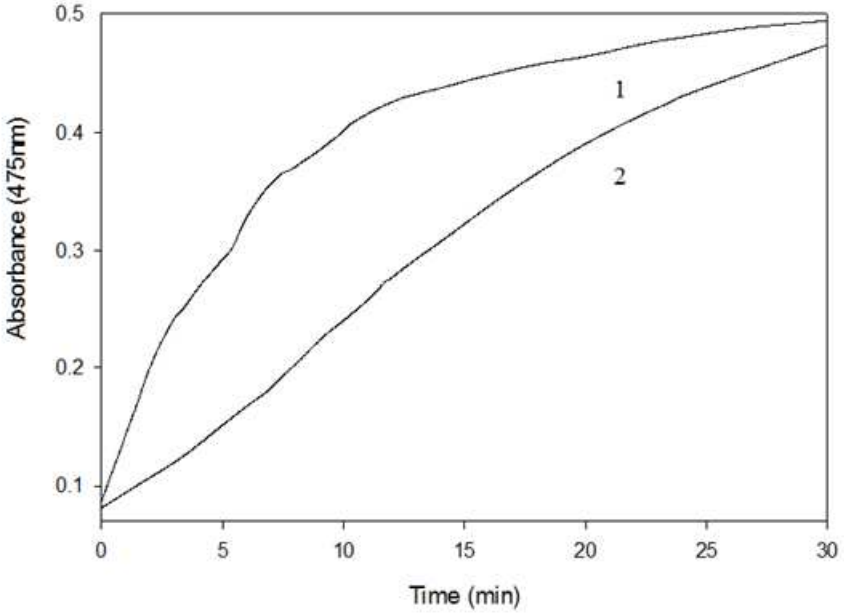

Figure 3.12 Absorbance of Dopachrome at 475nm in the presence of 3,4-dihydroxybenzaldhyde at 1000 μM (2) in the presence of L-DOPA (250 μM)(1)

In both the single- and 3,4 benzaldehydes, the hydroxyl moieties were shown to be more effective inhibitors than the methoxy groups on L-tyrosine suggesting they interfere more with the hydroxylation process. At 1000 μM 3,4-dihydroxybenzaldehyde (**8**), 3-hydroxybenzaldehyde (**4**) and 2-hydroxybenzaldehyde (**5**) were equally active inhibitors on L-tyrosine, reducing activity to 53%, 54% and 52% respectively. This shows that removing the 4-hydroxy did not reduce inhibitory activity. Preincubation did not increase these compounds activity on L-tyrosine so they are not likely enzyme inactivators. On L-DOPA 3,4-dihydroxybenzaldehyde and 3-hydroxybenzaldehydewere not strong inhibitors after 30 minutes, reducing activity by 10% and 3%, respectively, at 1000 μM. However, the reaction inhibited by 3,4-dihydroxybenzaldehyde initially does inhibit oxygen consumption and dopachrome formation (Figure 3.12). For example, after 2:50, dopachrome formation is 50% inhibited. These results suggest 3,4-dihydroxybenzaldehyde inhibits by a reversible mechanism, allowing the enzyme activity to recover. A 10 minute preincubation period on L-DOPA did not potentiate additional 3,4-dihydroxybenzaldehyde oxygen consumption., suggesting the inhibition mechanism does not require additional oxygen.

The methoxy moieties were weaker inhibitors, 3,4-dimethoxybenzaldehyde (**9**) was a moderate inhibitor on L-tyrosine reducing, enzyme activity by 32% at 1 mM. For comparison anisaldehyde (4-methoxybenzaldehyde) at the same concentration reduced tyrosinase activity to 69%.

3,5-Benzaldehyde

Motivated by the example of (iso)vanillin, we continued to investigate the structure-activity relationship by considering 3,5 benzaldehydes. The above work performed on single moiety compounds suggested that isolated methoxy and hydroxyl groups did not suppress activity. Motivated by this, the 3,5 benzaldehydes have two moieties with no neighbors, which may make them accessible for additional binding and inhibition activity. However, the results, discussed in detail below, show that these were the least active of the examined compounds.

Both the single-moiety and 3,4 benzaldehydes showed that the compounds with hydroxyl groups were stronger inhibitors than those with methoxy moieties, suggesting that the –OH groups interfere with the enzyme. It is also notable that the 3,4-dihydroxybenzaldehyde, and 3-hydroxybenzaldehyde and 4-hydroxybenzaldehyde all had similar inhibitory activity (≈53% at 1 mM) , suggesting that the additional hydroxyl group does not affect activity.

The first 3,5 benzaldehyde tested had two hydroxyl groups, 3,5-dihydroxybenzaldehyde (**10**). This compound slightly extended the lag phase, and inhibited dopachrome formation by 52% at 1 mM after 30 minutes, showing similar activity as the other hydroxyl compounds. Oxygen consumption assays showed a 42% reduced oxygen consumption (Figure 3.13). A 10-minutepreincubation did not increase activity. The fact that 3,5-dihydroxybenzaldehyde and 3-hydroxybenzaldehyde have similar inhibitory efficacy suggests that the -OH group plays a support role in determining efficacy, rather than a direct role. It also implies that the -OH group in 3,5-dihydroxybenzaldehyde is not consumed during the inhibition process, as the product would be 3-hydroxybenzaldehyde; we would expect twice the inhibitory activity for the same concentration. It should be noted that 3,5-dihydroxybenzaldehyde did not inhibit oxidation on L-DOPA, nor did preinciubation potentiate any activity.

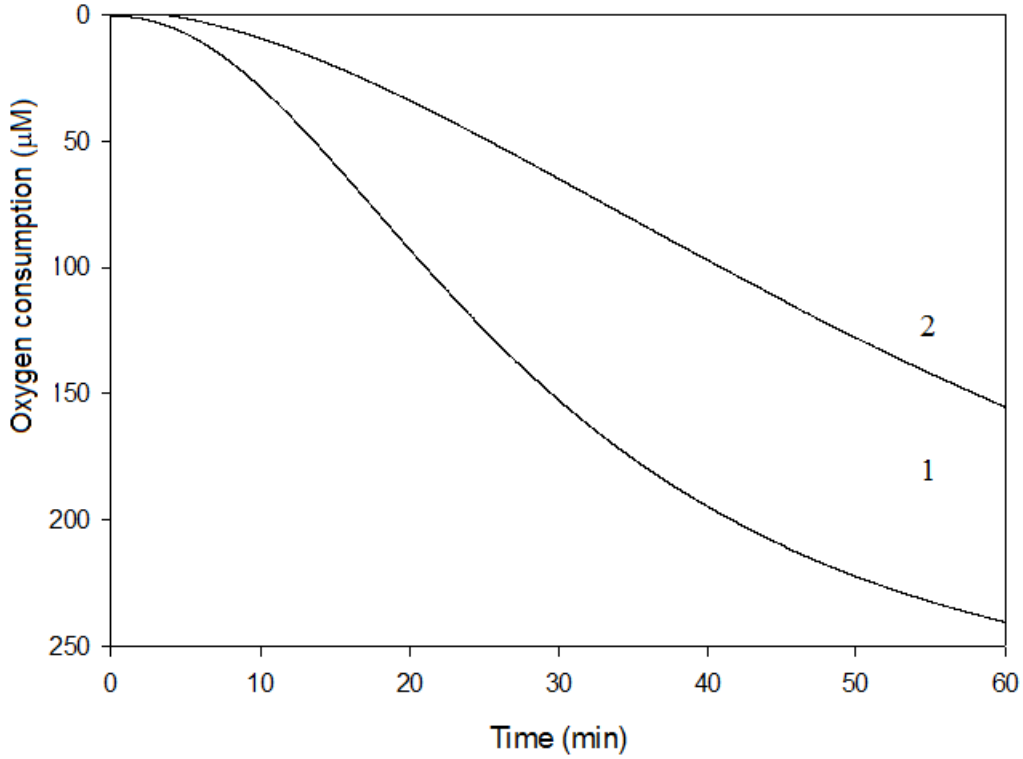

Figure 3.13 Oxygen consumption of 3,5-dihyroxybenzaldehyde at 1000 µM in the presence of L-tyrosine at (500 µM)(2)

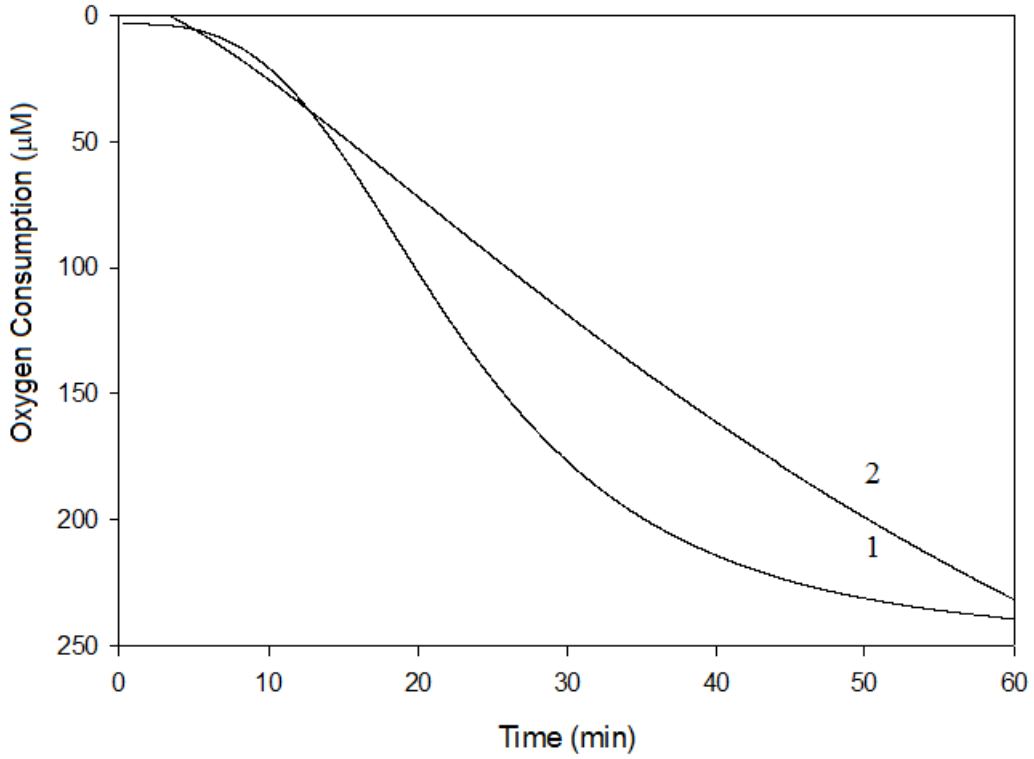

Figure 3.14 Oxygen consumption of 3,5 dimethoxybenzaldehyde at 1000 500 µM in the presence of L-tyrosine at (500 µM)

3,5-dimethoxybenzaldehyde (**11**), which has two -OCH_3 groupslocated at the *meta*-position, was shown to be a weak monophenolase inhibitor. Dopachrome formation and oxygen consumption were both suppressed by <5% on L-tyrosine at 1000 µM (Figure 3.14). Inhibition assays performed on L-DOPA also showed weak suppression of oxygen consumption, less-than 14% (Figure 3.15), indicating it is a weak diphenolase inhibitor. Notably, similar to the 3,4-dihydroxybenzaldehyde, 3,5-dimethoxybenzaldehyde (**11**) at 500 µM initially suppressed oxygen consumption on both substrates by 35% at 30 minutes, but recovered by 60 minutes. Preincubation of 3,5-dimethoxybenzaldehyde with L-DOPA at 1 mM did not increased activity suggesting this compound acts as a weak inhibitor.

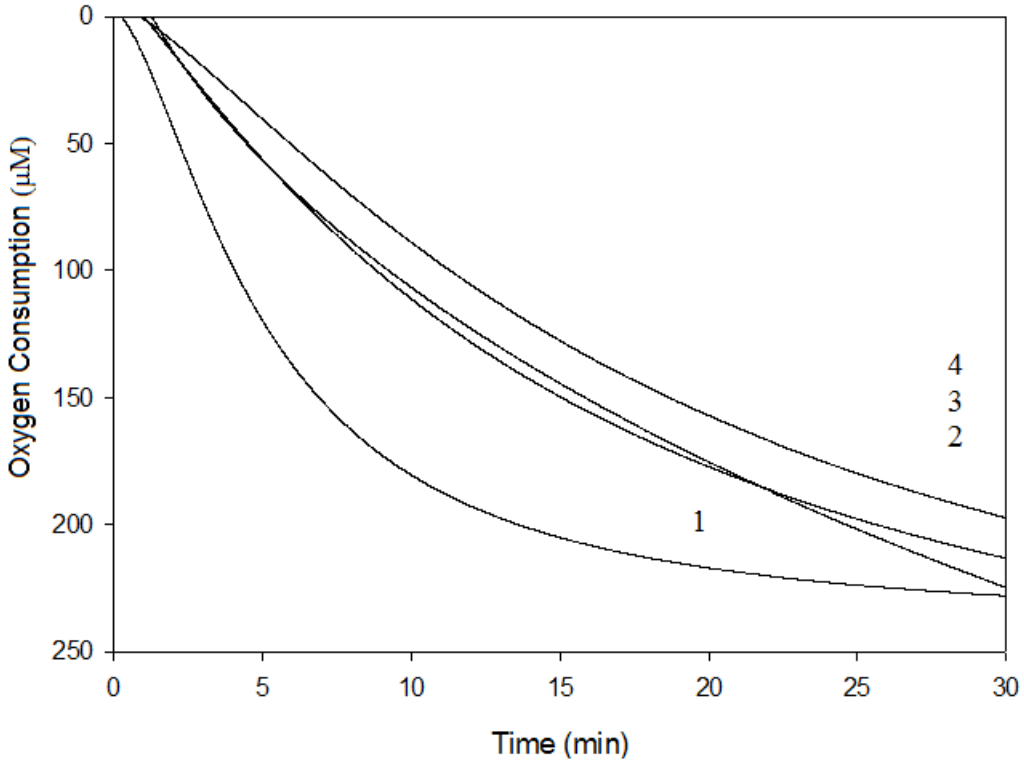

Figure 3.15 Oxygen consumption of 3,5-dimethoxybenzaldehyde at 0.25mM (2), 0.5mM (3) and 1mM (4) in the presence of L-DOPA at 0.250mM (1)

Fluorescence measurements performed on 3,5-dimethoxybenzaldehyde showed decreased intensity by 38% after only 5 minutes, supporting that initially the inhibitor binds at the active site. The fluorescence continues to decrease until 15 minutes then reversed, ending at 85%. This suggests that the compound is interacting at the tyrosinase active site, slightly suppressing enzyme activity but this is interaction maybe reversible.

Time (minutes)	1 mM3,5-dimethoxybenzaldehyde with L-DOPA	L-DOPA Control
0	100	100
5	62	95
15	58	-
30	85	125

Table 3.5 Percentage fluorescence on L-DOPA of 3,5-dimethoxybenzaldehyde at 1 mM

Above, the inhibitory properties of single moiety (2, 3, or 4) benzaldehydes and two moiety 3,5 benzaldehydes have been investigated. This section investigates 2,4 benzaldehydes, with hydroxyl or methoxy groups located at the *para*- and *ortho*-positions; moieties located at the *ortho*-position could block access to the aldehyde, which was suggested to be the critical reactive end-member (demonstrated with benzaldehyde and in Chapter 2). Alternative, electrostatic forces originating from these electronegative (or electropositive) sites could aid in drawing the inhibitor into the active site and orienting it, and thus may enhance the activity. The results, discussed in detail below, show that some of these compounds are extremely effective inhibitors; 2-hydroxy, 4-methoxybenzaldehyde (HMB) was demonstrated to be as effective inhibitor as its parent compound, benzaldehyde (Figure 3.1).

2,4-benzaldehydes

Above, the inhibitory properties of single moiety (2, 3, or 4) benzaldehydes and two moiety 3,5 benzaldehydes have been investigated. This section investigates 2,4 benzaldehydes, with hydroxyl or methoxy groups located at the *para*- and *ortho*-positions;moieties located at the *ortho*-position could block access to the aldehyde, which was suggested to be the critical reactive end-member (demonstrated with benzaldehyde and in Chapter 2). Alternative, electrostatic forces originating from these electronegative (or electropositive) sites could aid in drawing the inhibitor into the active site and orienting it, and thus may enhance the activity. The results, discussed in detail below, show that some of these compounds are extremely effective inhibitors; 2-hydroxy-4-methoxybenzaldehyde (HMB) was demonstrated to be as effective inhibitor as its parent compound, benzaldehyde (Figure 3.2).

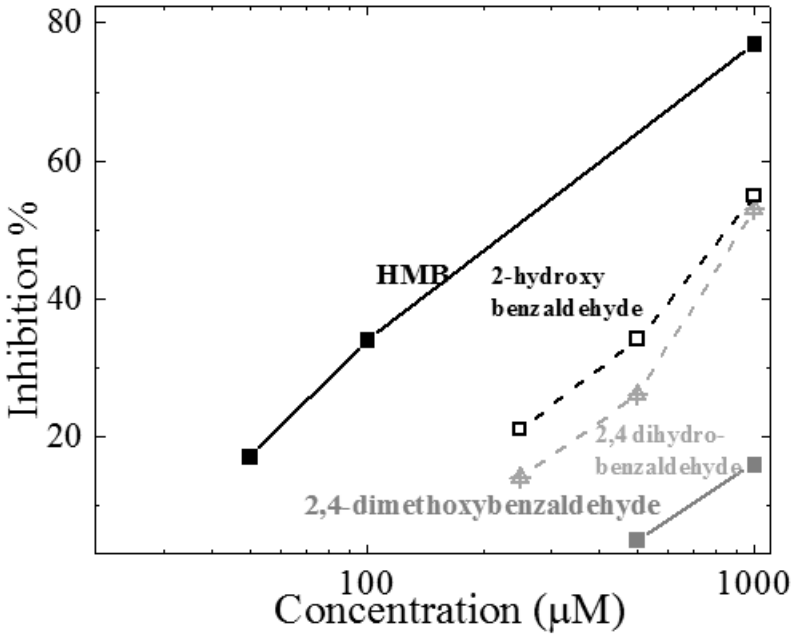

Figure 3.16 Percentage of enzyme activity on L-tyrosine (500 μM) by 2,4-benzaldehydes

The first tested compound was HMB (**12**), which is structurally similar to anisaldehyde, but with a -OH at the *ortho*-position. This compound had strong monophenolase activity when following the oxidation of L-tyrosine, inhibiting dopachrome formation by 17%, 34% and 77% for 50μM, 100μM and 1000μM respectively (Figure 3.16). This compound showed comparable to the parent benzaldehyde. Inhibitory assays were performed using HMB on *N*-acetyl-L-tyrosine. These results confirmed that the substrate was not oxidized, indicating that HMB inhibited the tyrosinase catalyzed monophenolase oxidation.

HMB had a unique extended lag phase on L-DOPA, and significantly suppressed the initial rate of the dopachrome formation up to 10 minutes. Similar to 3,4-dihydroxybenzaldehyde, 3,5-dimethoxybenzaldehyde, after a 60 minutes dopachrome formation recovered and approached the control measurement. Preincubation of HMB with tyrosinase for 10 minutes and 30 minutes (Figure 3.17) showed enhanced activity, suggesting it is an inhibitor. The strong activity against L-tyrosine, and extended lag phase suggests HMB likely inhibits the Eoxy conformation. We compared 2,4-dimethoxybenzaldehyde to determine if the methoxy group effected activity and after 60 minutes enzyme activity was only reduced by 16% at 1000 μM on L-tyrosine.

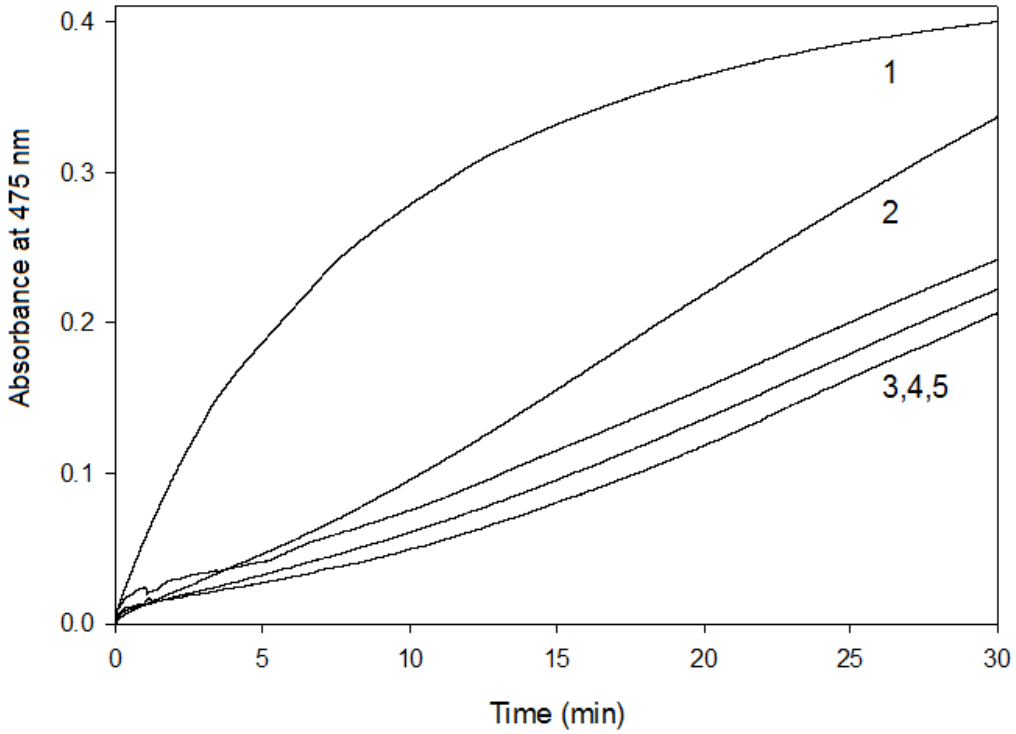

Figure 3.17 Dopachrome formation in the presence of HMB (2-hydroxy-4-methoxybenzaldehyde) either preincubated for 30minutes at 1000µM(5) or 500µM (2), Inhibition at 1000 µM(3) and preincubated for 10minutes at 1000 µM(4). L-DOPA (500 µM)(1)

Based on the previous works on L-tyrosine inhibitors, we expect HMB to bind at the active site. Indeed, fluorescence measurements showed HMB decreased fluorescence by 34% after 30 minutes compared to the control, supporting that it is able to bind at the tyrosinase active site and displace the fluorescence probe (Table 3.6).

Time (min)	500µM HMB with L-tyrosine	500 µM 2,4-dimethoxybenzaldehyde with L-tyrosine	L-tyrosine control
0	100	100	100
10	88	55	97
20	72	101	87
30	66	100	84
60	55	113	85

Table 3.6 Fluorescence change over 30 minutes assay period of HMB and 2,4-dimethoxybenzaldehyde

Recalling that anisaldehyde (4-methoxybenzaldehyde) was a strong inhibitor, as was isovanillin (3-hydroxy, 4-methoxybenzaldehyde) and HMB (2-hydroxy, 4-methoxybenzaldehyde), suggests that the *para*-position methoxy group may encourage inhibitory activity. To test this, weperformed inhibitory assays with 2,4-dimethoxybenzaldehyde (**13**), which has both *para*-position and *ortho*-position methoxy groups. Inhibition assays performed on L-tyrosine, at 1000 μM showed enzyme activity was only reduced by 16% after 60 minutes. Fluorescence measurements performed on 2,4-dimethoxybenzaldehyde show initially binding but by the end of the assay period was not longer interacting at the active site, further supporting the methoxy groups are not as strong contributors to inhibition activity as their hydroxyl counter parts.

Aromatic chloro aldehydes

The last group of compounds have a chlorine moiety, and are not natural products. The chlorinated analogue of 3,5-dihydrobenzaldehyde is 3,5-dichlorobenzaldehyde (**14**). This compoundsuppressedmonphenolase activity by 3% against L-tyrosine at 1000 μM, compared to 3,5-dihydrobenzaldehyde, which showed suppression of 55% at 1 mM.Above, it was suggested that a *para*-positioned methoxy group may promote activity, thus 3,5-Dichloro-4-methoxybenzaldehyde (**15**) was investigated for activity. While the activity was better than its non-methoxy counterpart, dopachrome formation was suppressed by only 10% at 1000 μM. Lastly, the chlorinated analogue of vanillin, 3-chloro-4-methoxybenzaldehyde (**16**), was tested. This compound also showed a 10% reduction in dopachrome formation at 1000 μM .Interestingly, this is better than vanillin, but still would be classified as a weak inhibitor. The chlorine moieties are expected to be non-reactive, thus, these results emphasize the role of the active moieties (-OH and -OCH_3) in determining inhibitory activity. This may be through direct interactions, stabilizing/destabilizing the aromatic ring, providing electrostatic forces, or by manipulating the electron distributions in the compound.

Insect

Compound	Actual weight change (g)± SD	Mean rank
Control	0.0160± 0.031	118
Anisaldehyde	-0.0004± 0.001	5.8
4-hydroxybenaldehyde	0.0006± 0.0016	19
3,4-dimethoxybenzaldehye	0.0009± 0.0016	11.4
Isovanillin	0.00164± 0.0013	22
3,4-dihydroxybenzaldehyde	0.00206± 0.0013	19
Vanillin	0.0027± 0.0003	20.6

Table 3.7 Change in larval weight based on diet incorporation, concentrations were 8 mM unless otherwise noted. N=5 for each treatment level

Several of the tested compounds were selected for organism-level testing in *S. exigua*, the beet armyworm, a common agricultural pest insect. A diet incorporation assay was performed by including 8 mM of the tested compound into their diet. To determine efficacy, the percent weight change during their late 2nd/early 3rdinstar larval stages was measured. The results were not normally distributed, a Shapiro-Wilks test revealed a p>0.001. We then tested the data with a Kruskal Wallis test and the mean ranking (Table 3.7) showing was a statistical difference between the treatments and control (H= 15.67, DF=6, p=0.0155). The results do loosely follow the results from the cell-free assays. Specifically, anisaldehyde was the strongest inhibitor tested at the organism-level, and also showed the suppression of insect growth at -22% (Table 3.7) loss in weight change. The next strongest inhibitors were 4-hydroxybenzaldehyde and lastly vanillin. Organisms tested with these compounds all showed positive weight change, but greatly suppressed compared to the control (<50%). Vanillin was the weakest compound tested, and also had the smallest effect on insect growth, <10% compared to the control. The compound 3,4-dimethoxybenzaldehyde was the only stand-out, with showing significant inhibition of the insect growth, but showing little activity in the cell-free experiments. This is likely a consequence of the complexity within these organisms; 3,4-dimethoxybenzaldehyde may inhibit other biological functions within the insect, but this is outside of the scope of our work. Contact assays showed no mortality for any of the compounds, indicating the insect epidermis is robust against these chemicals and/or the insect midgut is particularly susceptible.

Melanoma cell

Compounds tested	IC_{50} (μM)	log*P*
Benzaldehyde	2000	1.38
4-methoxybenzaldehyde	815	1.64
4-hydroxybenzaldehyde	720	1.27
3-hydroxy-4-methoxybenzaldehyde	705	1.10
3-methoxy-4-hydroxybenzaldehyde	428	1.28
2,4-dihydroxybenzaldehyde	289	0.72
2-hydroxy-4-methoxybenzaldehyde	187	1.4
3-Chloro-4-methoxybenzaldehyde	179	-
2,4-Dimethoxybenzaldehyde	86	1.61
3,5-Dichloro-4-methoxybenzaldehyde	52	2.71

Table 3.8 Cytotoxicity against B16-F10 melanoma cells and log*P* values of benzaldehyde derivatives

In addition to organism-level testing and cell-free testing, several of the compounds were tested for melanogenesis inhibition in cultured B16-F10 murine melanoma cells. Melanin formation and cell viability were determined, and an IC50 calculated (Table 3.8).The compound 3,5-Dichloro-4-methoxybenzaldehyde (IC50 of 52μM) and 2,4-dimethoxybenzaldehyde (IC50 of 86 μM) had the lowest IC50 and showed no melanin inhibition at these concentrations. The compound 2-hydroxy-4-methoxybenzaldehye (HMB) showed a higher IC50 of 187 μM and, critically, showed a decrease in the per-cell melanin formation by 20% at 25μM (Figure 3.18). In the cell-free testing HMB was shown to be one of the strongest inhibitors, even at low concentrations, acting on the Eoxy confirmation of the enzyme. Replacing the *para*-positioned methoxy group with a hydroxyl, forming 2,4-dihydroxybenzaldehyde, decreased activity in the cell free experiments (Table 3.8). In the cellular-level testing, this replacement more than doubled the IC50 to 289 μM, but preserved the decrease in melanin formation (Figure 3.18). Of significance, there is a 20% reduction in melanin formation before the onset of any statistically significant cell death at 100μM. Lastly, we recall that removing the *ortho*-position hydroxyl group, forming 4-hydroxybenzaldehyde (*p*-hydroxybenzaldehyde) significantly increased the inhibitory activity in cell free experiments (Figure 3.19). Cellular-level testing showed that *p*-hydroxy has double the IC50 of 2,4-dihydroxybenzaldehyde at 720μM, however, it loses its ability to inhibit melanin formation, and in-fact increases melanin formation (Table 3.20). The remaining compounds were significantly weaker cytotoxic compounds and poor melanin suppressers. Cytotoxicity was generally shown to increase inversely with tyrosinase inhibitory activity.

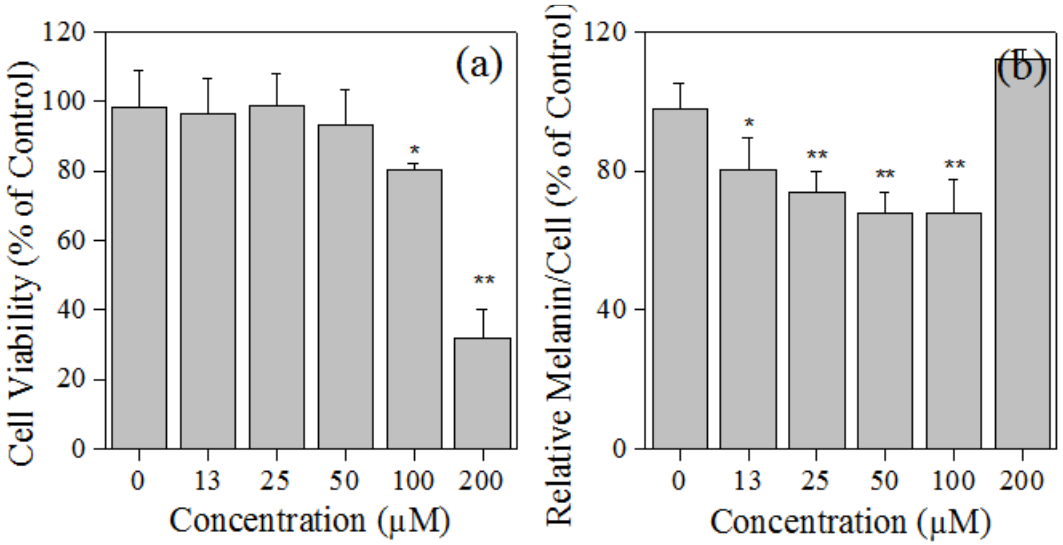

Figure 3.18 (a) Viability of melanoma cells after treatment with 2-hydroxy-4-methoxybenzaldehye (HMB (b) Cellular melanin content of melanoma cells after treatment with 2-hydroxy-4-methoxybenzaldehye HMB

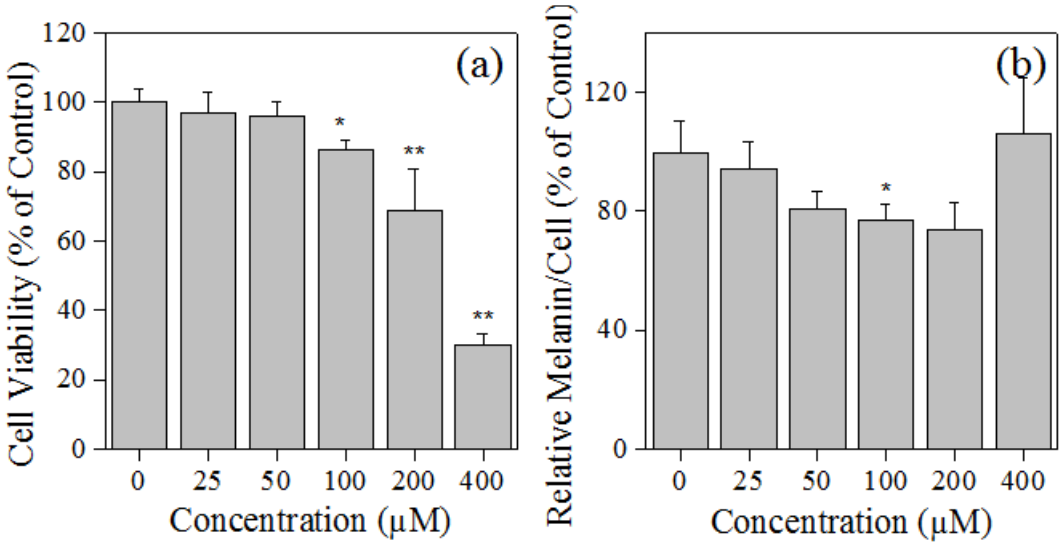

Figure 3.19 (a) Viability of melanoma cells after treatment with 2,4-dihydroxybenzaldehyde,(b) Cellular melanin content of melanoma cells after treatment with 2,4-dihydroxybenzaldehyde

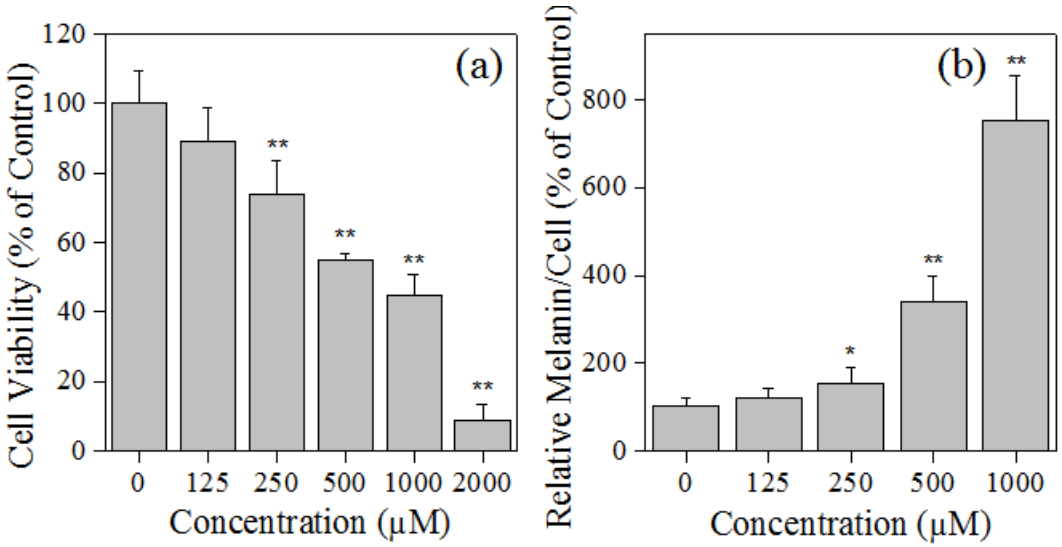

Figure 3.20 (a) Viability of melanoma cells after treatment with 4-hydroxybenzaldehyde (b) Cellular melanin content of melanoma cells after treatment with 4-hydroxybenzaldehyde

Discussion

The above works investigated the structure-activity relationship of 16 benzaldehyde-derived compounds as tyrosinase inhibitors. These compounds generally had hydroxyl- and methoxy moities added to the aromatic ring at the *ortho*-, *meta*-, and *para*-positions. Activity was tested by inhibitory and pre-incubation assays. Three compounds stood out as strong inhibitors: benzaldehyde, 2-hydroxy-4-methoxybenzaldehye (HMB), and 4-hydroxybenzaldehye (p-hydroxybenzaldehyde) in cell-free testing (Figure 2). With the exception of benzaldehyde, these compounds, and several others to a lesser degree, showed strong inhibitory activity specifically on L-tyrosine substrates, but little activity against L-DOPA, suggesting they inhibit specifically the Eoxy confirmation of the enzyme (Figure 3.2); benzaldehyde was the only inhibitor which acted strongly against L-DOPA (Figure 3.5). Organism-level testing showed insect viability suggestively coupled to growth inhibition. Cellular-level testing showed most of the chemicals to be cytotoxic before melanogenesis was inhibited. However, one chemical of note, 2,4-dihydroxybenzaldehye, showed inhibition activity without the compromising cell viability, making it a promising candidate for treatments. In the following section, we interpret the underlying mechanism responsible for the above results.

Inhibitory Mechanisms

Benzaldehyde is the simplest aromatic aldehyde and was a strong tyrosinase inhibitor of both monphenolase and diphenolase activity. The benzene ring is less reactive to electrophilic attack because the aldehyde head moiety is an electron-withdrawing group (LoPachin and others 2009), thus we expect the aldehyde head group to be the source of inhibitory activity. Empirically, we observed weak enhancement of the inhibitory activity in the preincubation assays (<10%), suggesting that benzaldehyde inhibits tyrosinase directly, by binding (possibly reversibly) at the active site, as supported by fluorescence.

It is important to note that the conformation of tyrosinase determines its activity on each substrate; there are three relevant conformations: Emet, Eoxy, and Edeoxy. The Emet structure has a single protonated oxygen bound to the one of the copper ions located at the active site (Ramsden and Riley 2014); Emet accounts for ≈85% of the enzyme conformation (Chang 2009) and is active only on L-DOPA (a diphenolase substrate). The Eoxy structure has a pair of oxygen ions each bound to both copper ions, and accounts for ≈15% of the enzyme conformation and is active on both L-DOPA and L-Tyrosine. Lastly, the Edeoxy confirmation has no oxygen at the active site and is not active on either substrate. Enzyme conformation has been previously identified as crucial to the inhibitory activity of benzaldehyde, which has been reported as a non-competitive inhibitor (Kubo and others 2003b) against L-DOPA (catalyzed by Emet and Eoxy).

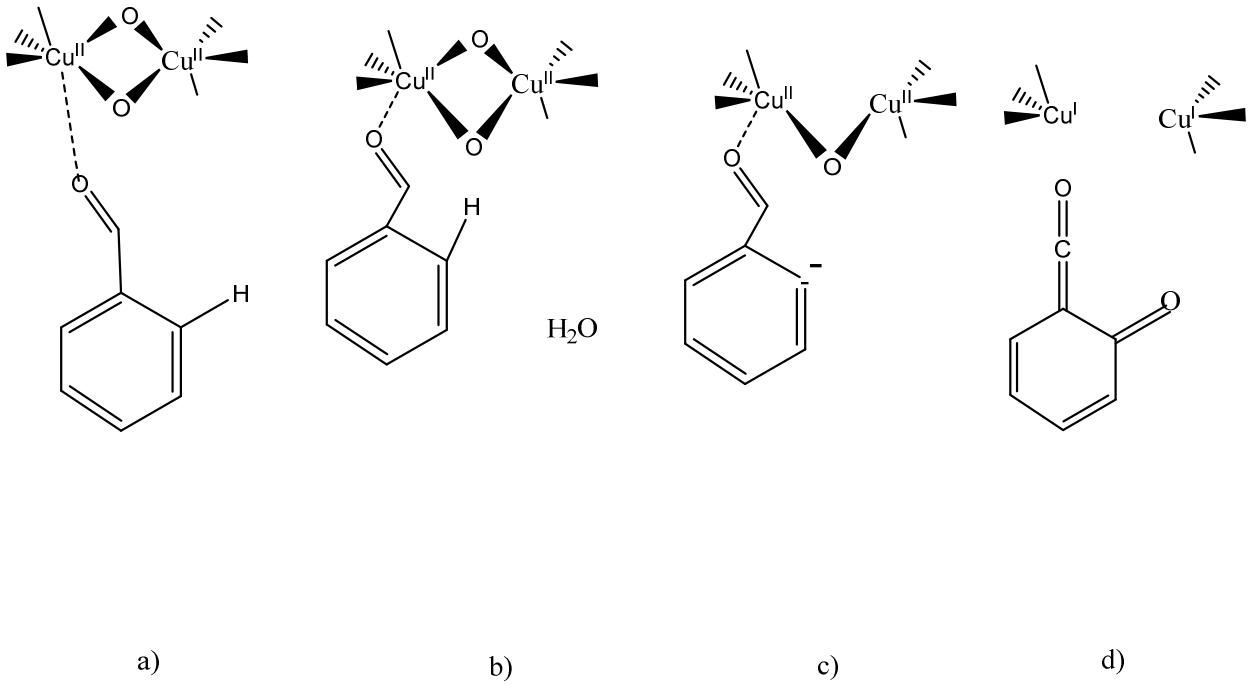

Figure 3.21 Proposed benzaldehyde inhibition mechanism

We propose that the aldehyde head group is converting Eoxy to inactive Edeoxy, and in doing so suppressing both L-tyrosine and L-DOPA catalyzation, and reducing the observed activity on both substrates. In our proposed mechanism the strongly electronegative oxygen on the aldehyde is attracted to the two electropositive copper ions in the Eoxy (Cu+2) state (Figure 3.21a). This specific activity is supported by previously reported x-ray crystallography results that showed the primary oxygen moiety on tropholone (2-hydroxyl-cycloheptatrien-1-one, a structurally similar analogue to benzaldehyde) would bind to a copper ion located at the active site (Ismaya and others 2011). The hydrogen from the aldehyde and the lone hydrogen at the two position on the aromatic ring are electrostatically attracted towards the bound oxygen within the active site, forming a water molecule which is then released (Figure 3.21b). A similar water release occurs when Eoxy is converted to Emet in the presence of catechols. The resultant electron vacancy at the two position is attracted towards the second copper ion which inserts the remaining oxygen at the two position (Figure 3.21c). The benzaldehyde is thus reduced to 6-(Oxomethylene)-2,4-cyclohexadien-1-one (CAS no. 21083-33-0) and tyrosinase is converted from the Eoxy state to the Edeoxy state. Once the enzyme is in the Edeoxy state it becomes inactive on either substrate.

The above inhibitory mechanism only requires the aldehyde head group and an adjacent protonated carbon, and thus is expected to be valid for all of the tested chemicals. However, this mechanism is only active on the minority (15%) Eoxy state, leaving the (85%) Emet state intact. As a result, this mechanism will strongly inhibit on L-Tyrosine, which can only be oxidized by Eoxy, but will only weakly inhibit activity on L-DOPA, which can be oxidized by either Eoxy or Emet. Indeed, all of the compounds tested, with the exception of vanillin, were shown to be inhibitors of L-Tyrosine at >50%. In comparison, activity on L-DOPA was inhibited by <13.5%

for the majority of compounds examined. Specific inhibitory activity for each compound is expected to be partly determined by their various electron donating or accepting moieties, which will affect the ring's stability. A previous study reported that hydrogen bonding interactions stabilized the Eoxy form of *Streptomyces glaucescens* tyrosinase (Jackman and others 1992). Yet, we suggest the major source of this activity is the depletion of available Eoxy.

The lack of activity shown by most of the aromatic aldehydes acting on the diphenol substrate (L-DOPA) shows that the moieties in the 3,4 or 5 positions do not contribute directly to the activity. However, the structure dependent activity does suggest that they play a crucial role in determining the overall efficacy. One possible explanation relates to the charge distribution in the aromatic ring. Specifically, electron resonance favors the charge density to be higher at the 2 and 4 position on the aromatic ring. Adding a less reactive –OCH3moiety at these positions reduces the reactivity of the aromatic ring, allowing the aldehyde to be the primary reactive site. These compounds (**3, 6, 8, 12, 13, 15, 16**) have notably higher Log *P* values (Table 3.7), meaning they are more hydrophobic, which may encourage the inhibitor to interact more-strongly at the enzyme hydrophobic active site.

Comparison of 3,4 benzaldehydes

To better understand the inhibition mechanism we compared isovanillin, vanillin, 3,4-dihydroxybenzaldehyde and 3,4-dimethoxybenzaldehyde. This comparison helps determine how antagonistic or cooperative the interaction of electron donating groups may affect inhibitor activity.

Isovanillin (3-hydroxy-4-methoxybenzaldehyde) was the most active of the 3,4 compounds on L-DOPA, with 14.7% inhibition activity, and when measured on L-tyrosine showed an unprecedented lag phase up to 10 minutes. An extended lag phase identifies specifically inhibition of the L-tyrosine hydroxylation (and hence the Eoxy confirmation).By comparison, anisaldehyde (4-methoxybenzaldehyde) had the second-longest lag phase. The only difference in the structure of these compounds is the *meta*-position -OH. This pair of compounds demonstrates an additive effect, with additional moieties enhancing activity, which is key in inhibiting enzyme activity. However, switching the *meta*- and *para*-position groups, forming vanillin, entirely suppressed activity. Our initial consideration was that, for isovanillin, the hydroxyl group at the *meta*-position interacts with the copper B site (Ramsden and Riley 2014), resulting in the methoxy group at the *para*-position sterically blocking the copper A site. However, exchanging the hydroxyl and methoxy groups, as is the case for vanillin, does not change this argument, suggesting other factors must be responsible. One possible explanation for the site-dependent activity in vanillin and isovanillin is electron resonance. Specifically, in simple benzaldehyde, the electron resonance favors charge accumulation at the 2 and 4 position, and disfavors charge accumulation at the 3 positions. This results in a site-dependent contribution to the reactivity of the decorating moieties, especially electron donating and accepting groups. In isovanillin, the strongly electron donating hydroxyl group located at the *meta*-position is expected to be more reactive than the more-weakly electron donating methoxy group located at the same (*meta*) site in vanillin. Similarly, the hydroxyl group located at the

para-site in vanillin is expected to be stabilized by the local charge accumulation in the aromatic ring. As a result, isovanillin is expected to show higher activity than its structural analogue vanillin, which indeed is consistent with the data.

In addition to these mechanisms, some of the mechanisms presented in Chapter 2 may also be active. For example, these aromatic aldehydes could be binding at the active site by a Schiff base (Cozzi 2004), which are considered less reversible in this aromatic system.It should be noted that in general the compounds with hydroxyl moieties were generally better at reducing enzyme activity than their methoxy counter parts, likely donating electrons to stabilize the Schiff base. However, we would expect the inhibitory activity to increase with moiety decoration, and no dependence on the moiety location. This is not entirely consistent with our data, and thus may not be the main mechanism in determining activity.

Melanoma cells

For the cell assays, we did identify effective melanogenesis inhibitors, as well as compounds which resulted in cell death. Bioavailability of benzaldehydes is relatively high and they are stable, neutral and able to cross cell membranes. The interfacial region of a membrane is known to establish electrostatic, hydrophobic, and other interactions with various types of small molecules and can explain much of the activity we observed. Regarding cell cytotoxicity, aldehydes are reactive by nature so there are various ways the aldehydes can impair cell activity. These interactions can occur at the surface of the phospholipid bilipid membrane, to the interior cytosol of the cell and with intracellular proteins (Correia and others 2015; Sakaguchi and others 1979).

It is possible that our aromatic aldehydes are binding with the phospholipid layer on the cell membrane, interfering with membrane dynamics leading to cell cytotoxicity (Solis-Calero and others 2010). This is supported by the near universal activity of our aromatic aldehydes. Aromatics are also known to interact with and accumulate in biological membranes(Engelke and others 1996; Almeida and others 2007). This accumulation in the lipid bilayer is governed by a partition coefficient that is specific to the compound being tested. The partition coefficient, Log *P*, is how well a compound dissolves in either water or octanol. Aromatic aldehydes hydrophobicity varies with the decorating moieties (Klyosov 1996). This interaction affects the function and structure of the membrane. Once the aromatics accumulate on the membrane, the membrane can begin to swell, increases membrane fluidity in the form of proton outflow from the membrane, which can disrupt important biological functions (Odinokov and Ostroumov 2015). It has been published that the neutral methyl *p*-coumarate was able to permeate the membrane (Song and others) and further inhibit melanin formation. Also as more compounds disturb the phospholipid layer, the more the lipid bilayer interior is disrupted (Okamura 1999). These studies support that neutral aromatic benzaldehyde such as those tested here can pass through the membrane disrupting critical biological activity (How and others 2014).

The mechanism by which the compounds are passing through the cell membrane is not considered in the cell free experiments. Once inside the cells, aldehydes bind with important

biological targets such as proteins ultimately deactivating them (LoPachin and Gavin 2014).Aldehydes generally react with amino groups or imino compounds forming Schiff bases. The Schiff base is expected to be largely governed by those factors affecting the stability of the carbon-nitrogen double bond. The simple 2-hydroxybenzaldehyde forms a quasi six-member ring through intramolecular hydrogen bonding and produces a stable chelate structure, indicating the possibility to chelate essential metals in the cell (Kubo, 1999). This suggests that metal ions might have a role in cytotoxicity by reducing their availability for cells. However, the strongest cellular inhibitors had a *para*-methoxy moieties and the addition of an electron-donating hydroxyl or methoxy group at the 2- position improved activity. In line with this 2,4-dimethoxybenzaldehyde (**13**) had potent cytotoxicity against the B16-F10 cells. Yet, this activity was unexpected since this compound was a weak monophenolase and diphenolase inhibitor.

Another aspect to consider is the effects of the cell metabolism on the benzaldehyde analogues after they enter the cell. Aromatic aldehydes have been reported to deplete glutathione, an antioxidant, levels prior to the inhibition of cellular respiration and glutathione depleted cells were more susceptible to cytotoxicity. Specifically, 2-hydroxybenzaldehyde was poorly detoxified (Niknahad and others 2003) in hepatocytes so metabolism was a major factor in the aldehydes cytotoxicity. Poorly metabolized aldehydes are very cytotoxic binding to intracellular targets such as proteins or mitochondrial forming adducts that lead to cell death (O'Brien and others 2005). If these targets are critical for cellular function then their reactivity with aldehydes could be related to lipophilicity and electrophilicity since these parameters are contributors to cytotoxicity (Rutkowska and others 2013). The lipophilicity can be measured by Log *P*, a lower value means greater water miscibility. The efficacy of cytotoxicity can be summarized in decreasing order of activity; 2,4-dimethoxybenzaldehyde > 4-methoxysalicylaldehyde > 2,4-dihydroxybenzaldehyde>4-hydroxybenzaldehyde indicating that the potency is in proportion to their log *P* values. Yet, the electrophilicity the measure of a compounds ability to accept electrons of these compounds is decreasing, which is the same pattern we observed on tyrosinase inhibition. While other 2-hydroxy-4-alkylbenzaldehydes and 2-hydroxy-4-alkoxybenzaldehydes could be expected to show potent cytotoxicity there are few compounds reported in literature as natural products. The remaining tested compounds had significantly higher inhibitory concentrations, nor did they significantly suppress melanin formation. Thus, melanin production by mammalian pigment cells is a process involving a series of multifaceted cellular events.

Additionally, the activity we observed on the benzaldehyes did not translate to strong control of insect development. Lepidopteran larva likely detoxify the benzaldehydes upon ingestion blunting their activity. The ligand glutathione S-transferase has been reported to detoxify benzaldehyde in larval fall army worm (Capinera, 2008). *S. exigua* produces glutathione S-transferase in its larval mid-gut (Wan and others 2016) so it is very possible that these aromatic aldehydes were metabolized to a less toxic form. This strong detoxification is consistent with *S. exigua* being an aggressive generalist species.

Conclusion

The ability of aromatic aldehydes to reduce melanin production and inhibit tyrosinase activity was much stronger than their aliphatic counterparts presented in Chapter 2. The aromatic ring structure complicates the inhibition mechanism, but functionally provided a better basis for nucleophilic and electrostatic interactions that disrupted enzyme and cellular activity. This work demonstrated the complex role played by moieties decorating the aromatic ring in determining inhibitory activity. Several strong tyrosinase inhibitors and non-inhibitors were identified. Cellular testing identified two compounds that were effective melanogenesis inhibitors and did not cause cell mortality. This knowledge could be applied to develop useful natural products that can have applications for potential cancer treatments.

Structures

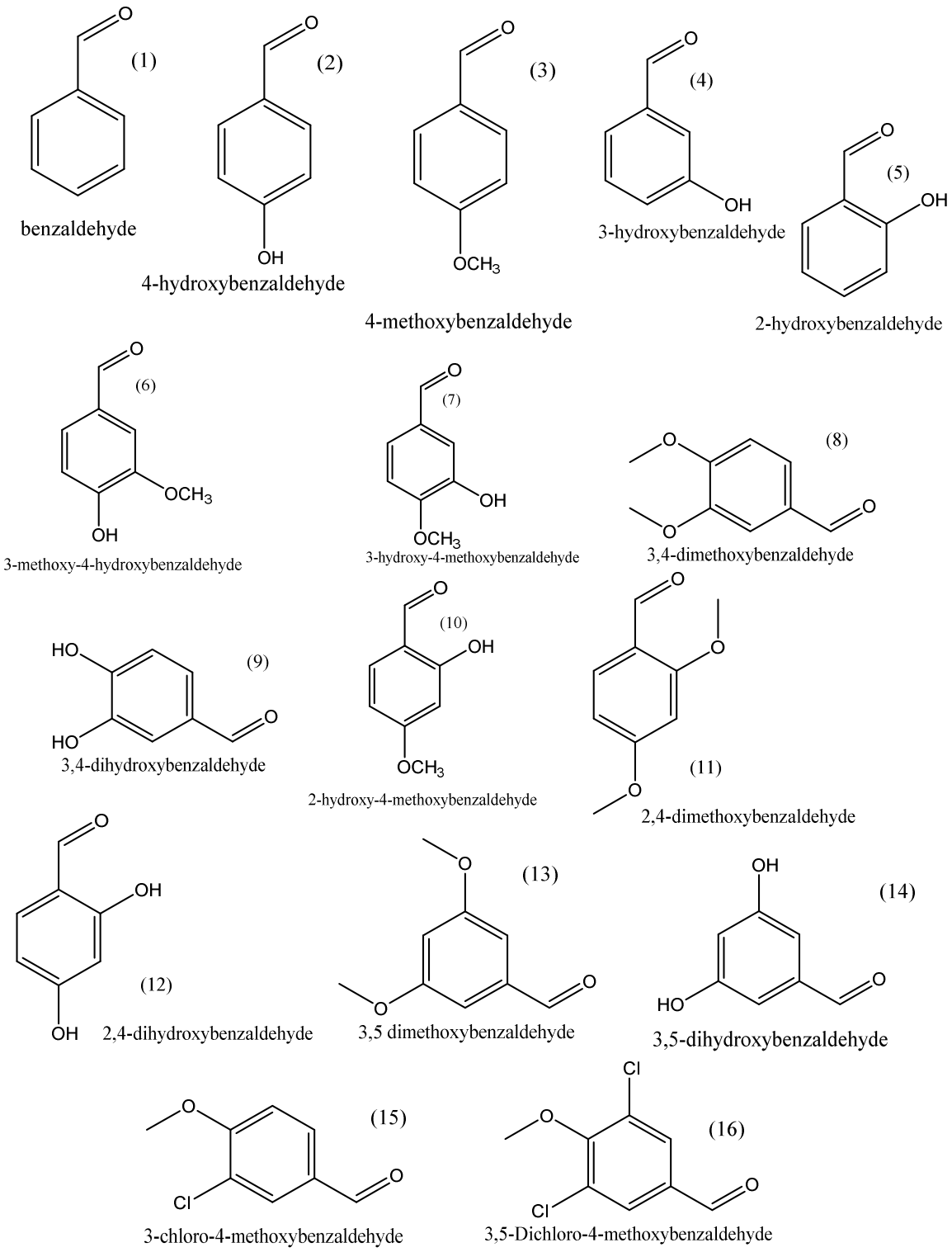

Figure 3.22 Structural diagrams of tested benzaldehyde compounds

Materials and Methods

General methods

General procedures were as previously reported (Satooka and Kubo 2011; Nitoda and others 2007) with slight modifications. Assays were performed in triplicate.

Methods

Chemicals

Benzaldehyde (**1**)(Figure 3.22) is presented as the foundational structural compound. Inhibitory and preincubation assays, fluorescence testing, measuring dopachrome formation and oxygen consumption were performed as described in the methods section. The first group of compounds examined have a single additional moiety, either an –OH (*para*-hydroxybenzaldehyde)(**2**) or $–OCH_3$ (anisaldehyde)(**3**) at the *para*-position (4- position) relative to the aldehyde head group. Two other compounds were investigated with a single moiety, 3-hydroxybenzaldehyde (**4**) has an additional -OH at the *meta*-position (3-position) and (**5**) 2-hydroxybenzaldehyde, which has an additional -OH at the *ortho*-position (2-position). The second group of compounds have an additional hydroxyl or methoxy moiety at the *meta*-position. Vanillin (**6**) has a hydroxyl at the *para*-position with a methoxy at the adjoining *meta*-position; isovanillin (**7**) is similar to vanillin, but has the hydroxyl and methoxy moieties interchanged, with the –OH at the *meta*-position and $–OCH_3$ the *para*-position; 3,4-dimethoxybenzaldehyde (**8**) has methoxy groups at both the *meta*- and *para*-positions and 3,4-dihydroxybenzaldehye (**9**) has hydroxyl groups at both the *meta*- and *para*-positions. The next set of compounds had a hydroxyl group in the *ortho*-position; HMB (**10**) has a hydroxyl at the *ortho*-position and a methoxy at the *para*-position; 2,4-dimethoxybenzaldehyde (**11**) has a methoxy at both the *ortho*- and *para*-positions; 2,4-dihydroxybenzaldehyde (**12**) has a hydroxyl at both the *ortho*- and *para*-position. The third class of chemicals have moities located at both of the *meta*-positions, e.g. 3,5 benzaldehydes; 3,5-dimethoxybenzaldehydes (**13**) has methoxy groups at both *meta*-positions; 3,5-dihydroxybenzaldehydes (**14**) has hydroxyl groups at both *meta*-positions. Lastly, non-natural products were also screened; 3-Chloro-4-methoxybenzaldehyde (**15**) has a chlorine group at the *meta*-position and a methoxy at the *para*-position; 3,5-Dichloro-4-methoxybenzaldehyde (**16**) has chlorine groups at both *meta*-positions, and a methoxy group at the *para*-position. No compounds with a methoxy group in the *ortho*-position were tested due to steric hindrance. These compounds were purchased from Sigma-Aldrich (Milkwalkee, WI, USA).

Enzyme

Assays investigate tyrosinase inhibition as a mechanism to suppress melanogenesis. Tyrosinase – mushroom derived– used in the inhibition assays was purchased from Sigma Aldrich and was purified by anion-exchange chromatography using DEAE-Sepharose Fast Flow (Pharmacia, Uppsala, Sweden) as previously described (Espin and Wichers 1999). Tyrosinase initiates the melanin formation cascade by catalyzing the hydroxylation of L-tyrosine, and thenthe oxidation L-DOPA into dopaquinone, then non-enzyamatically into dopachrome, and eventually into melanin, as discussed in the General Introduction.

Spectrometry

Photo-spectroscopy (UV-VIS) measurements were performed on a Shimadzu 1700 (Tokyo, Japan) to identify the formation of dopachrome. Absorbance was measured at 475 nm, which corresponds to a strong absorbance of dopachrome. Samples were dissolved in DMSO and only used for experimentation after dilution. The final concentration of DMSO was always 3%. For inhibition assays, a test solution of 3 ml was prepared consisting of 1.95 ml distilled and filtered H_20, 0.725 ml of 67mM phosphate buffer (pH=6.8), 0.125 ml L-DOPA (from a 6 mM stock) were mixed and incubated at 30° C for 5 minutes. At this point, the 100 µl of the sample solution and 100 µl of the purified tyrosinase in phosphate buffer was added (1 µg/ml) to the mixture in this order. Once tyrosinase was added to the solution the absorbance was measured for 30-60 minutes. For preincubation assays, the preincubation solution- 1.95 ml distilled and filtered H_20, 0.725 ml of 67mM phosphate buffer (pH=6.8), 100 µl of the sample solution and 100 µl of the purified tyrosinase was added (1 µg/ml) and incubated for 10 minute (or 20 minutes) at 30° C, prior to the addition of L-DOPA. Each assay was repeated three times on separate occasions; data was recorded in Probe 2.1v.

Oxygen consumption

Oxygen consumption inhibitory assays can monitor both the catalyzation of L-tyrosine into L-DOPA and L-DOPA into dopaquinone, since both steps consume a single molecular oxygen from solution. Measurements were taken using an OBH 100 oxygen electrode with a water jacket chamber using an YSI 5300 oxygen monitor. (all from Yellow Springs Instruments Co., Yellow Springs, OH).

For inhibition assays, a test solution of 3 ml was prepared consisting of 1.95 ml distilled and filtered H_20, 0.725 ml of 67mM phosphate buffer (pH=6.8), 0.125 ml L-DOPA (from a 6 mM stock) and the candidate inhibitor dissolved in DMSO were incubated at 30° C for 5 minutes. At this point, 100 µl of the purified tyrosinase in phosphate buffer was added (1 µg/ml). Oxygen consumption was then monitored at 30° C for up to 60 minutes. Each assay was repeated three times on separate occasions to confirm repeatability. Preincubation assays investigated interactions of the inhibitor with tyrosinase. The preincubation solution was prepared as described above. The results were expressed as oxygen consumption in the unit µM.

HPLC

The high-performance-liquid-chromotography (HPLC) analysis was performed on EYELA pump (Tokyo Rikakikai Co. Ltd., Tokyo, Japan) with an EYELA UV-7000 detector (Tokyo Rikakikai Co. Ltd., Tokyo, Japan) and Develosil ODS-UG-5 column (4.6 x 150 mm, Nomura Chemical Co., Ltd., Japan). The operating conditions were as follows unless otherwise noted: the solvents were 7% MeCN (Acetonitrile) and H_2O containing 0.2 % Trifluoroacetic (TFA), flow rate of 1 ml/min, detection at 280 nm (UV), injected volume of 25 µl from the above described 3 ml assay system. The peak area was used to monitor the consumption of substrates and the results were described as the ratio of the area of sample peaks to the control.

Fluorescence

Fluorescence measurements were performed using *N*-Phenyl-1-naphthylamine (1-NPN) to probe the occupancy of the active site. This compound strongly fluoresces in hydrophobic environments (Yin and others 2015), which includes the tyrosinase active site. Thus, as the substrate and/or inhibitor occupy the active site, the fluorescence intensity is expected to decrease. In this work specifically, control fluorescence assays performed on the native L-tyrosine substrate showed an initial drop in signal intensity during the conversion of L-tyrosine to L-DOPA. This drop can be understood as the substrates occupying the active site, and consequentially displacing 1-NPN. Assays performed on the L-DOPA substrate also showed an initial decrease in fluorescence due to the same displacement mechanisms (Yin and others 2015). After this initial decrease, the fluorescence intensity increased, indicating that the probe can access the active site. Generally, the fluorescence signal in the control experiments increase over the 30 minute assay period due to the shrinking amount of L-DOPA available to bind.

Fluorescence measurements were performed on an EnVision Plate reader 2104i (Perkin-Elmer, Waltham, MA,USA), using a 340 nm excitation light and monitoring emissions at 460 nm. Inhibitory assay solutions (3 ml) were prepared as described in the spectroscopy experiments, with the addition of 100 µL of 1-NPN for (20 µM) was added and the solution incubated at 30° C for 10 minutes.. Of this solution 300 µL were then loaded into wells of a 96 well plate, then the candidate inhibitor was added to this solution, then 10 µl tyrosinase was added. Emissions were measured every 5 minutes for 30 minutes. To avoid light interference measurements were taken only after the light path way shut for at least 10 seconds.

Cellular assays

Cell mortality assays were performed on B16-F10 murine melanoma cells purchased from ATCC (Manassas, VA, USA), and cultured in continuous log phase growth in Dulbecco's Modified Eagle medium (DMEM) containing 10% fetal bovine serum (FBS). Cells were seeded in 96-well plates (≈2000 cells/well) and incubated at 37° C for 24 hours at 5% CO_2 prior to chemical treatment. Each chemical was applied in duplicate (N=6) with a final content of 0.1% DMSO, and treated cells were cultured for 72 hours prior to scoring. The melanin content was quantified as described (Kageyama and others 2004; Venkatasamy and others 2004) with some adjustment. Cells were washed with phosphate-buffered saline (PBS), harvested by trypsinization, and centrifuged for 10 minutes at 1500×*g*. The cell pellets were then dissolved in 1.0 M NaOH that contained 10% DMSO for a 2 hour incubation period at 80° C. Melanin content was determined at 475 nm using a SpectraMax Plus spectrophotometer and SoftMax Pro software (Molecular Devices, Union City, USA). Cell viability was evaluated through trypan blue exclusion using a Nikon Diaphoto TMD (Nikon, Tokyo, Japan), and a 50% viable cells lost (IC_{50}) was determined. PBS was used to wash cells, and then they were dispersed by trypsinization. A sample of the cells was then diluted with DMEM containing 10% FBS, and then mixed with the trypan blue solution (for a final concentration of 0.1%) at room temperature. Unstained cells (viable cells) were counted within 10 minutes using a hemocytometer after being mixing with the trypan blue solution.

Insect

S. exigua and were purchased from BioServ (Frenchtown, NJ). Larvae were reared on and tested on BioServ generalist lepidoptera artificial diet (Frenchtown, NJ). For diet incorporation assays late second and early 3rd *S. exigua* larvae were individually weight then placed in a petri dish. The dish was covered with parafilm and a single hole was pierced through the cover to allow air flow and placed in the incubator. The test chemical was added in replacement of dry diet base if a powder. Diet was then weight out to approximately one gram, the value recorded then placed in a plastic petri dish. Insects were weighted on day 5. There were a minimum of 5 larvae per treatment level. The percentage change in weight was calculated for both the insect and diet. Insects were incubated at 27 ºC at 12/12 hours light and dark.

Statistical analysis

For cellular assay the statistical significance was evaluated by either Student's or Welch's t-test depending on the variance and $p < 0.05$ was considered statistically significant. For insect assays normality was tested using Shapiro Wilks testing for normality and then a Kruskal Wallis ANOVA was used to determine statistical difference and $p < 0.05$ was considered statistically significant.

References

1. Almeida JRM, Modig T, Petersson A, Hähn-Hägerdal B, Lidén G, Gorwa-Grauslund MF. 2007. Increased tolerance and conversion of inhibitors in lignocellulosic hydrolysates by Saccharomyces cerevisiae. Journal of Chemical Technology & Biotechnology 82(4):340-9.

2. Chang T-S. 2009. An Updated Review of Tyrosinase Inhibitors. Int. J. Mol. Sci. 10(6).

3. Correia HD, Marangon J, Brondino CD, Moura JJG, Romao MJ, Gonzalez PJ, Santos-Silva T. 2015. Aromatic aldehydes at the active site of aldehyde oxidoreductase from Desulfovibrio gigas: reactivity and molecular details of the enzyme-substrate and enzyme-product interaction. J. Biol. Inorg. Chem. 20(2):219-29.

4. Cozzi PG. 2004. Metal-Salen Schiff base complexes in catalysis: practical aspects. Chemical Society Reviews 33(7):410-21.

5. Engelke M, Tähti H, Vaalavirta L. 1996. Perturbation of artificial and biological membranes by organic compounds of aliphatic, alicyclic and aromatic structure. Toxicology in Vitro 10(2):111-5.

6. Espin JC, Wichers HJ. 1999. Slow-binding inhibition of mushroom (Agaricus bisporus) tyrosinase isoforms by tropolone. Journal of Agricultural and Food Chemistry 47(7):2638-44.

7. How CW, Teruel JA, Ortiz A, Montenegro MF, Rodríguez-López JN, Aranda FJ. 2014. Effects of a synthetic antitumoral catechin and its tyrosinase-processed product on the structural properties of phosphatidylcholine membranes. Biochimica et Biophysica Acta (BBA) - Biomembranes 1838(5):1215-24.

8. Ismaya WT, Rozeboom HJ, Weijn A, Mes JJ, Fusetti F, Wichers HJ, Dijkstra BW. 2011. Crystal Structure of Agaricus bisporus Mushroom Tyrosinase: Identity of the Tetramer Subunits and Interaction with Tropolone. Biochemistry 50(24):5477-86.

9. Jackman MP, Huber M, Hajnal A, Lerch K. 1992. Stabilization of the oxy form of tyrosinase by a single conservative amino acid substitution. Biochemical Journal 282(Pt 3):915-8.

10. Kageyama A, Oka M, Okada T, Nakamura S, Ueyama T, Saito N, Hearing VJ, Ichihashi M, Nishigori C. 2004. Down-regulation of melanogenesis by phospholipase D2 through ubiquitin proteasome-mediated degradation of tyrosinase. Journal of Biological Chemistry 279(26):27774-80.

11. Klyosov AA. 1996. Kinetics and specificity of human liver aldehyde dehydrogenases toward aliphatic, aromatic, and fused polycyclic aldehydes. Biochemistry 35(14):4457-67.

12. Kubo I, Chen QX, Nihei K, Calderon JS, Cespedes CL. 2003a. Tyrosinase inhibition kinetics of anisic acid. Zeitschrift Fur Naturforschung Section C-a Journal of Biosciences 58(9-10):713-8.

13. Kubo I, Kinst-Hori I. 1998. Tyrosinase inhibitors from cumin. Journal of Agricultural and Food Chemistry 46(12):5338-41.

14. Kubo I, Kinst-Hori I. 1999. 2-hydroxy-4-methoxybenzaldehyde: A potent tyrosinase inhibitor from African medicinal plants. Planta Medica 65(1):19-22.

15. Kubo I, Kinst-Hori I, Nihei K, Soria F, Takasaki M, Calderon JS, Cespedes CL. 2003b. Tyrosinase inhibitors from galls of Rhus javanica leaves and their effects on insects. Zeitschrift Fur Naturforschung Section C-a Journal of Biosciences 58(9-10):719-25.

16. LoPachin RM, Gavin T. 2014. Molecular Mechanisms of Aldehyde Toxicity: A Chemical Perspective. Chemical Research in Toxicology 27(7):1081-91.

17. LoPachin RM, Gavin T, Petersen DR, Barber DS. 2009. Molecular Mechanisms of 4-Hydroxy-2-nonenal and Acrolein Toxicity: Nucleophilic Targets and Adduct Formation. Chemical Research in Toxicology 22(9):1499-508.

18. Niknahad H, Shuhendler A, Galati G, Siraki AG, Easson E, Poon R, O'Brien PJ. 2003. Modulating carbonyl cytotoxicity in intact rat hepatocytes by inhibiting carbonyl metabolizing enzymes. II. Aromatic aldehydes. Chemico-Biological Interactions 143:119-28.

19. Nitoda T, Fan MD, Kubo I. 2007. Anisaidehyde, a melanogenesis potentiator. Zeitschrift Fur Naturforschung C-a Journal of Biosciences 62(1-2):143-9.

20. O'Brien PJ, Siraki AG, Shangari N. 2005. Aldehyde sources, metabolism, molecular toxicity mechanisms, and possible effects on human health. Critical Reviews in Toxicology 35(7):609-62.

21. Odinokov A, Ostroumov D. 2015. Structural Degradation and Swelling of Lipid Bilayer under the Action of Benzene. The Journal of Physical Chemistry B 119(48):15006-13.

22. Ramsden CA, Riley PA. 2014. Tyrosinase: The four oxidation states of the active site and their relevance to enzymatic activation, oxidation and inactivation. Bioorganic & Medicinal Chemistry 22(8):2388-95.

23. Sakaguchi K, Miyakawa T, Takeuchi S, Nakagawa K, Hayase E. 1979. Interaction of benzaldehyde to the membrane-protein of escherichia-coli. Agricultural and Biological Chemistry 43(8):1775-7.

24. Satooka H, Kubo I. 2011. Effects of Thymol on Mushroom Tyrosinase-Catalyzed Melanin Formation. Journal of Agricultural and Food Chemistry 59(16):8908-14.

25. Solis-Calero C, Ortega-Castro J, Munoz F. 2010. Reactivity of a Phospholipid Monolayer Model under Periodic Boundary Conditions A Density Functional Theory Study of the Schiff Base Formation between Phosphatidylethanolamine and Acetaldehyde. Journal of Physical Chemistry B 114(48):15879-85.

26. Song K, An SM, Kim M, Koh J-S, Boo YC. Comparison of the antimelanogenic effects of coumaric acid and its methyl ester and their skin permeabilities. Journal of Dermatological Science 63(1):17-22.

27. Venkatasamy R, Faas L, Young AR, Raman A, Hider RC. 2004. Effects of piperine analogues on stimulation of melanocyte proliferation and melanocyte differentiation. Bioorganic & Medicinal Chemistry 12(8):1905-20.

28. Wan H, Zhan S, Xia XD, Xu PF, You H, Jin BR, Li JH. 2016. Identification and functional characterization of an epsilon glutathione S-transferase from the beet armyworm (Spodoptera exigua). Pest. Biochem. Physiol. 132:81-8.

29. Wang W, Guo J, Zhang JN, Peng J, Liu TX, Xin ZH. 2015. Isolation, identification and antioxidant activity of bound phenolic compounds present in rice bran. Food Chemistry 171:40-9.

30. Yin J, Choo YM, Duan HX, Leal WS. 2015. Selectivity of odorant-binding proteins from the southern house mosquito tested against physiologically relevant ligands. Frontiers in Physiology 6.

Chapter 4

Effect of phenolics on tyrosinase and B16 melanoma cells

Introduction

In this chapter, I present my work using plant-derived phenols as tyrosinase inhibitors. Phenolics contain six member carbon rings with at least one attached hydroxyl group. In plants, phenols are present as secondary metabolites, responsible for antioxidant activity (Dillard and German 2000). Specifically, free radicals are generated by biological processes and, particularly when produced in excess, can damage cell membranes, DNA and proteins (La and others 2008).The hydroxyl group in phenols is itself reactive and is able to donate its hydrogen group to neutralize the radicals in a process called free radical scavenging (Lobo and others 2010).The ability to destroy free radicals and provide antioxidant protection makes phenols attractive for various applications, including medical therapies (Karlsson and Lindquist 2016). In this work, I focus specifically on phenolic acids which are made up of hydrolysable tannins (HT).These compounds are known to have antibacterial, anticarcinogenic, and antifungal activity, as well as anti-inflammatory activity (Koleckar and others 2008; Ayala-Zavala and others 2012). The most basic HT is gallic acid (3,4,5-trihydroxybenzoic acid, Figure 1a), a six carbon ring with three hydroxyl and one carboxylic acid group. All HT are derivatives of this parent phenol. Gallic acid is present in several plant species, including *Fuchsia tetradactyla* (Onagraceae) (Haraguchi and others 2000), *Bersamaabys sinica* (Melianthaceae) (Kubo and others 1985), *Arctostaphylosuva-ursi* (Ericaceae) and other sources (Matsuo and others 1997; Kubo and others 2003a; Kim 2007), and has been demonstrated as an effective tyrosinase inhibitor.

As discussed in Chapters 1 and 2, inhibiting tyrosinase offers opportunities for regulating melanin production. Yet, in the literature there is significant variation in the reported inhibitory efficacy of phenols, which points to the lack of understanding of the inhibition mechanism. In addition to exploring a different class of chemicals, in this chapter we investigate tyrosinase inhibition in the scope of regulating insect activity. As discussed in the General Introduction, tyrosinase plays a crucial role in insect sclerotization (Bittner 2006), immune response (Marmaras and others 1996) and pigmentation. Thus using tyrosinase inhibitors as insect pest control agents is of great interest in agricultural applications. Here we will explore phenolics ability to inhibit enzyme ability and hydrolysable tannins ability to impact insect development.

Results

Gallic acid

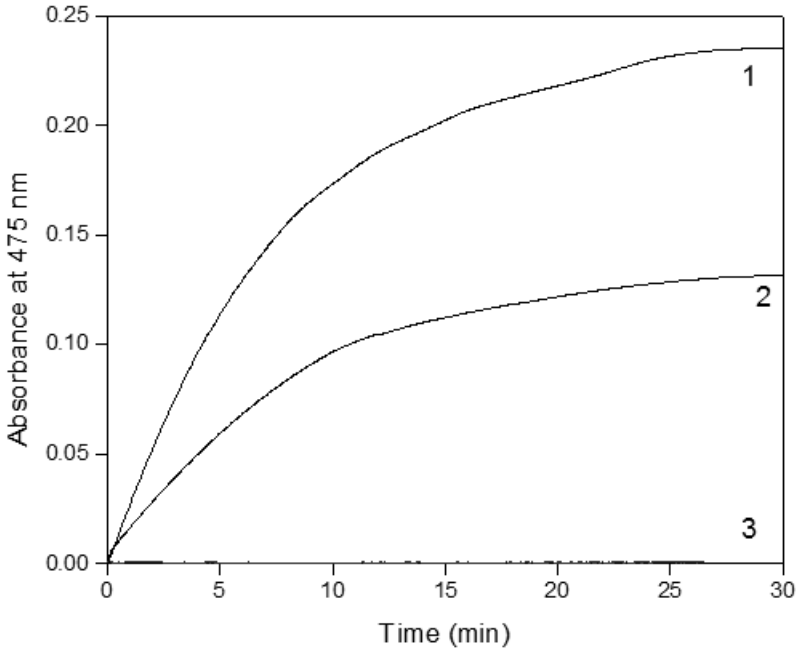

Figure 4.1 UV-Vis of dopachrome formation of Gallic acid and the oxidation of L-DOPA (0.250mM)(1) L-DOPA only, (2) L-DOPA (0.250 mM) and gallic acid (mM), 3: gallic acid (0.1 mM) only

Gallic acid (**1**) was previously reported as a tyrosinase inhibitor (Kim 2007). UV-VIS spectroscopy performed on an L-DOPA substrate confirmed its inhibitory efficacy (Figure 4.1), reducing enzyme activity by 45% at the previously reported IC_{50} of 4.5 mM (Kubo and others 2003b). Yet, during the reaction, the solution became a yellow/brown color rather than the typical orange/red color (Harborne 1998) characteristic of dopachrome formation. Further, the reaction was not accelerated by adding a catalytic amount (10 μM) of L-DOPA. One possibility is that the gallic acid is oxidized by tyrosinase, forming an ortho-quinone similar to dopachrome. Due to the oxidizable nature of gallic acid inhibitory kinetics were not investigated.

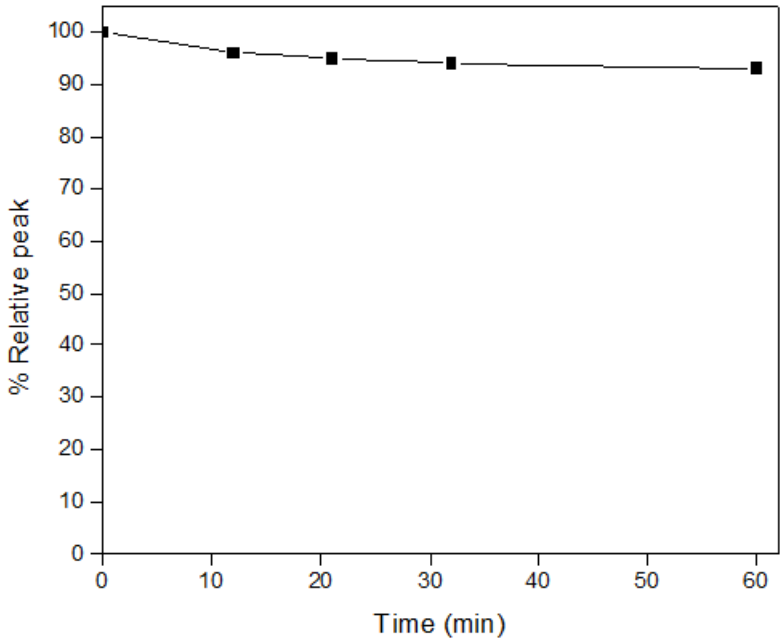

Figure 4.2 Percent relative peak of HPLC analysis of the reaction mixture with gallic acid (4.5 mM) and tyrosinase(closed squares)

To determine if gallic acid is indeed oxidized by tyrosinase, an assay was performed in which gallic acid (4.5 mM) and tyrosinase were combined in a test solution; the gallic acid concentration was monitored using HPLC. The gallic acid peak area remained relatively constant for the 60 minute assay period (Figure 4.2) only decreasing by 6%, yet gallic acid is known to undergo auto-oxidation (Gao and others 1998). Notably, the color of the solution did not change. An additional oxygen consumption (Figure 4.3) showed a small amount of oxygen consumption in this test solution, which can be attributed to naturally occurring auto-oxidation of gallic acid (Nikolic and others 2011).Introducing catalytic amounts (≈10 μM) of L-DOPA did not significantly increase in the amount of oxygen consumed after 30 minutes, supporting the HPLC data. However, the most oxygen was consumed for the solution with the highest gallic acid concentration (4.5 mM). The full UV-VIS spectrum of the solution also showed no new peaks, or peak evolution (Figure 4.4).

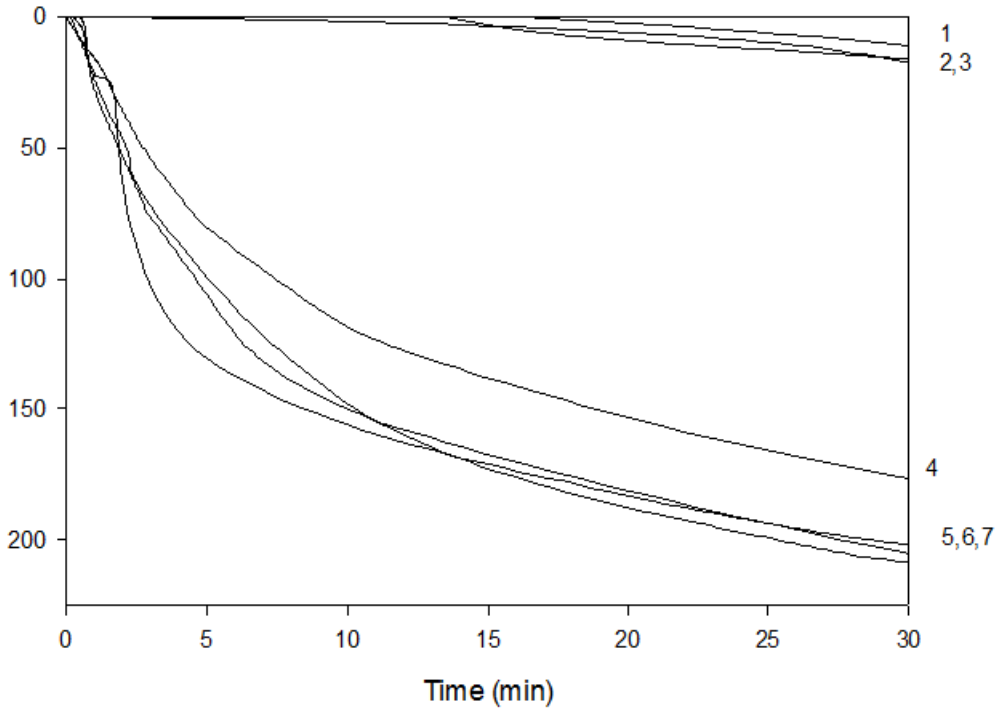

Figure 4.3 Oxygen consumption of gallic acid at 1mM and tyrosinase only (1),gallic acid at 0.1 mM and L-DOPA 0.1mM only (2),gallic acid at 0.1 mM and tyrosinase with catalytic amount of L-DOPA 0.01 mM added (3),gallic acid 1mM and L-DOPA 0.5mM (4), L-DOPA 0.5 mM control (5), gallic acid 0.5mM and L-DOPA 0.5mM (6) and gallic acid 4.5mM and L-DOPA 0.5 mM (7)

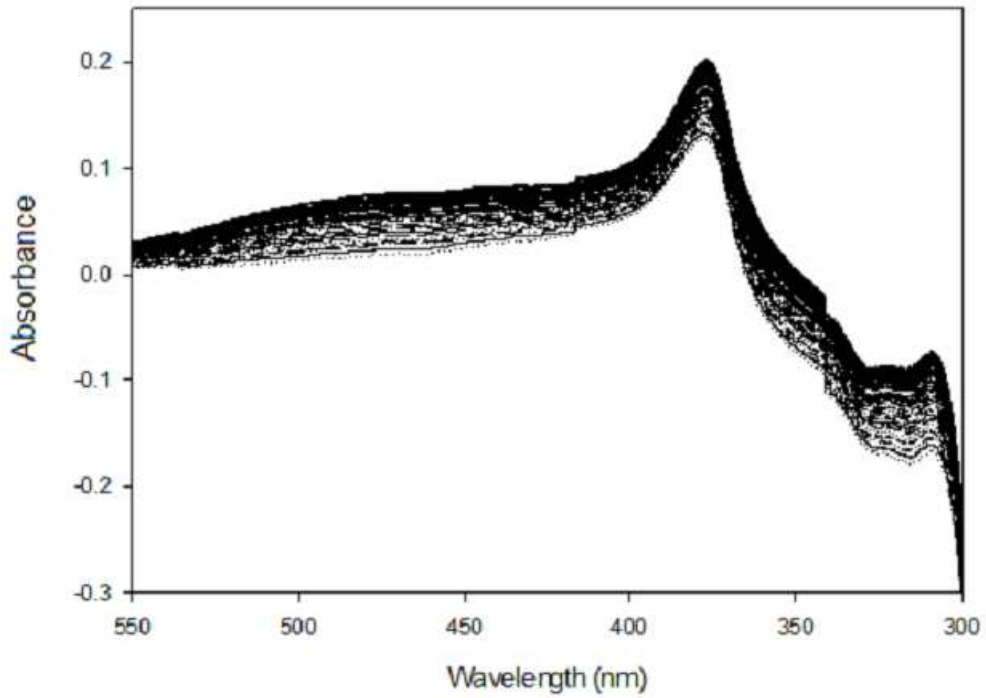

Figure 4.4 UV Spectrum of tyrosinase with gallic acid (0.500 mM) only

We then continued to determine the reaction mechanism by combining tyrosinase with gallic acid at 0.5 mM and L-DOPA at 0.5 mM and followed the reaction on the HPLC (Figure 4.5). We observed that the L-DOPA peak area decreased by 28 % after 50 minutes, which can be attributed to the standard oxidation of L-DOPA into dopaquinone. The gallic acid peak area also decreased by 38% which was surprising since there was no change when gallic acid and tyrosinase were combined with L-DOPA. These changes suggest there is interaction between the substrate and inhibitor. However, control experiments of L-DOPA and gallic aciddid not show any change over 60 minutes (data not shown), suggesting the reaction was *not* with L-DOPA, but rather one of the oxidized products (dopaquinone, leucodopachrome, or dopachrome).

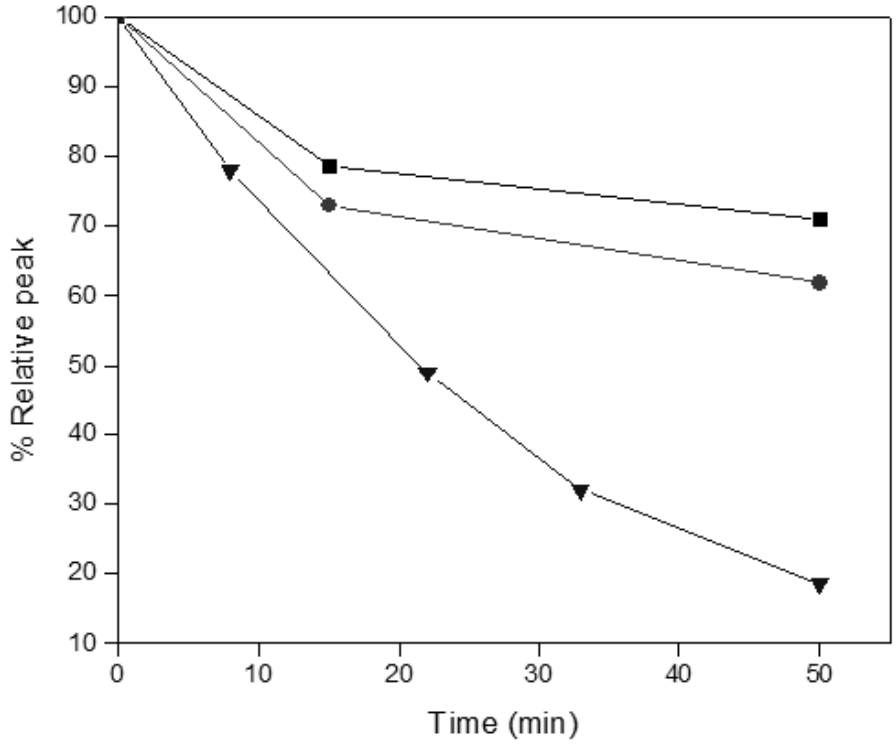

Figure 4.5 Reaction mixture with gallic acid (0.5 mM) and L-DOPA (0.5 mM), closed square and closed circle respectively. L-DOPA at 0.5mM with tyrosinase (upside down triangle)

Oxygen consumption assays performed on the gallic acid at 0.5 mM and L-DOPA 0.5 mM (Figure 4.4) concentration confirmed only weak inhibitory activity. After 30 minutes oxygen consumption was reduced by only 4% compared to the control, and then did not consume any further oxygen through the end of the assay (70 minutes). By comparison, the control assay consumed oxygen for the entire 70 minutes. Doubling the gallic acid concentration (to 1 mM) more-than tripled the oxygen consumption inhibition (to 13%). Similarly, oxygen consumption halted before the end of the measurement time. However, increasing the gallic acid concentration to 4.5 mM showed enhanced oxygen consumption compared to the control, and visually reduced melanin formation (as identified by the color of the solution). Increasing the L-DOPA concentration to 1 mM (gallic acid at 0.5 mM), the compound concentrations were monitored throughout the reaction using HPLC (Figure 4.6). Over the 50 minute reaction period, the L-DOPA peak area decreased by 29 % while the gallic acid peak area decreased by 82% (Figure 4.6). Recalling the L-DOPA (0.5 mM) and gallic acid (0.5 mM) HPLC assay, the L-DOPA peak decreased by 28%, and gallic acid by 38%. The gallic acid peak area change suggests that the L-DOPA concentration strongly effects gallic acid consumption.

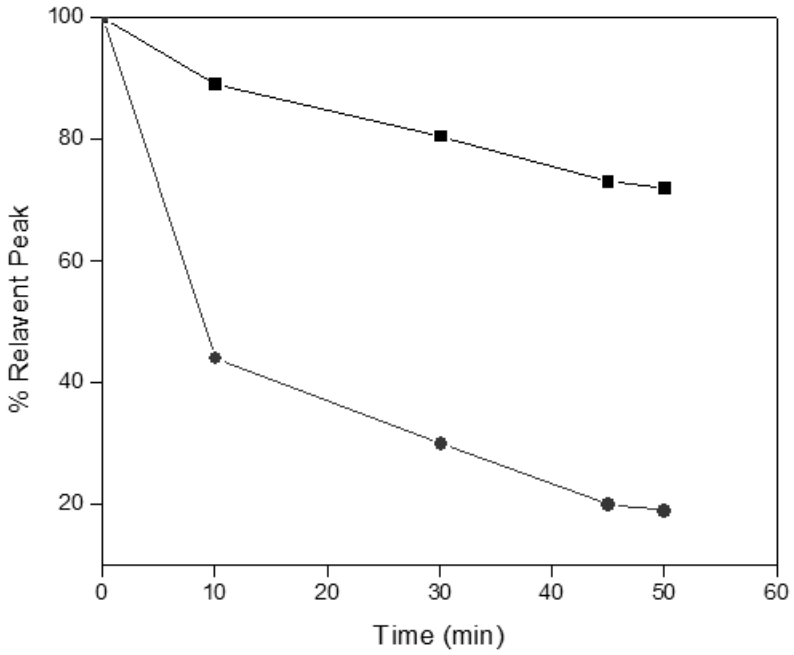

Figure 4.6 Quantitative metrics of HPLC data of gallic acid 0.5 mM (closed square) and 1 mM L-DOPA (closed circle)

The above data further support a reaction between the L-DOPA products and gallic acid. To investigate the possibility of a reaction, the L-DOPA (0.5 mM) with gallic acid (0.5 mM) and tyrosinase reaction was monitored with full-spectrum UV-VIS spectroscopy (Figure 4.7). The spectrum shows the emergence of a peak at 390 nm, which grows with reaction time and was not observed in the control spectrum. We suggest that this must be the product of the gallic acid reaction with the L-DOPA products. A similar peak was observed in the spectrum of L-DOPA (0.5 mM) with gallic acid (1 mM) and tyrosinase (not shown).

The above data show-that oxygen consumption was only weakly effected by the inhibitor, but also that the gallic acid was preferentially consumed. Refocusing back to inhibiting melanogenesis, UV-VIS spectroscopy (Figure 4.8), which monitors dopachrome formation, we also return to the IC_{50} concentration (L-DOPA 0.85 mM, gallic acid 4.5 mM). Previous results hinted at the role of oxygen in this reaction mechanism. Spectroscopy (Kubo and others 1995) was consistent with the previous results inhibiting 47% of enzyme activity at this concentration. Yet, when these measurements were repeated with the same solution being mixed, introducing oxygen to the system the inhibitory effects of gallic acid were erased. This clearly shows that oxygen concentration was a limiting factor in the gallic acid inhibitory mechanism. Full spectrum measurements (Figure 4.9) again confirm the emergence of the product peak at 300-400 nm.

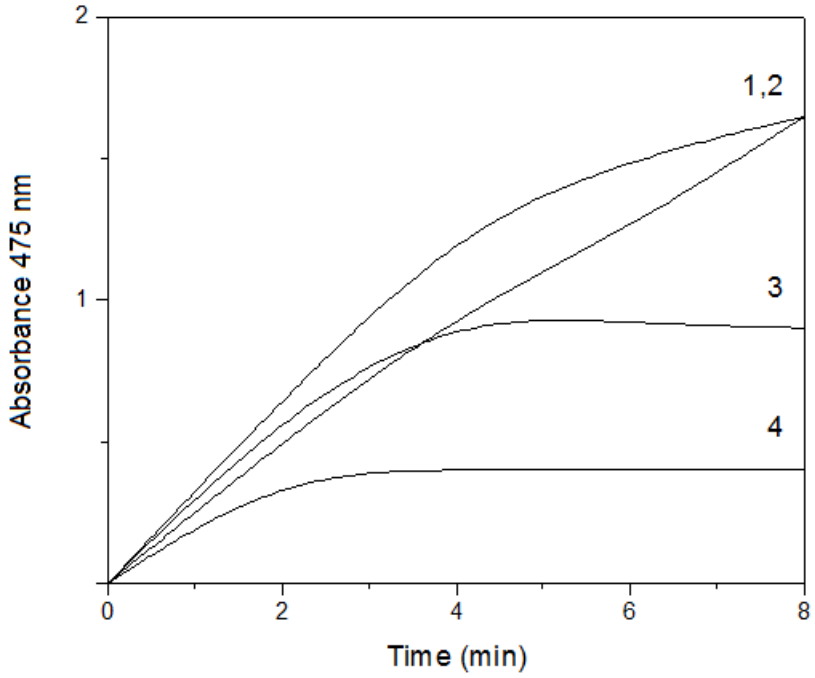

Figure 4.8 Mixing effect on gallic acid (4.5mM) with L-DOPA(0.8) at 475 nm. L-DOPA only no mixing (1), L-DOPA with gallic acid and mixing (2), L-DOPA only no mixing (3), L-DOPA with gallic acid mixing (4)

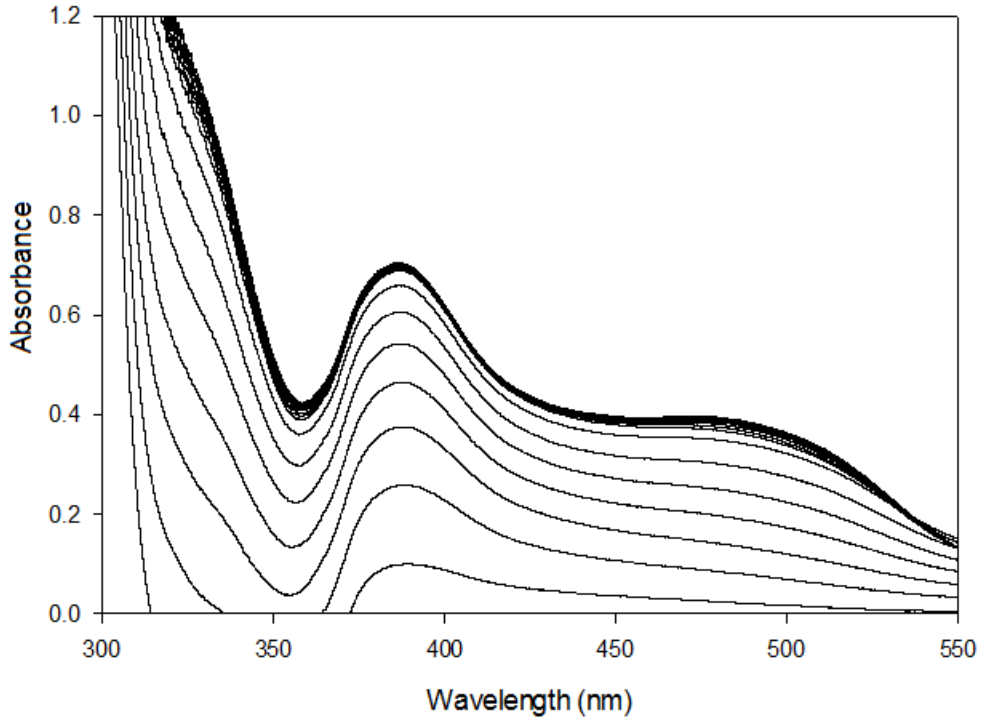

Figure 4.9 Consecutive spectra obtained in the oxidation of L-DOPA (0.85 mM) in the presence of gallicacid (4.5 mM).

To identify the peak observed in the spectroscopy (Figure 4.7, 4.9), we used thin layer chromatography (TLC) and spectroscopy, and determined the unidentified compound to be purpurogallincarboxcylic acid (**2**)(PA). Then gallic acid was oxidized by $K_3Fe(CN)_6/NaHCO_3$ as described (Bailey and others 1993) confirming the structure. Based on the above results, we propose an inhibitory mechanism in which gallic acid interrupts the melanin formation pathway by reacting with dopaquinone (Figure 4.10). Specifically, recalling the melanin formation pathway, tyrosinase oxidizes L-DOPA to form dopaquinone. In our proposed mechanism, dopaquinone then oxidizes gallic acid to an ortho-quinone by a redox reaction, and removes two of its hydrogens. In the process, dopaquinone itself is reduced back to L-DOPA. The redox reaction generates ortho-quinones (gallic acid derived) that condensed with one another through a Michael type addition, yielding a moderately stable dibenzotropolone intermediate, purpurogallincarboxylic acid (PA)(**2**) (Figure 4.1). To confirm this mechanism, PA was methylated by CH_2N_2 to yield the stable tetramethyl derivative (**5**). The structure of purpurogallincarboxylic acid (**2**) was indirectly characterized mainly based on extensive spectroscopic studies of **5**. This dibenzotropolone intermediate was relatively stable, but gradually further oxidized.

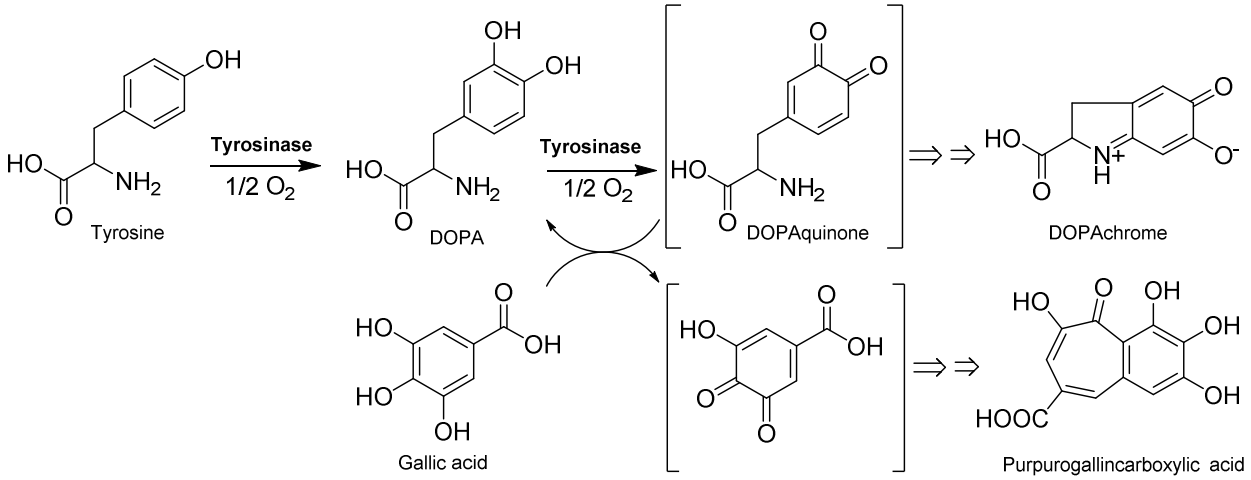

Figure 4.10 Proposed pathway of formation of purpurogallincarboxylic acid

We then continued to determine the reaction mechanism by combining gallic acid at 4.5 mM and L-DOPA at 0.5mM and followed the reaction on the HPLC. We observed that the L-DOPA peak area decreased overall by 25.5% after 65 minutes, while the gallic acid area decreased by 24.5%.overall. This was a one-to-one correspondence that is expected in the above proposed mechanism. The percent composition of gallic acid increased 0.6% while L-DOPA increased 0.6% by 65 minutes. Of note, both the height and area of each compound stabilized by 45 minutes suggesting that any further reactions ceased. It should be noted that PA was difficult to quantify on the HPLC because of this oxidizable nature.

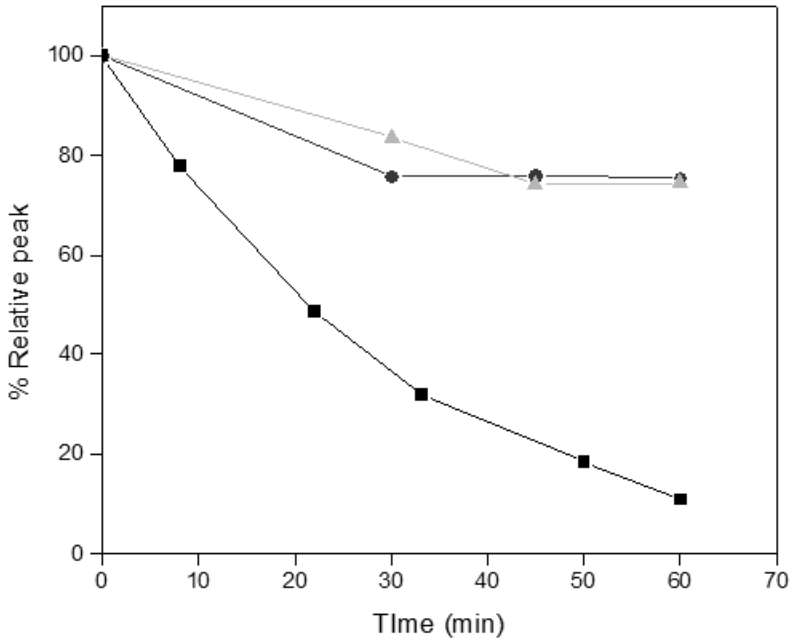

Figure 4.11 Quantitative HPLC values for gallic acid at 4.5mM (closed circle) and L-DOPA at 0.5mM (closed triangle) with L-DOPA only for comparison (upside down triangles)

Based on the above mechanism, we do not expect the inhibitor to be located at the enzyme active site. To confirm the non-interaction between the gallic acid and the active site, fluorescence measurements were performed (Table 4.1). The results showed an immediate increase in fluorescence signal when gallic acid was combined with L-DOPA and tyrosinase. This suggests that gallic acid was not actively binding during the first 10 minutes of the reaction. After 30 minutes we see a substantial decrease in fluorescence (Table 4.1). According to previous work (Conrad and others 1994), an aromatic ring with carboxyl moiety group - including hydroxyphenolic acids such as *para*- and *meta*-hydroxybenzoic acids and mimosine - will bind directly to the binuclear copper active center (Solomon 2014) through the acidic carboxylic group. It is possible that gallic acid was binding at the active site, but not inhibiting dopachrome formation.

Time (minutes)	Gallic acid (4.5mM)	Control
0	100	100
5	180	91
15	30	110
30	30	110

Table 4.1 Gallic acid at 4.5 mM on L-DOPA (0.500 mM) interacting with 1-NPN

While L-DOPA is a convenient substrate for testing due to its fast reaction time, L-tyrosine is considered the state of the melanin formation pathway. Inhibition testing performed on L-tyrosine (0.5 mM) and gallic acid (0.1 mM) showed no suppression of activity for the first 20-30 minutes (Figure 4.12), including no change to the lag phase. After 20-30 minutes, dopachrome formation was not significantly suppressed, but was suppressed by 15% after 60 minutes. The absence of suppression followed significant inhibition suggests there was a critical gallic acid to dopaquinone ratio at which the above redox-cycling reaction occurs.

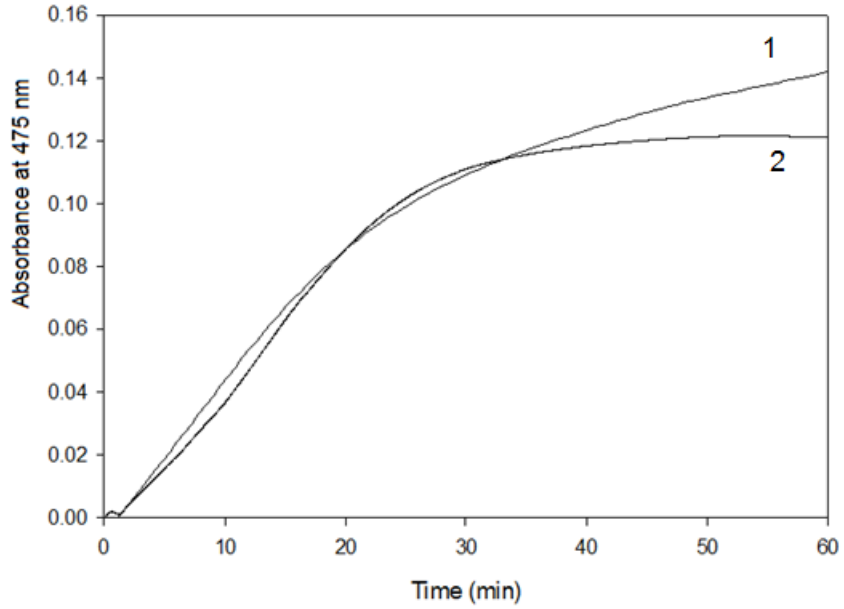

Figure 4.12 The change in absorbance at 475 nm during the oxidation of L-tyrosine 0.5 mM (1) in the presence of gallic acid (0.1 mM) (2)

Oxygen consumption assays performed on L-tyrosine at high concentrations of gallic acid show significant enhancement of oxygen consumption after 15 minutes (Figure 4.13). The above suggested redox-cycling reaction returns the dopaquinone to L-DOPA, which then can be oxidized by tyrosinase again. Thus oxygen consumption was expected to increase during redox-cycling, consistent with the data. The fact there was no inhibition activity for 15 minutes suggests that L-tyrosine does not facilitate redox cycling directly, and a critical gallic acid to dopaquinone concentration ratio was crucial to achieve inhibition.

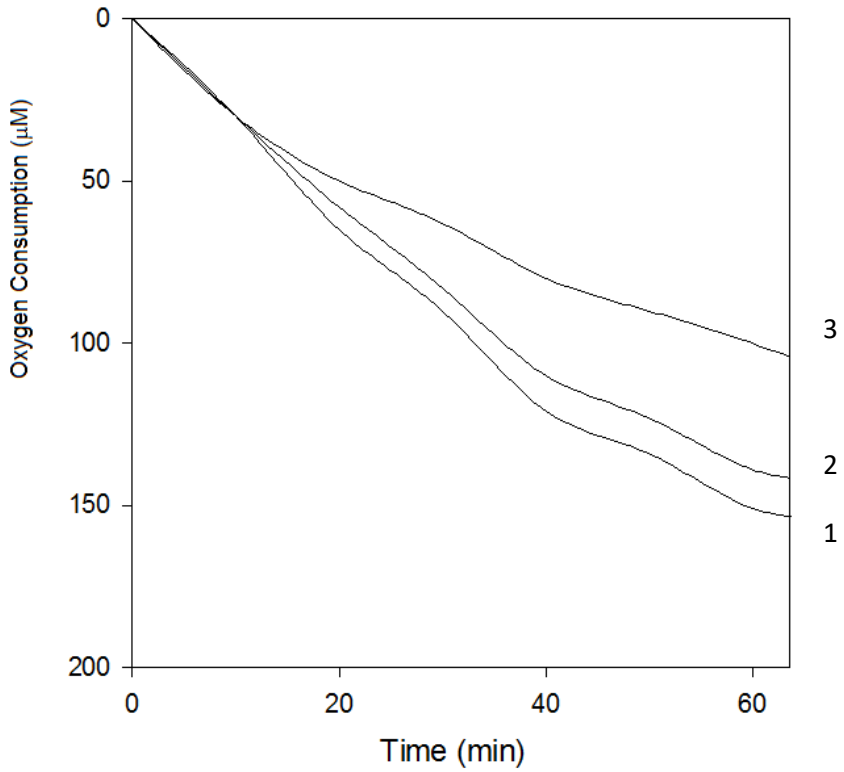

Figure 4.13 Oxygen consumption during the oxidation of L-tyrosine alone at 0.125 mM (1) and in the presence of gallic acid at 1.0 mM (2) and 2.0 mM (3)

Structural analogues

Next we wanted to determine if structurally similar phenols would also act as redox-cycler inhibitors. The structurally analogue methyl gallate (Methyl 3,4,5-trihydroxybenzoate) (**3**) a methyl ester of gallic acid was examined. This compound retains the three hydroxyl groups at the *para*- and *meta*-positions, but replaces the hydroxyl group on the head with a methoxy group.

Initially, we combined methyl gallate (0.5 mM) with L-DOPA (0.5mM) and tyrosinase. The reaction mixture turned yellow, compared to the control which turns red/orange, suggesting a similar inhibitory mechanism exists for gallic acid and methyl gallate. However, a control experiment with only tyrosinase and methyl gallate also turned yellow. This suggests that the methyl gallate may be directly interacting with tyrosinase and consuming oxygen - and/or the reacted methyl gallate products react with the L-DOPA products.

HPLC measurements on a test solution of methyl gallate (0.5 mM), L-DOPA (0.5 mM) and tyrosinase (Figure 14.14) show that the methyl gallate quickly decreased. Both the L-DOPA peak and methyl gallate peaks decreased significantly. It should be noted that small peaks emerged after 10 minutes that were likely the oxidation products we observed in the solution above.

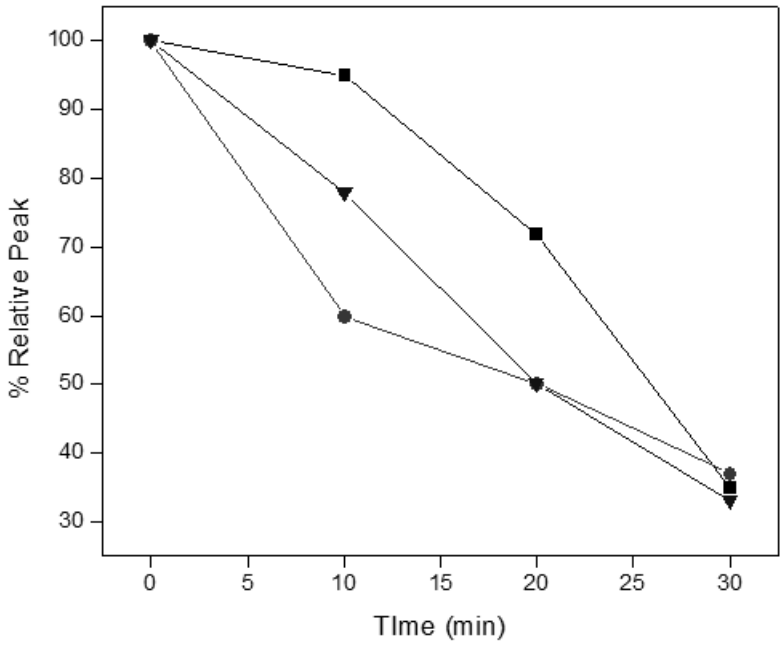

Figure 4.14 HPLC values for methyl gallate at 0.5 mM (closed triangle) in the presence of L-DOPA (closed square) at 0.5 mM and only L-DOPA (closed circle)

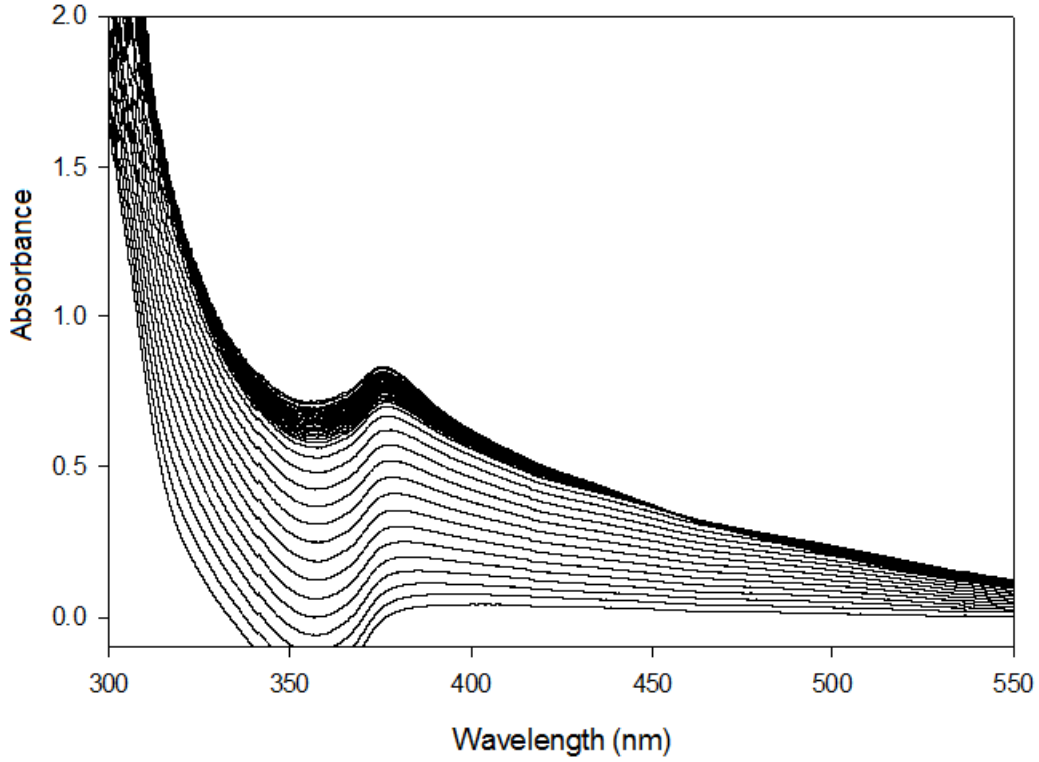

Figure 4.15 UV-Vis spectrum of methyl gallate (0.5 mM) and L-DOPA (0.5 mM) with tyrosinase

UV-VIS spectroscopy was measured on a similar test solution (methyl gallate (0.5 mM) and L-DOPA (0.5 mM) with tyrosinase) and showed both dopachrome formation and the emergence of a peak at 350-375 nm which was absent in the control experiment (Figure 4.15). This peak likely identifies the product of the methyl gallate oxidation. These products are likely different than the gallic acid UV-VIS data, as it the peak in that data appears at a lower wavelength.

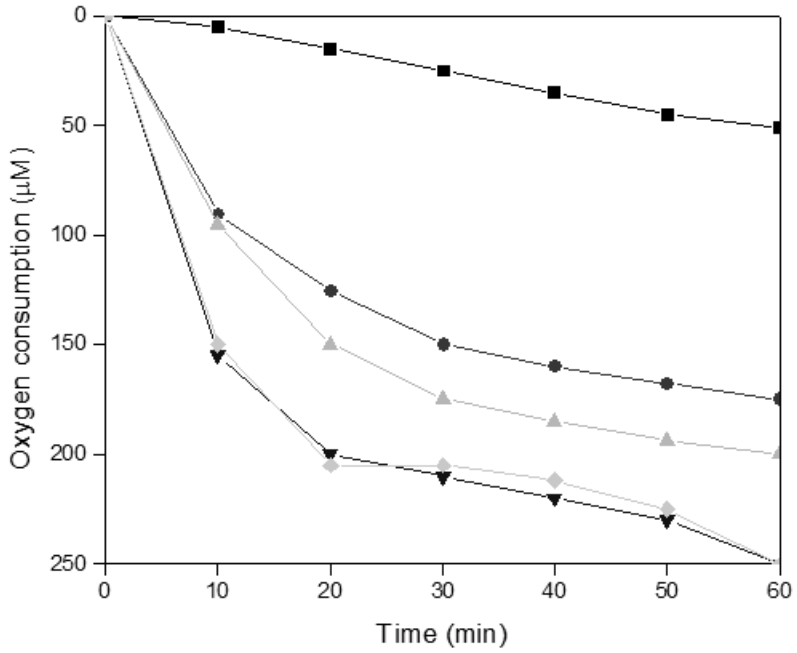

Figure 4.16 Oxygen consumption of methyl gallate at 1 mM (closed triangle) in the absence of tyrosinase; methyl gallate at 0.5 mM (closed square) and 1 mM (closed triangle) in the presence of only tyrosinase; methyl gallate at 0.5 mM (closed diamond) and 1 mM (closed upside down triangle) with L-DOPA (10 μM) added after 3 minutes

Oxygen consumption data further confirms the tyrosinase catalyzed oxidation of methyl gallate (Figure 4.16). In the absence of tyrosinase, there was minimal oxygen consumption in solutions of methyl gallate; the inclusion of tyrosinase significantly increases oxygen consumption. Introducing L-DOPA to the methyl gallate tyrosinase solution increased oxygen consumption. This suggests that methyl gallate was a competitive inhibitor which depletes the solution of available oxygen and thus stymies the oxidation of L-DOPA. Thus, while methyl gallate may or may not enter into the same redox-cycling mechanism as gallic acid, the fact that it was oxidized rapidly by tyrosinase precludes it from inhibiting by this mechanism. However, the oxidation of methyl gallate does cause inhibition by depleting the oxygen in the solution, and thus stymieing the tyrosinase catalyzed oxidation processes in general.

Next, we investigated another structurally similar compound, protocatechuic acid (3,4-dihydroxybenzoic acid) (**4**), which has only two hydroxyl groups on the ring structure, but returns the hydroxyl side chain to the carboxyl group.We began by combining 0.5 mM of protocatechuic acid and L-DOPA at 0.5 mM with tyrosinase. Assays monitored by HPLC on solutions of protocatechuic acid (0.5 mM) and L-DOPA (0.5 mM) with tyrosinase, show no reduction of the protocatechuic acid throughout the 40-minute measurement Figure 4.17).

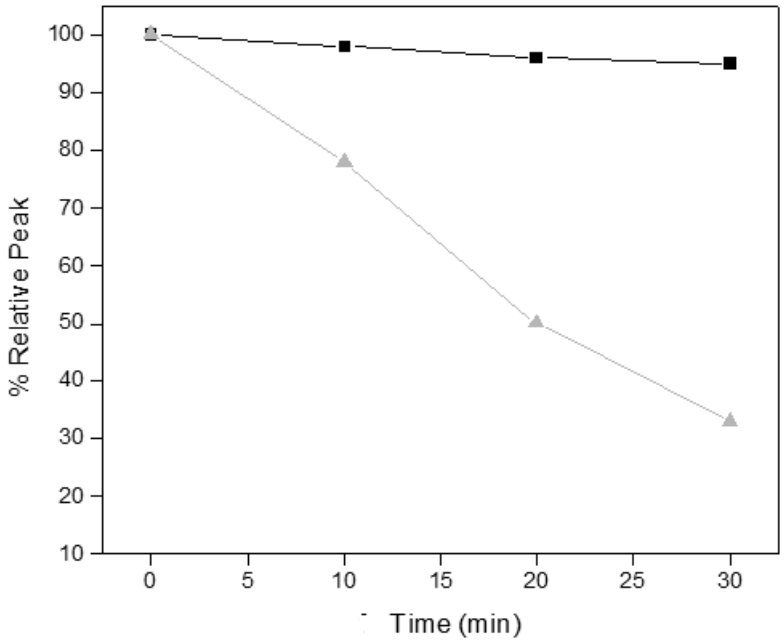

Figure 4.17 Relative peak of protocatechuic acid at 0.5mM (closed circle) with tyrosinase and only L-DOPA at 0.5mM (closed triangle)

The peak identified as L-DOPA decreased throughout the measurement and a peak corresponding to dopachrome formation appeared after 8 minutes. This suggests that protocatechuic acid does not inhibit the tyrosinase-catalyzed, oxidation of L-DOPA, nor was it oxidized as a substrate. This was further supported by the UV-VIS spectrum of the above solution which decreased dopachrome formation by only 4% (Figure 4.18) relative to the control.

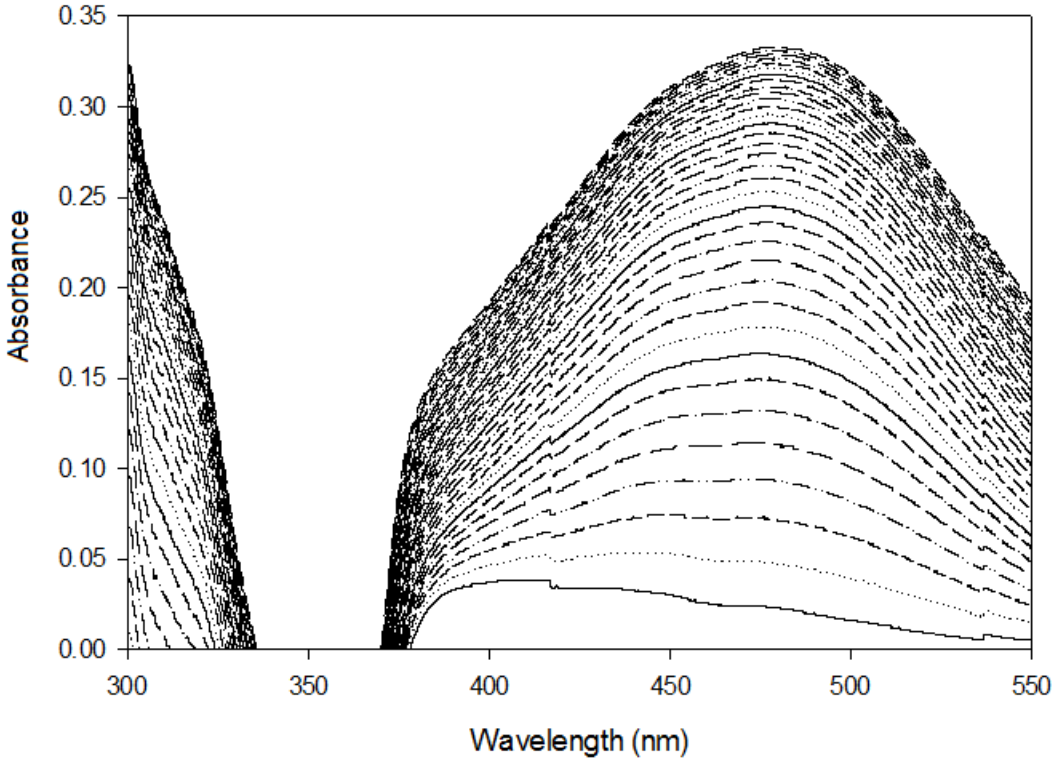

Figure 4.18 UV-Vis spectrum of protocatechuic acid (0.5 mM) and L-DOPA (0.5 mM)

To determine if redox cycling occurred we combined excess protocatechuic acid (0 mM, 1 mM, and 2mM) with tyrosinase and L-DOPA (0.5 mM) and measured oxygen consumption (Figure 4.19). The oxygen consumption changed very little over these concentration ranges, confirming that there was no oxidation of protocatechuic acid, nor was there redox.

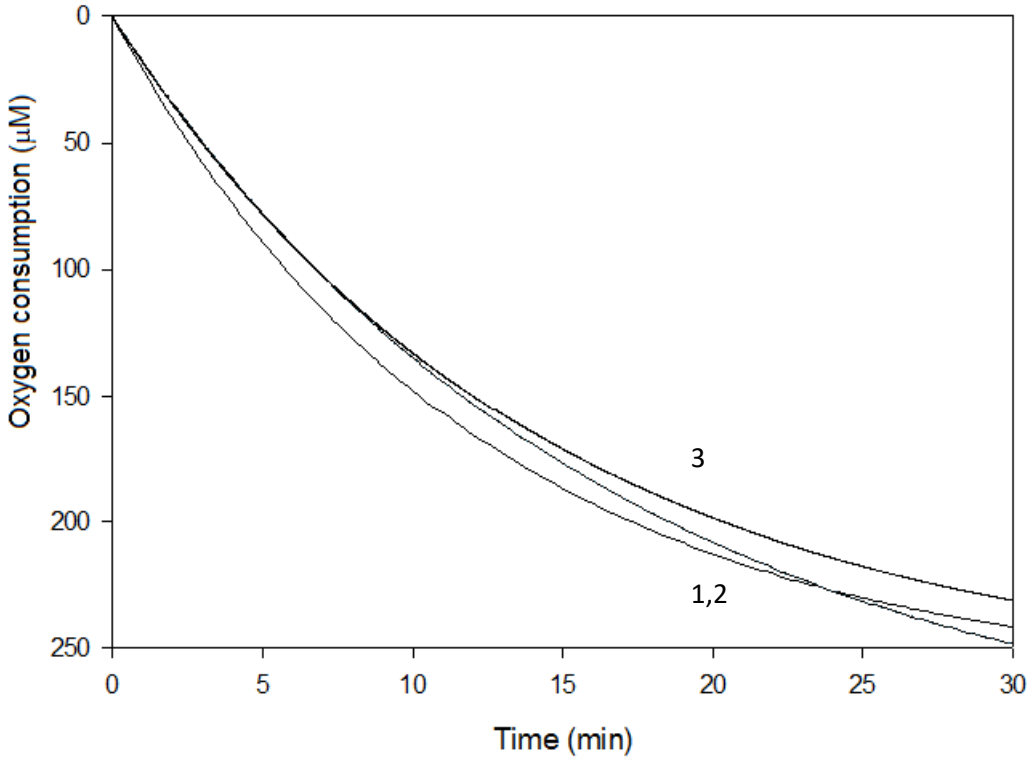

Figure 4.19 Oxygen consumption of Protocatechuic acid at 1 mM and 2 mM in the presence of L-DOPA (0.5 mM)

In addition to the above assays which show no activity from protocatechuic acid, assays performed with L-tyrosine also showed no activity (not shown). Fluorescence assays confirmed protocatechuic acid does not occupy the tyrosinase active pocket. Comparing these three structurally similar compounds suggests that the triple hydroxyl group was crucial to the redox cycling, but the carboxyl headed phenol can be made susceptible to oxidation by tyrosinase by changing the head group. Gallic acid was the only compound tested so-far which scavenges radicals in the melanin formation pathway, but methyl gallate still inhibited dopachrome formation by directly interacting with tyrosinase. The inactivity of protocatechuic acid can likely be attributed to the electron donating property of the third hydroxyl group, and its contribution to the overall stability of the other moieties.

A third HT, Tannic acid (**6**),was also investigated as it was the major compound isolated from a natural medicine Gallae Rhois and reported as a strong tyrosinase inhibitor with a very low IC_{50} of 76µM (Kubo and others 2003a). The structure of tannic acid (Figure 4.26) shows that it is comprised of 10 gallic acid compounds, cross-linked at the meta-hydroxyl site and the hydroxide side chain. These are the same sites investigated in methyl gallate and protocatechuic acid, emphasizing their reactivity. Tannins have been previously shown to react with proteins

through cross linking or 'tanning', hydrogen bonding and hydrophobic effects (Hagerman 1989) and thus is a promising candidate for tyrosinase inhibition.

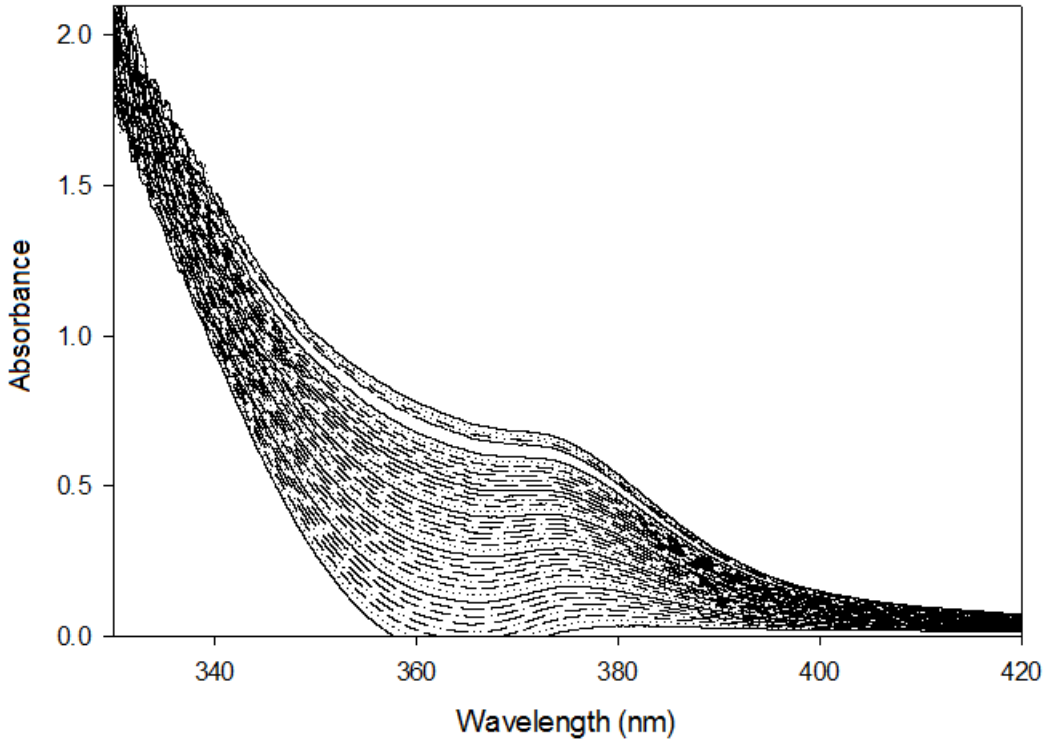

Figure 4.20 UV-VIS spectrum of preincubation of tyrosinase with tannic acid (100 μM) only

Starting with a simple visual confirmation, tannic acid (0.1 mM) and tyrosinase were combined (no L-DOPA or L-tyrosine), resulting in a color change in the solution. UV-VIS spectroscopy shows the weak build-up of a shoulder λ_{max} in the range of 330-380 nm which was likely a quinone or oxidized product, suggesting tyrosinase was oxidized, similar to methyl gallate (data not shown). Using the same test solution with a catalytic amounts of L-DOPA (10 μM) significantly enhanced the peak at 380 nm (Figure 4.20), at a similar absorbance intensity compared to the formation of PA. This was unexpected since tannic acid has not been reported to directly participate in Michael type condensation (even in the presence of oxidases) but it appears that oxidized products were forming. Testing of the tannic acid as an inhibitor on higher concentrations of L-DOPA (0.1 mM) confirmed it was a very strong inhibitor of dopachrome formation, even at the low concentration of 100 μM (Figure 4.21). The UV-VIS data shows that any products of tannic acid oxidation do not absorb at 475 nm, allowing us to directly contribute the absorption at this wavelength exclusively to dopachrome. Also, preincubation for 10 minutes did not increase the inhibitory activity.

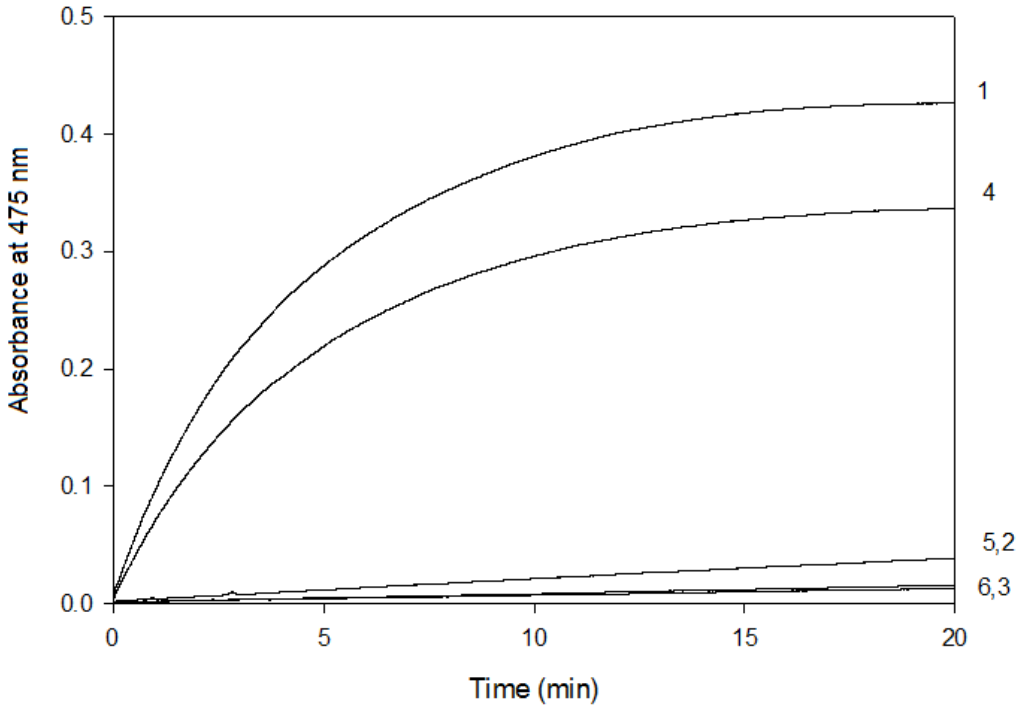

Figure 4.21 UV-VIS of absorbance at 475 nm of tyrosinase with L-DOPA (250μM) preincubated for 10 minutes (**1**), and inhibition assay (**4**) (negative control); tyrosinase and tannic acid (100 μM) preincubated for 10 minutes (**3**), and inhibition assay (**6**) (positive control); L-DOPA (100 μM) and tannic acid (100 μM) preincubated for 10 minutes (**2**), and inhibition assay (**5**)

Based on the structurally similar compounds we did not expect activity of tannic acid at the tyrosinase active site. Fluorescence measurements performed with 1-NPN on tyrosinase (100 μM) with L-DOPA (100 μM) and tyrosinase shows a 50% reduction of fluorescence signal (Table 4.2). The tannic acid structure is expected to be too large to enter the active site, and thus may be binding nearby and mechanically inhibiting access. Alternatively, the structure of tannic acid has 12 un-bonded electrons around the central aromatic ring, which may draw the structure towards the copper ions at the active site by electrostatic attraction, blanketing the active site and impeding access. We also note tannic acid was oxidized by the tyrosinase, so the inhibition could also be occupation of the active site during oxidation, or by the products of the oxidation.

Time	Tannic acid (100 μM)	Control
0	100	100
5	91.3	91
15	58.9	120
30	43.4	130

Table 4.2 Fluorescence of tannic acid at 100 μM with L-DOPA (0.250 mM) and tyrosinase

Insect Testing

With both tannic acid and gallic acid being demonstrated as effective enzyme inhibitors of dopachrome formation, these compounds were tests for efficacy in organism-level testing. The insect species *Spodopteraexigua* (Beet Armyworm) and *Trichoplusiani* (Cabbage Looper) were chosen as general agricultural pest insects of interest; efficacy was determined by growth inhibition assays performed during their larval stage. Topical feeding assays were performed in the late second and early third instar larvae. The dose at which 50% mortality of the insects was observed, ED_{50}, of tannic acid was 54 ppm, and ED_{50} of gallic acid was 3100 ppmfor *Trini.* The stronger effectiveness of tannic acid was consistent with the cell-free results, which showed tannic acid as a very strong inhibitor. Comparing to *S.exigua* the $ED_{50}$of gallic acid was 4970 ppmand 140 ppmfor tannic acid (Table 4.3). Again tannic acid was shown to be a significantly stronger inhibitor. The strong difference in the ED50 of the different insects emphasizes the variability between insects and their ability to manage these compounds.

	Tannic acid	**Gallic acid**
Spodoptera exigua	140ppm	4970ppm
Tricluplosia ni	54 ppm	3100 ppm

Table 4.3 Topical ED_{50} on two species of insect

Diet incorporation assays were performed with tannic acid on late secondary and early third instars *Tri ni*.and *S. exigua.* On day 5 larvae were weighted and were recorded. (The data met the assumption for normality testing, using a Shapiro-Wilks test). A one way ANOVA test showed there was a statistically significant difference ($p<0.05$) between the weights of the *S. exigua* individuals in the control treatment and methyl gallate, tannic acid and eugenol (Figure 22, Figure 23). This suggests that these compounds were feeding reducers. Yet, there was no statistically significant difference between the control larvae and those fed gallic acid for either species.

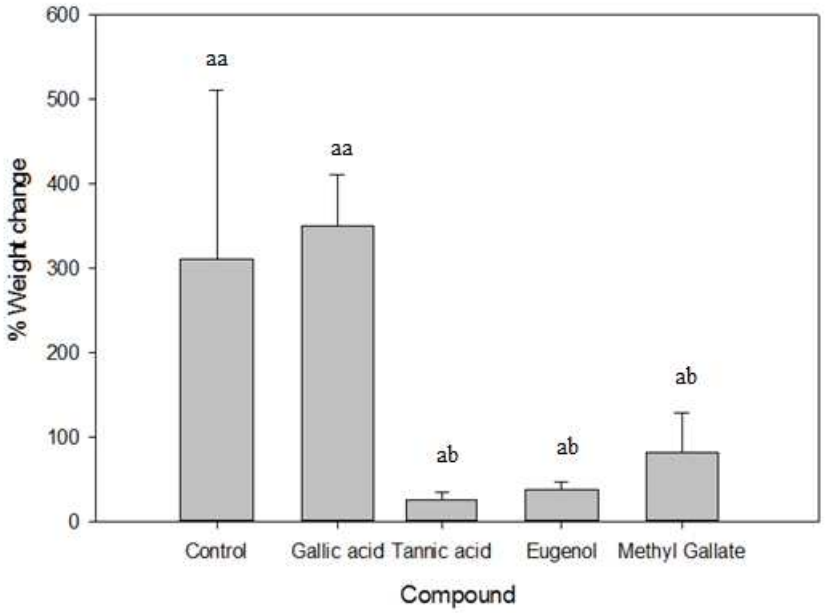

Figure 4.22 Change in weight % of *Tri ni* larvae

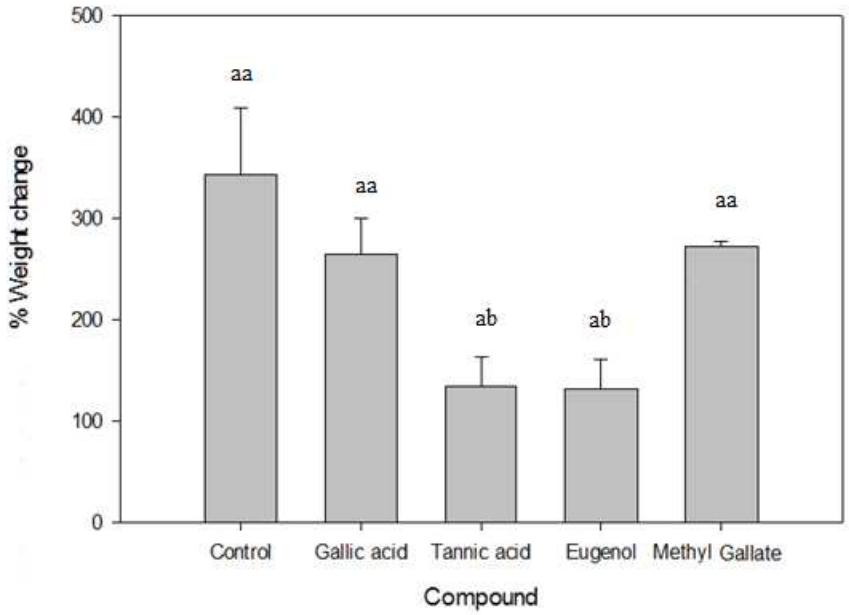

Figure 4.23 Change in weight % of *Spodoptera exigua* larvae

Moderate (28.6%) contact mortality was observed with gallic acid at the ED50 on second instar *S.exigua*; contact assays performed using tannic acid at the above ED50 showed no effect at this dose. In line with this *Tricluplosia ni* was not affected by gallic acid or tannic acid contact assay at the relative concentrations above. A synergy contact at the same concentration on *Tri ni*

combining gallic acid and tannic acid showed no mortality. Contact assays performed using methyl gallate at 500 ppm showed no mortality on *S. exigua* by the end of the assay period.

To determine if insect longevity was affected by gallic acid, tannic acid and methyl gallate *T. ni* eggs were dosed in a contact assay and monitored for emergence .The treatments of tannic acid (25 ppm) and methyl gallate (500 ppm) did not survive beyond the first day of emergence. *T. ni* eggs treated with gallic acid (at 30 ppm) hatched and the neonates survived through pupation. However, the treated population had a statistically significantly (p>0.05) lower pupal weight compared to the control. To determine how much gallic acid was processed by the larvae we collected frass samples and quantified the amount of gallic acid in them. On average, each insect consumed 1.4174 mg (+/-0.092855) of gallic acid from their artificial diet. In the frass we detected a range of 0.04-2.45mg of gallic acid. Nearly all of the gallic acid was either processed or oxidized to secondary products. We did not examine tannic acid because it was more likely to dissociate which makes HPLC quantification unreliable.

Insect Cells

Compounds tested	IC_{50} (μM)	
	Cell	log*P*
Protocatechuic acid	167	1.11
Methyl gallate	331	1.54
Gallic acid	380	0.91
Tannic acid	510	6.2
Trans-methylcinnamic acid	185	2.50
Cinnamic acid	447	2.55
Methylcinnamic acid	875	2.26
Methyleugenol	435	2.85
Eugenol	831	2.61

Table 4.3 Cytotoxicity against *S. exigua*gut cells by phenolics and structural analogues with log *P* values

The above insect assays suggest ingestion has significantly more activity than contact assays. To determine the effect of phenolics on the lepidopteran digestion track, we cultured mid-gut cells from *Spodoptera exigua* and directly exposed them to the test compounds, and report on cell viability (Table 4.3). Gallic acid was cytotoxic and actually potentiated growth at the lowest tested concentration of 50 μM. The IC50was estimated to be 380 μM. There was a statistically significant difference between the control and treatments above 400 μM

(p<0.05).Next, we examined methyl gallate because of it's structurally similarities to gallic acid. The IC50 was a comparable to gallic acid at 331 μM. Above 100 μM the cell viability was reduced by a statistically significant (p<0.05) amount. However, there was no statistical difference between the 100μM and 800μM treatments and control. This suggests the cells may be susceptible up to some saturation effect. Next, we examined protocatechuic acid to determine if the hydroxyl group effected activity. Protocatechuic acid was a cytotoxic compound in a dose responsive manner. The IC50 was estimated to be 167μM, much lower than the other compounds. There was a statistically significant difference in cell viability between the control and treatment (p>0.05), but no statistical difference amongst the treatments themselves. Protocatechuic acid was the most cytotoxic compound which was unexpected since it showed very weak enzyme activity. This emphasizes that, while the activity mechanism of these compounds may be related to L-DOPA, the complexity of cell functionality offers many opportunities for these chemicals to be toxic. Next, we examined tannic acid which showed dose dependent cytoxocity. The IC50was estimated to be 510 μM, much higher than the other compounds. Cell mortality was statistically (p<0.05) higher than the control between 200-400 μM. At the highest test concentration of 800 μM there was a two sigma difference (p<0.01). Overall, tannic acid was the weakest phenolic compound examined which was also unexpected since it was the most effective insect control agent. Structural analogues (phenolic acids) were also examined but they were generally lower in cytotoxicity than the tannins.

Recalling that some of the phenols were oxidized in the test solution during the enzyme assays, it becomes important to test compound stability in the cell medium using HPLC. Over a two hour period, the gallic acid peak decreased by 6.3%, methyl gallate decreased by 14%, and protocatechuic acid decreased by 8% (data not shown). The decrease in peak area suggests the compounds are possibly reacting in the medium to form structurally similar secondary reaction products, which was consistent with the enzyme assays (Figure 4.3, for example). Specifically for gallic acid we observed 10% of the available oxygen being used within the first 5 minutes after introducing the compound to the insect cell medium. Overall about 20% of the oxygen was consumed, which could be the source of some activity against the mid-gut cells. This was not the case for the other tannins examined.

Melanoma Cell

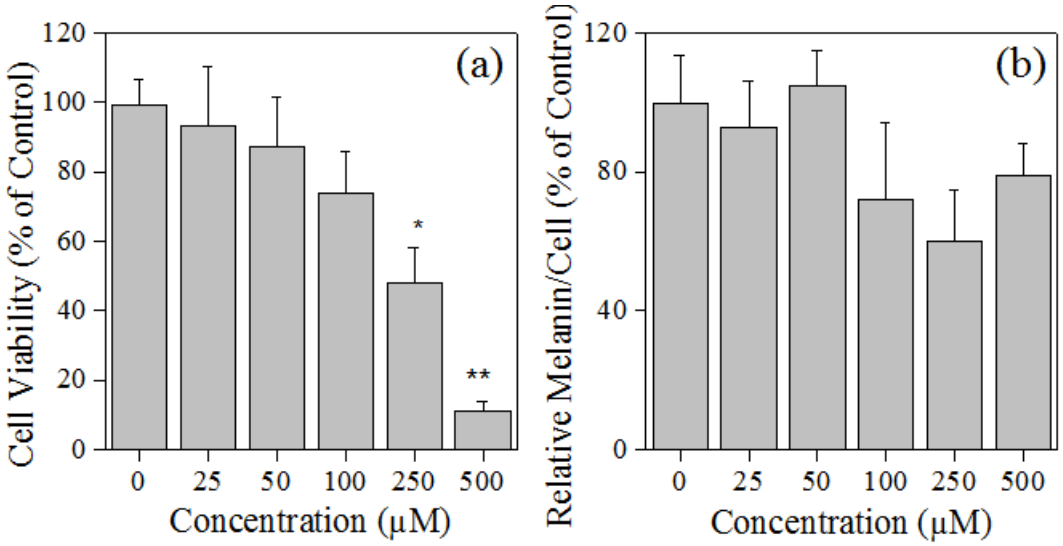

Figure 4.24 (a) Cell viability and (b) relative melanin per cell for murine cells tested with gallic acid

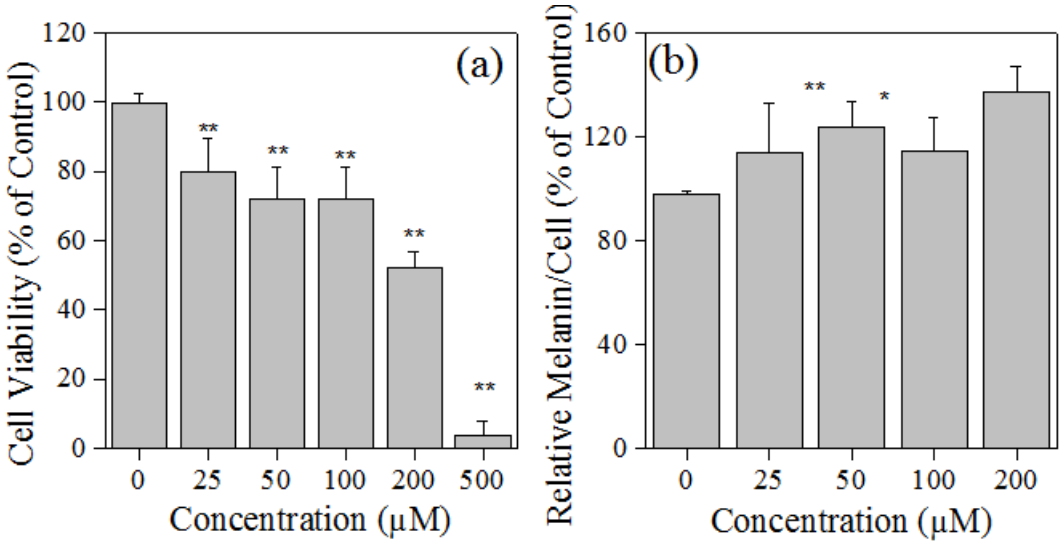

Figure 4.25 (a) Cell viability and (b) relative melanin per cell for murine cells tested with purpurogallincarboxylic acid

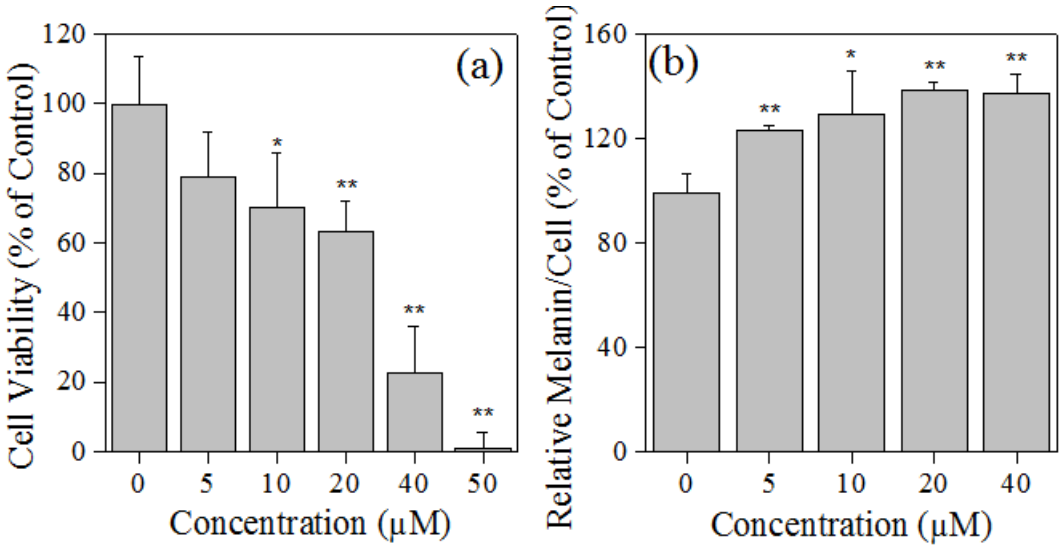

Figure 4.26 (a) Cell viability and (b) relative melanin per cell for murine cells tested with tannic acid

The phenolics that were tyrosinase inhibitors were expected to inhibit melanogenesis in the cultured murine B16-F10 melanoma cells without affecting cell growth. We began by measuring cell viability and determining an IC50, then measured the per-cell melanin concentration. Gallic acid was shown to be cytotoxic in a dose dependent manner with an estimated IC50of 229 μM (Figure 4.24). Cell viability above 250 μM was significantly reduced compared to the control (with statistical significance $p<0.05$). Gallic acid did not significantly suppress melanogenesis. Next, purpurogallincarboxylic acid was tested for activity; the highest concentration of purpurogallincarboxylic acid tested was 500 μM due to the compounds limited solubility in the testing medium. The IC50 was estimated at 219 μM. The purpurogallincarboxylic acid enhanced melanin formation, rather than inhibiting it (Figure 25).Lastly, tannic acid was tested for its melanin suppression ability and was found to be cytotoxic (Figure 4.26). Cell viability was shown to decrease in a concentration dependent manner up to 40 μM.Cell mortality was statistically significant ($p<0.01$) in the range of 10-50 μM. The IC50 was estimated to be 24 μM. Tannic acid did not suppress melanin production in the murine B16-F10 melanoma cells but increased its production.

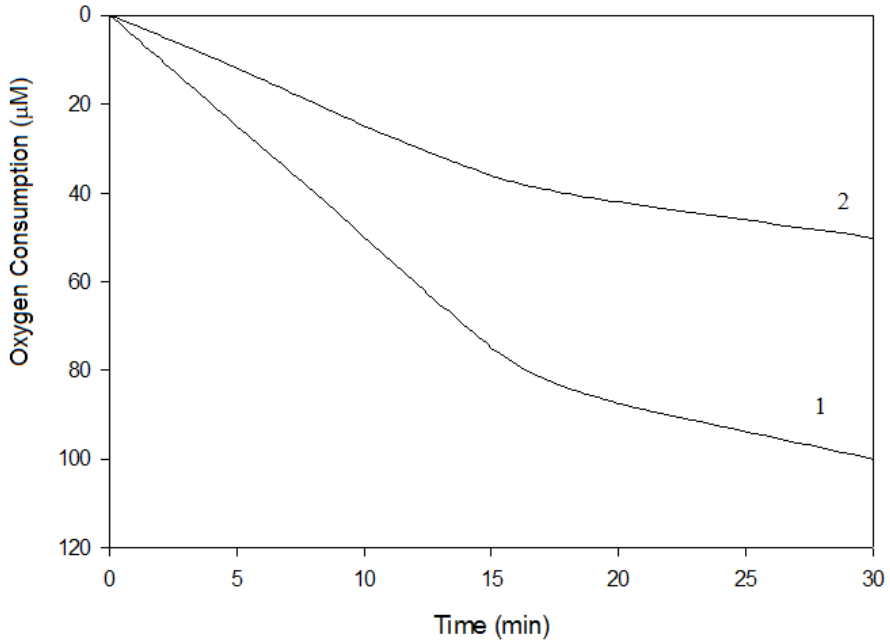

Figure 4.27 Oxygen consumption of oxidation of gallic acid at 100 µM. (1) and tannic acid at 100 µM. (2) in Dulbecco's Modified Eagle Medium (DMEM) containing 10 % of fetal bovine serum (FBS) for 30 minutes

We performed control experiments to confirm the stability of the compounds in the cell medium (Figure 4.27). Combining the compounds with only melanoma cell media resulted in approximately 60% and 75% of the available oxygen being by gallic and tannic acid, respectively. This implies that the activity we observed on the melanoma cells may not have been that only of gallic acid or tannic acid but rather their oxidized products or the oxygen depletion.

Discussion

Gallic acid, the principle compound identified in a number of plant extracts and parent compound of all hydrolysable tannins, was shown to be ineffective as a tyrosinase inhibitor. However, simple visual tests, as well as more complex UV-VIS spectroscopy, HPLC, and oxygen consumption assays confirm gallic acid was inhibiting the formation of dopachrome. In our proposed mechanism, the melanin formation pathway is interrupted by a gallic acid moderated redox cycle. Specifically, in the standard melanin formation pathway, L-DOPA is oxidized by tyrosinase to form dopaquinone and this quinone undergoes an intramolecularnon enzymatic 1,4-addition to the benzene ring, which caused its cyclization to leukodopachrome. This intermediate is quickly oxidized to dopachrome by another molecule of dopaquinone, which is itself reduced back to L-DOPA (Sanchezferrer and others 1995).Control experiments show thatgallic acid does not interact with tyrosinase or L-DOPA, even at high concentrations, but undergoes only weak auto-oxidation. However, in a solution of tyrosinase, gallic acid and L-DOPA, UV-VIS spectroscopy shows the emergence of a peak at 390-400 nm which was not observed in the control experiments. This suggests gallic acid reacts with one of the L-DOPA products; we suggest that gallic acid is oxidized by dopaquinone. In this reaction, dopaquinone accepts hydrogen from two of the hydroxyl groups on gallic acid at its two double-bonded oxygen sites, located at the meta- and para- positions. After accepting these hydrogens, dopaquinone once more becomes L-DOPA. Thus, L-DOPA becomes dopaquinone, which is then reduced by gallic acid to become L-DOPA, forming a redox cycle. Thus, with dopaquinone not progressing to form dopachrome, we observe the suppression of the color change in our solution. As a consequence, the subsequent formation of melanin is inhibited. A redox cycler protracts this oxidation reduction reaction. After the redox cycling interaction, gallic acid was oxidized to an ortho-quinone, which then condenses with other ortho-quinones through a Michael type addition to form the dibenzotropolone intermediate, purpurogallincarboxylic acid. A similar process was reported for potato polyphenol oxidase (Herrmann 1954).

Our HPLC data showed that in solutions of L-DOPA, gallic acid and tyrosinase consumed both compounds, and that consumption was depended both on reaction time and concentration. The data showed that the higher the gallic acid concentration was, compared to the L-DOPA concentration, inhibition began earlier, and was stronger. During redox cycling, the gallic acid must interact with the dopaquinone before it is converted to leucodopachrome. Thus, early in the interaction - when dopaquinone concentrations are low - or at low concentrations of gallic acid, redox cycling will not occur, consistent with our results. Thus, gallic acid neither inhibited the enzymatic oxidation nor acted as a substrate, but was oxidized by redox reaction.

Quantitative support for our suggested mechanism can be shown using the HPLC data. Specifically, control experiments using only L-DOPA and tyrosinase identify the uninhibited consumption rate of L-DOPA. Since gallic acid does not inhibit tyrosinase, this rate is expected to be unchanged. However, the measured L-DOPA consumption in the experiments with gallic acid will have some fraction of the L-DOPA returned from dopaquinone, due to the redox cycle. In the suggested mechanism, each of the returned L-DOPA will correspond to one oxidized gallic acid. Thus, the measured consumption of L-DOPA and gallic acid is expected to correspond to the total L-DOPA consumed. Indeed, the HPLC results confirm this quantitative agreement.

Gallic Acid Concentration	L-DOPA Concentration	Gallic Acid % Area Change	L-DOPA % Area Change	Relative Consumption (Sum of area × % change) / L-DOPA Concentration	Control
0.5 mM	0.5 mM	37%	28%	65%	89%
0.5mM	1 mM	82%	23%	64%	83%
4.5 mM	0.5 mM	25%	24%	249%	89%

Table 4.4 Gallic Acid and L-DOPA consumption fractions

The results show a similar consumption of L-DOPA and Gallic acid as the control performed on L-DOPA, with the exaction of the highest concentration of gallic acid (Table 4.4). This is likely due two contributing factors: (1) the auto-oxidation of gallic acid will enhance its consumption by approximately 10%, (2) the formation of purpurogallincarboxylic acid consumes two gallic acids per molecule, further increasing the apparent concentration. The fact that we do not see the formation of purpurogallincarboxylic acid at low concentrations suggests that the condensation does not occur at low concentrations, and thus must only be taken into account at the highest concentrations. Accounting for these factors (10% auto-oxidation, 2 gallic acid per L-DOPA), the relative consumption in the 4.5 mM gallic acid test was calculated to be 92%, in very good agreement with the control.

The role of electron donating hydroxyl groups on gallic acid was investigated in two structurally similar phenols. In phenolic compounds, the electron donating or withdrawing groups strongly influence their redox potential. Specifically, the electron donating groups, includinghydroxyl groups, make the aromatic structure rich in electrons. The high electron density confers a higher degree of instability to the phenol and increases its reactivity and reduces efficiency of the redox cycling process (Ullah and others 2009). This was demonstrated by the methyl gallate HPLC data which shows it was quickly oxidized and it is known to be a pro-oxidant at biological pH (Hagermann 1998). In contrast, protocatheutic acid has one fewer hydroxyl groups on the aromatic ring, compared to gallic acid or methyl gallate, and does not show redox activity. Gallic acid was shown to initiate redox cycling, but at higher concentrations can have pro-oxidant properties due to its structure.

Melanoma cells

Gallic acid was of great interest because of its anti-inflammatory, antioxidant and possible anticancer activity (Salcedo and others 2014). Gallic acid and its structural analogues were described to induce apoptosis in human leukemia (HL60 RG), human osteosarcoma bone cancer (HOS-1), human lung cancer cells, glioblastoma cancer cells (DBTRG-05MG) (Hsu 2016) and showed cytotoxic effects on other cell lines (Yoshioka and others 2000; Saleem and others 2002). The compound was able to form hydrogen bonds between its hydroxyl groups and residues on the surface lipids, such as the phosphate and carbonyl groups (Salcedo and others

2014). The structurally similar tannic acid is also known to induce cell apoptosis in human gingival cancer cells (YD-38 cell)(Darvin and others 2015), breast cancer cells (MCF7) and other cancer cells(Ngobili and others 2015). One way apoptosis, or programmed cell death, is initiated through the interaction with reactive oxygen species (ROS) which can damage important biomolecules and cellular components such as proteins and lipid (Apel and Hirt 2004).Gallic acid has been reported to have antioxidant properties by scavenging free radicals, including hydrogen peroxide and inhibiting lipid peroxidation (Sroka and Cisowski 2003). Lipid peroxidation occurs when ROS remove electrons from lipids that make up, for example, the cell membrane layer, and is one of the major causes of cellular damage. It has been reported previously that gallic acid moieties in tannins at high concentrations also generate superoxide radicals and hydrogen peroxide (Serrano and others 1998), which may be a source of its cellular mortality activity. However, the larger compound, tannic acid, inhibits the generation of superoxide anions and hydrogen peroxide at moderate concentrations (Gulcin 2009). It has been reported that polyphenols, such as tannic acid, can interact with lipid membranes and cause a collapse of the water space between bilayers which would disrupt the entire membrane structure (Salcedo and others 2014).

In cell membranes the electron transport chain (ETC) converts energy and powers essential biological functions (Molecular Biology, 4th edition). The ETC functions at the interface of the cytoplasmic membrane and is a chain of specialized electron carriers (redox agents), which allow for electrons to be shuttled through the membrane. Gallic acid may enter into the lipid-bilayer portions of membranes (Franks and Lieb 1986). permeating the plasma membrane and reaches the ETC. Once inside the lipid bilayer portions, gallic acid may inhibit the ETC, perhaps by interfering with the redox reaction (Mondal and others 2012).Gallic acid was described to increase activity of mammalian glutathione *S*-transferase, an important drug metabolizing enzyme, through oxidative modification of the enzyme (Hossain 2009).This same study found that gallic acid was able to passively enter through pores in the mitochondrial membrane, supporting our above suggestion that gallic acid can interfere with ETC.

On the other hand, tannins are known to chelate low valence metal ions, including copper. Yet gallic acid did not inhibit tyrosinase activity when preincubated together so this was an unlikely route of inhibition for gallic acid. On the other hand, tannic acid is known to reduce Fe(III) to Fe(II) (Lopes and others 1999) preventing the metal ions from being able to interact in solution. The variation in activity on melanoma murine cell depends on the compounds structure since tannic acid IC_{50} was 24 μM compared to gallic acid 229 μM. It has been shown in the previous chapters that metal chelators are often more efficient inhibitors so tannic aids ability to bind with the copper ions and form covalent bonds gives it an advantage over the radical oxygen generating gallic acid. Tannic acids metal chelation capacity is important because it forms aternary complex with the copper ions and stabilizes the oxidized form of the metal ionTA-Cu (II)-X (Henle and Linn 1997; Fraga and Oteiza 2002, (Zubair and others 2013). This complex can undergo redox reactions generating the above mentioned Cu (III) in a redox cycling mechanism that removes tyrosinase copper ions from the solution or other essential metal ions there by reducing essential metal availability for the cell (Scalbert 1991, Kubo and Kinst-Hori 1999, Pham 2013)and prohibiting cellular functions that require copper like the chromatin complex structure (Shamim and others 2008), leading to cell death. Furthermore, tannins can irreversibly inactivate enzymes (proteins) by cross-links, via tanning covalent bonds between phenolic compounds and proteins form a cross-linking structure which is more rigid and

thermally stable than other interactions. When tannic acid was preincubated with tyrosinase we observed a decrease in enzyme activity that we did not observed with gallic acid. Overall, we did not see a reduction in the amount of melanin produced so a general non enzymatic copper dose dependent mechanism that was not related to melanin production as described above is most likely. These results indicate that enzyme inhibition may not directly result in melanin suppression due to secondary reactants and complex structure interactions.

Insect

Overall, the most effective compound in controlling insect growth and development was tannic acid. The mid-gut cellular assays generally showed the opposite pattern of activity as the enzyme and organism level assays. This suggests different mechanisms of action which is not unexpected. Phytochemicals are well known to act by a variety of mechanisms in insects (Rattan 2010). The larval response to ingested phenols may be a consequence of the alteration the compounds undergo in the high pH (>12) lepidopteron mid-gut environment. Of the gallic acid consumed by the insects, only a small portion remained intact after digestion. The insect mid-gut has a high pH (>12) and the pKa of gallic acid hydroxyl groups is 9, of tannic acid is 10, and both methyl gallate is 8. This results in the test compounds deprotonating and increasing their ability to hydrogen bond with biomolecules. It should be noted however that the most effective compound in the mid-gut assay was protocatechuic acid which has the simplest structure of the tannins examined and may be the key to the compounds efficacy. This structure could make it more likely to be oxidized damaging cellular components. Additionally, oxygen present in the mid-gut (albeit at low concentrations) would likely modify any of the examined compounds to form quinones (Bernays and others 1993, Barbehenn and Constabel 2011). Quinones are known to be highly toxic to insect as well as many other organisms and have anti-nutritive effects. In addition, quinones can redox cycle to produce ROS in the gut lumen (Pardini 1995) damaging tissue. Alkyl gallates, which are structurally similar to the phenols tested here, were previously described to increase production of ROS (Sakaguchi and others 1979). Tannic acid at low concentrations does not generate superoxide anions but at higher concentrations they do in the hemolymph of mussels (Bouki, 2003). It is possible once in the gut lumen tannic acid at higher concentrations acts as a pro-oxidant, causing cellular damage. Due to the high number of hydroxyl groups, tannic acid is a much more effective growth reducer compared to those compound with fewer hydroxyls. Thus, we suggest some chemical modification of the compound is at the core of the larval defenses in the midgut and/or phenol ROS generation in the gut lumen (Barbehenn and Martin 1994; Barbehenn and Constabel 2011) may be the key factors in the observed efficacy in inducing cell mortality and reducing larval growth.

Conclusion

Structurally similar phenols are shown to behave as melanogenesis inhibitors. Gallic acid, the fundamental hydrolysable tannin, was shown to be a melanogenesis inhibitor by initiating a redox cycle with dopaquinone. This process interrupts dopachrome formation and depletes the available oxygen in the solution, halting the reaction. This is likely due to the strongly interacting hydroxyl groups on the phenol, which are well-known to be the source of antioxidant activity and pro-oxidant activity in the compounds. However, removing a meta-position hydroxyl, forming protocautheic acid, completely suppressed all inhibitory activity, as well as pro- or anti-oxidant activity. This suggests that the meta-position hydroxyl group is key to inducing redox activity. On the other hand, tannic acid was shown to be a strong scavenger and chelator and showed strong activity against the enzyme and insect. Depending on the testing environment phenols express different inhibitory properties.

Structures

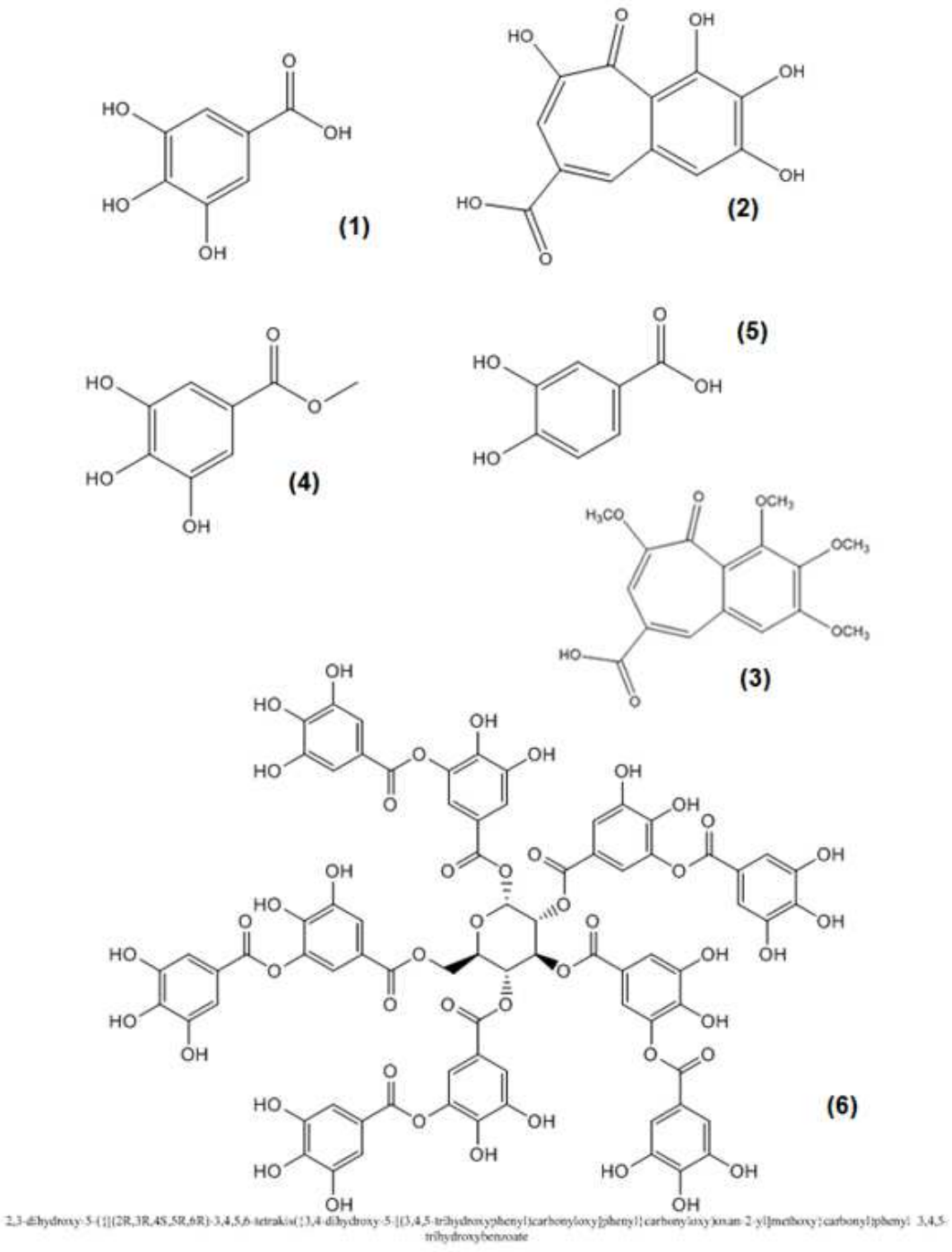

Figure 4.26 Structures of the tested compounds: (**1**) gallic acid, (2) purpurogallincarboxcylic acid, methylated purpurogallincarboxcylic acid (3), methyl gallate (4), protocatechuic acid (5) and tannic acid (6)

Materials and Methods

General methods

General procedures were as previously reported (Satooka and Kubo 2011; Nitoda and others 2007) with slight modifications. Assays were performed in triplicate.

Materials

Core testing materials such as L-DOPA, L-tyrosine and tyrosinase were purchased from Sigma-Aldrich (Milwaukee, MN, USA). All compounds were purchased from Sigma-Aldrich (Milwaukee, MN, USA).

Enzyme

Assays investigate tyrosinase inhibition as a mechanism to suppress melanogenesis. Tyrosinase – mushroom derived– used in the inhibition assays was purchased from Sigma Aldrich and was purified by anion-exchange chromatography using DEAE-Sepharose Fast Flow (Pharmacia, Uppsala, Sweden) as previously described (Espin and Wichers 1999). Tyrosinase initiates the melanin formation cascade by catalyzing the hydroxylation of L-tyrosine, and thenthe oxidation L-DOPA into dopaquinone, then non-enzymatically into dopachrome, and eventually into melanin, as discussed in the General Introduction.

Spectrometry

Photo-spectroscopy (UV-VIS) measurements were performed on a Shimadzu 1700 (Tokyo, Japan) to identify the formation of dopachrome. Absorbance was measured at 475 nm, which corresponds to a strong absorbance of dopachrome. Samples were dissolved in DMSO and only used for experimentation after their dilution. The final concentration of DMSO was always 3%. For inhibition assays, a test solution of 3 ml was prepared consisting of 1.95 ml distilled and filtered H_20, 0.725 ml of 67mM phosphate buffer (pH=6.8), 0.125 ml L-DOPA (from a 6 mM stock) were mixed and incubated at 30° C for 5 minutes. At this point, the 100 µl of the sample solution and 100 µl of the purified tyrosinase in phosphate buffer was added (1 µg/ml) to the mixture in this order. Once tyrosinase was added to the solution the absorbance was measured for 30-60 minutes. For preincubation assays, the preincubation solution- 1.95 ml distilled and filtered H_20, 0.725 ml of 67mM phosphate buffer (pH=6.8), 100 µl of the sample solution and 100 µl of the purified tyrosinase was added (1 µg/ml) and incubated for 10 minute (or 20

minutes) at 30° C, prior to the addition of L-DOPA. Each assay was repeated three times on separate occasions; data was recorded in Probe 2.1v.

Oxygen consumption

Oxygen consumption inhibitory assays can monitor both the catalyzation of L-tyrosine into L-DOPA and L-DOPA into dopaquinone, since both steps consume a single molecular oxygen from solution. Measurements were taken using an OBH 100 oxygen electrode with a water jacket chamber using an YSI 5300 oxygen monitor (all from Yellow Springs Instruments Co., Yellow Springs, OH).For inhibition assays, a test solution of 3 ml was prepared consisting of 1.95 ml distilled and filtered H_20, 0.725 ml of 67mM phosphate buffer (pH=6.8), 0.125 ml L-DOPA (from a 6 mM stock) and the candidate inhibitor dissolved in DMSO were incubated at 30° C for 5 minutes. At this point, 100 µl of the purified tyrosinase in phosphate buffer was added (1 µg/ml). Oxygen consumption was then monitored at 30° C for up to 60 minutes. Each assay was repeated three times on separate occasions to confirm repeatability. Preincubationassays investigated interactions of the inhibitor with tyrosinase. The preincubation solution was prepared as described above.The results were expressed as oxygen consumption in the unit µM.

HPLC

The high-performance-liquid-chromotography (HPLC) analysis was performed on EYELA pump (Tokyo Rikakikai Co. Ltd., Tokyo, Japan) with an EYELA UV-7000 detector (Tokyo Rikakikai Co. Ltd., Tokyo, Japan) and Develosil ODS-UG-5 column (4.6 x 150 mm, Nomura Chemical Co., Ltd., Japan). The operating conditions were as follows unless otherwise noted: the solvents were 3% MeCN (Acetonitrile) and H_2O containing 0.2 % Trifluoroacetic (TFA), flow rate of 1 ml/min, detection at 280 nm (UV), injected volume of 25 µl from the above described 3 ml assay system. The peak area was used to monitor the consumption of substrates and the results were described as the ratio of the area of sample peaks to the control.

Fluorescence

Fluorescence measurements were performed using *N*-Phenyl-1-naphthylamine (1-NPN) to probe the occupancy of the active site. This compound strongly fluoresces in hydrophobic environments (Yin and others 2015), which includes the tyrosinase active site. Thus, as the substrate and/or inhibitor occupy the active site, the fluorescence intensity is expected to decrease. In this work specifically, control fluorescence assays performed on the native L-tyrosine substrate showed an initial drop in signal intensity during the conversion of L-tyrosine to L-DOPA. This drop can be understood as the substrates occupying the active site, and consequentially displacing 1-NPN. Assays performed on the L-DOPA substrate also showed an

initial decrease in fluorescence due to the same displacement mechanisms (Yin and others 2015). After this initial decrease, the fluorescence intensity increased, indicating that the probe can access the active site. Generally, the fluorescence signal in the control experiments increase over the 30 minute assay period due to the shrinking amount of L-DOPA available to bind. Fluorescence measurements were performed on an EnVision Plate reader 2104i (Perkin-Elmer, Waltham, MA,USA), using a 340 nm excitation light and monitoring emissions at 460 nm. Inhibitory assay solutions (3 ml) were prepared as described in the spectroscopy experiments, with the addition of 100 µL of 1-NPN for (20 µM) was added and the solution incubated at 30° C for 10 minutes.. Of this solution 300 µL were then loaded into wells of a 96 well plate, then the candidate inhibitor was added to this solution, then tyrosinase was added. Emissions were measured every 5 minutes for 30 minutes total. To avoid light interference measurements were taken only after the light path way shut for at least 10 seconds.

Cellular assays

Cell mortality assays were performed on B16-F10 murine melanoma cells purchased from ATCC (Manassas, VA, USA), and cultured in continuous log phase growth in Dulbecco's Modified Eagle medium (DMEM) containing 10% fetal bovine serum (FBS). Cells were seeded in 96-well plates (≈2000 cells/well) and incubated at 37° C for 24 hours at 5% CO_2 prior to chemical treatment. Each chemical was applied in duplicate (N=6) with a final content of 0.1% DMSO, and treated cells were cultured for 72 hours prior to scoring. The melanin content was quantified as described (Kageyama and others 2004; Venkatasamy and others 2004) with some adjustment. Cells were washed with phosphate-buffered saline (PBS), harvested by trypsinization, and centrifuged for 10 minutes at 1500×*g*. The cell pellets were then dissolved in 1.0 M NaOH that contained 10% DMSO for a 2 hour incubation period at 80° C. Melanin content was determined at 475 nm using a SpectraMax Plus spectrophotometer and SoftMax Pro software (Molecular Devices, Union City, USA). Cell viability was evaluated through trypan blue exclusion using a Nikon Diaphoto TMD (Nikon, Tokyo, Japan), and a 50% viable cells lost (IC_{50}) was determined. PBS was used to wash cells, and then they were dispersed by trypsinization. A sample of the cells was then diluted with DMEM containing 10% FBS, and then mixed with the trypan blue solution (for a final concentration of 0.1%) at room temperature. Unstained cells (viable cells) were counted within 10 minutes using a hemocytometer after being mixing with the trypan blue solution.

Insect

S. exigua and were purchased from BioServ (Frenchtown, NJ). Larvae were reared on and tested on BioServ generalist lepidoptera artificial diet (Frenchtown, NJ). For diet incorporation assays, late second and early 3rd*S. exigua*larvae were individually weight then placed in a petri dish. The dish was covered with parafilm and a single hole was pierced through the cover to allow air flow and placed in the incubator. The test chemical was added in replacement of dry diet base if a

powder or from the amount liquid if in that state at room temperature. Diet was then weight out to approximately one gram, the value recorded then placed in a plastic petri dish. Insects were weighted on day 5. There were a minimum of 5 larvae per treatment level. The percentage change in weight was calculated for both the insect and diet. For contact assays, compounds were dissolved in methanol and administered via 1 µl drop on the thorax of early third instar larvae. Individuals were placed in a petri dish. Each treatment had 5 larvae per treatment level. The dish was covered with parafilm and a single hole was pierced through the cover to allow air flow and placed in the incubator. Larvae were scored on day 5 for mortality. For topical feeding assays 1 ml of untreated diet was loaded onto 12-well non treated flat bottom BD Falcon plates and allowed to solidify. Treatment and control solutions were dispensed and water was the control and briefly evaporated. Two control wells were present on each plate. In total there were 30 plates with both treatments present to account for any variation. Five day old *S. exigua*or *Tri ni* were loaded, one larvae per well. Plates were sealed with Fisher plate covers (Fisher scientific, Waltham, MA) and a single hole pierced through the center to allow air flow and then placed in the incubator. Insects were scored for mortality each day until day 4. If a larva became stuck on the plate lid it was not recorded and removed from the treatment pool. An Abbotts correction was used to determine mortality if it exceed 5% in the control. Insects were incubated at 27 ºC at 12/12 hours light and dark.

Insect cell

Midgut cells were cultured according to (Hakim and others 2009) with some modification from the tissue of early fifth instar *Spodoptera exigua* larva. Insects were obtained from an in house colony raised in standard conditions on a general Lepidoptera diet from BioServ (Frenchtown, NJ) reared at 26 ºC. In house cells were cultured in TNM-TH medium (Milwaukee, MN, USA) supplemented with 5% FBS and incubated at 27 ºC.96-well plates were first loaded with treatment and then aliquots from a cell solution was added to each well (2500 cells/ well). Each chemical was applied in duplicate. Plates were then sealed and incubated at 27 ºC for 48 hours. Cells viability was determined by the Trypan blue exclusion method with a Nikon Diaphoto TMD, and 50% viable cells lost (IC_{50}) was determined. An aliquot of suspension from the culture dish is mixed with 0.4% (w/v) Trypan blue (2:1) and rested for 5 minutes. Unstained cells (viable cells) were counted using a hemocytometer.

References

1. Apel K, Hirt H. 2004. Reactive oxygen species: Metabolism, oxidative stress, and signal transduction. Annual Review of Plant Biology 55:373-99.

2. Ayala-Zavala JF, Silva-Espinoza BA, Cruz-Valenzuela MR, Villegas-Ochoa MA, Esqueda M, Gonzalez-Aguilar GA, Calderon-Lopez Y. 2012. Antioxidant and antifungal potential of methanol extracts of Phellinus spp. from Sonora, Mexico. Rev. Iberoam. Micol. 29(3):132-8.

3. Bailey RG, Nursten HE, McDowell I. 1993. The chemical oxidation of catechins and other pehnolics- a study of the formation of black tea pigments. Journal of the Science of Food and Agriculture 63(4):455-64.

4. Barbehenn RV, Constabel CP. 2011. Tannins in plant-herbivore interactions. Phytochemistry 72(13):1551-65.

5. Bittner S. 2006. When quinones meet amino acids: chemical, physical and biological consequences. Amino Acids 30(3):205-24.

6. Conrad JS, Dawso SR, Hubbard ER, Meyers TE, Strothkamp KG. 1994. Inhibitor binding to the binuclear active-site of tyrosinase- temperature, pH, and solvent deuterium-isotope effects. Biochemistry 33(19):5739-44.

7. Dillard CJ, German JB. 2000. Phytochemicals: nutraceuticals and human health. Journal of the Science of Food and Agriculture 80(12):1744-56.

8. Espin JC, Wichers HJ. 1999. Slow-binding inhibition of mushroom (Agaricus bisporus) tyrosinase isoforms by tropolone. Journal of Agricultural and Food Chemistry 47(7):2638-44.

9. Franks NP, Lieb WR. 1986. The pharmacology of simple molecules. Archives of toxicology. Supplement. Archiv fur Toxikologie. Supplement 9:27-37.

10. Hagerman A. 1989. Chemistry and Significance of Condensed Tannins. Chemistry of Tannin-Protein Complexation [serial online]:323-33.

11. Hakim RS, Caccia S, Loeb M, Smagghe G. 2009. Primary culture of insect midgut cells. In Vitro Cell. Dev. Biol.-Anim. 45(3-4):106-10.

12. Haraguchi H, Honda S, Kamikawa T, Kondou Y, Kubo Y, Kubo I. 2000. Structural criteria of antioxidative activities of gallic acid esters. Abstracts of Papers of the American Chemical Society 219:U39-U.

13. Harborne AJ. 1998. Phytochemical Methods A Guide to Modern Techniques of Plant Analysis, 3rd ed: Chapman and Hill.

14. Herrmann K. 1954. The o-polyphenol oxidatses and their actions. Pharmazie 9((8)):670-82.

15. Kageyama A, Oka M, Okada T, Nakamura S, Ueyama T, Saito N, Hearing VJ, Ichihashi M, Nishigori C. 2004. Down-regulation of melanogenesis by phospholipase D2 through ubiquitin proteasome-mediated degradation of tyrosinase. Journal of Biological Chemistry 279(26):27774-80.

16. Karlsson O, Lindquist NG. 2016. Melanin and neuromelanin binding of drugs and chemicals: toxicological implications. Archives of Toxicology 90(8):1883-91.

17. Kim YJ. 2007. Antimelanogenic and antioxidant properties of gallic acid. Biological & Pharmaceutical Bulletin 30(6):1052-5.

18. Koleckar V, Kubikova K, Rehakova Z, Kuca K, Jun D, Jahodar L, Opletal L. 2008. Condensed and hydrolysable tannins as antioxidants influencing the health. Mini-Reviews in Medicinal Chemistry 8(5):436-47.

19. Kubo I, Chen QX, Nihei K, Calderon JS, Cespedes CL. 2003a. Tyrosinase inhibition kinetics of anisic acid. Zeitschrift Fur Naturforschung Section C-a Journal of Biosciences 58(9-10):713-8.

20. Kubo I, Kinst-Hori I, Nihei K, Soria F, Takasaki M, Calderon JS, Cespedes CL. 2003b. Tyrosinase inhibitors from galls of Rhus javanica leaves and their effects on insects. Zeitschrift Fur Naturforschung Section C-a Journal of Biosciences 58(9-10):719-25.

21. Kubo I, Matsumoto T, Hanke FJ, Taniguchi M. 1985. Flavan-2-ol causes seedling growth inhibitor to induce growth stimulation. Abstracts of Papers of the American Chemical Society 189(APR-):82-PEST.

22. Kubo I, Yokokawa Y, Kinsthori I. 1995. TYROSINASE INHIBITORS FROM BOLIVIAN MEDICINAL-PLANTS. Journal of Natural Products-Lloydia 58(5):739-43.

23. La P-H, Hua H, C P-H. 2008. Free Radicals, Antioxidants in Disease and Health. International Journal of Biomedical Science p. 89-96.

24. Lobo V, Patil A, Phatak A, Chandra N. 2010. Free radicals, antioxidants and functional foods: Impact on human health. Pharmacognosy Reviews 4(8):118-26.

25. Marmaras VJ, Charalambidis ND, Zervas CG. 1996. Immune response in insects: The role of phenoloxidase in defense reactions in relation to melanization and sclerotization. Arch. Insect Biochem. Physiol. 31(2):119-33.

26. Matsuo K, Kobayashi M, Takuno Y, Kuwajima H, Ito H, Yoshida T. 1997. Anti-tyrosinase activity constituents of Arctostaphylos uva-ursi. Yakugaku Zasshi-Journal of the Pharmaceutical Society of Japan 117(12):1028-32.

27. Ngobili TA, Shah H, Park JP, Kwist KW, Inskeep B, Burg KJL, Booth BW. 2015. Remodeling of Tannic Acid Cross linked Collagen Type I Induces Apoptosis in ER+ Breast Cancer Cells. Anticancer Research 35(3):1285-90.

28. Nikolic GM, Veselinovic AM, Nikolic RS, Mitic SS. 2011. Spectroscopic study of Mg(II) ion influence on the autoxidation of gallic acid in weakly alkaline aqueous solutions. Russian Journal of Physical Chemistry A 85(13):2270-3.

29. Nitoda T, Fan MD, Kubo I. 2007. Anisaidehyde, a melanogenesis potentiator. Zeitschrift Fur Naturforschung C-a Journal of Biosciences 62(1-2):143-9.

30. Rattan RS. 2010. Mechanism of action of insecticidal secondary metabolites of plant origin. Crop Protection 29(9):913-20.

31. Sakaguchi K, Miyakawa T, Takeuchi S, Nakagawa K, Hayase E. 1979. Interaction of benzaldehyde to the membrane protein of escherichiacoli. Agricultural and Biological Chemistry 43(8):1775-7.

32. Salcedo CL, Frias MA, Cutro AC, Nazareno MA, Disalvo EA. 2014. Antiradical activity of gallic acid included in lipid interphases. Biochimica Et Biophysica Acta-Biomembranes 1838(10):2656-61.

33. Saleem A, Husheem M, Harkonen P, Pihlaja K. 2002. Inhibition of cancer cell growth by crude extract and the phenolics of Terminalia chebula Retz. fruit. Journal of Ethnopharmacology 81(3):327-36.

34. Sanchezferrer A, Rodriguezlopez JN, Garciacanovas F, Garciacarmona F. 1995. Tyrosinase- a comprehensive review of it's mechanism. Biochimica Et Biophysica Acta-Protein Structure and Molecular Enzymology 1247(1):1-11.

35. Satooka H, Kubo I. 2011. Effects of Thymol on Mushroom Tyrosinase-Catalyzed Melanin Formation. Journal of Agricultural and Food Chemistry 59(16):8908-14.

36. Serrano A, Palacios C, Roy G, Cespon C, Villar ML, Nocito M, Gonzalez-Porque P. 1998. Derivatives of gallic acid induce apoptosis in tumoral cell lines and inhibit lymphocyte proliferation. Archives of Biochemistry and Biophysics 350(1):49-54.

37. Shamim U, Hanif S, Ullah MF, Azmi AS, Bhat SH, Hadi SM. 2008. Plant polyphenols mobilize nuclear copper in human peripheral lymphocytes leading to oxidatively generated DNA breakage: Implications for an anticancer mechanism. Free Radical Research 42(8):764-72.

38. Ullah MF, Shamim U, Hanif S, Azmi AS, Hadi SM. 2009. Cellular DNA breakage by soy isoflavone genistein and its methylated structural analogue biochanin A. Molecular Nutrition & Food Research 53(11):1376-85.

39. Venkatasamy R, Faas L, Young AR, Raman A, Hider RC. 2004. Effects of piperine analogues on stimulation of melanocyte proliferation and melanocyte differentiation. Bioorganic & Medicinal Chemistry 12(8):1905-20.

40. Yin J, Choo YM, Duan HX, Leal WS. 2015. Selectivity of odorant-binding proteins from the southern house mosquito tested against physiologically relevant ligands. Frontiers in Physiology 6.

41. Yoshioka K, Kataoka T, Hayashi T, Hasegawa M, Ishi Y, Hibasami H. 2000. Induction of apoptosis by gallic acid in human stomach cancer KATO III and colon adenocarcinoma COLO 205 cell lines. Oncology Reports 7(6):1221-3.

42. Zubair H, Khan HY, Sohail A, Azim S, Ullah MF, Ahmad A, Sarkar FH, Hadi SM. 2013. Redox cycling of endogenous copper by thymoquinone leads to ROS-mediated DNA breakage and consequent cell death: putative anticancer mechanism of antioxidants. Cell Death & Disease 4.